

The role of metabolically active brown adipose tissue in patients with phaeochromocytoma and paraganglioma

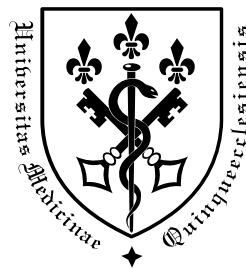
DOCTORAL (PH.D.) DISSERTATION

EDUARD OŠTARIJAŠ, M.D.

SUPERVISOR: Silvija Canecki-Varžić, M.D., PH.D.

HEAD OF THE DOCTORAL SCHOOL: PROF. Lajos Bogár, M.D., PH.D., D.SC.

HEAD OF THE DOCTORAL PROGRAMME: PROF. Emese Mezősi, M.D., PH.D., D.SC.



Doctoral School of Clinical Medical Sciences
University of Pécs, Medical School

PÉCS, 2025

Contents

List of abbreviations	4
1. Introduction	8
1.1. Pheochromocytoma and paraganglioma	8
1.1.1. Pathogenesis	9
1.1.2. Inherited syndromes	10
1.1.3. Clinical manifestations	12
1.1.4. Diagnosis	14
1.1.5. Management	16
1.2. Brown adipose tissue	17
1.2.1. Catecholamine-mediated activation	18
1.2.2. Regulatory factors	19
1.2.3. Detection	21
2. Cohort study	23
2.1. Methods	23
2.1.1. Patient characteristics and clinical assessment	23
2.1.2. Statistical analysis	24
2.1.3. Ethics	25
2.2. Results	26
3. Systematic review of literature	36
3.1. Methods	36
3.1.1. Study eligibility	36
3.1.2. Search strategy	36
3.1.3. Data collection	37

3.1.4.	Risk of bias assessment	38
3.1.5.	Statistical analysis	38
3.2.	Results	40
3.2.1.	Search and selection	40
3.2.2.	Risk of bias assessment	41
3.2.3.	Quantitative synthesis	42
3.2.4.	Qualitative synthesis	44
4.	Discussion	46
4.1.	Integration of findings.....	53
4.2.	Strengths and limitations	53
5.	Future perspectives	56
6.	Summary of findings	58
7.	Acknowledgments	59
8.	References.....	60
9.	Publications & author-level research metrics.....	72
9.1.	Author metrics	72
9.2.	Publications related to the dissertation.....	72
9.3.	Publications unrelated to the dissertation.....	73
9.4.	Abstracts and other publications	76

List of abbreviations

aBAT	activated brown adipose tissue
AJCC	American Joint Committee on Cancer
A_r	mean value
AT	adipose tissue
ATP	adenosine triphosphate
BAT	brown adipose tissue
BMI	body mass index
CAC	cancer-associated cachexia
cAMP	cyclic adenosine monophosphate
CI	confidence interval
COMT	catechol-O-methyltransferase
CT	computed tomography
df	degrees of freedom
DOPA	dihydroxyphenylalanine
DOTA	dodecane tetraacetic acid
DOTATATE	DOTA-[Tyr ³]-octreotate
e.g.	for example (Latin, <i>exempli gratia</i>)
ERK	extracellular signal-regulated kinase
¹⁸ F	fluorine-18
¹⁸ F-F-DA	¹⁸ F-6-fluorodopamine
¹⁸ F-FDG	¹⁸ F-fluorodeoxyglucose

Fig.	figure
⁶⁸ Ga	gallium-68
GafREC	Governance Arrangements for Research Ethics Committees
HIF	hypoxia-inducible factor
HNPGL	head-and-neck paraganglioma
HRz	hazard ratio
¹²³ I	iodine-123
¹³¹ I	iodine-131
i.e.	that is (Latin, <i>ita est</i>)
IQR	interquartile range
MAPK	mitogen-activated protein kinase
MED	median
MEDLINE	Medical Literature Analysis and Retrieval System Online
MEK	mitogen-activated protein kinase (MAPK) / extracellular signal-regulated kinase (ERK)
MEN	multiple endocrine neoplasia
MIBG	metaiodobenzylguanidine (iobenguane)
MRI	magnetic resonance imaging
3-MT	3-methoxytyramine
MTC	medullary thyroid carcinoma
mTOR	“mammalian target of rapamycin”
N/A	not applicable <i>or</i> not available
NCT	National Clinical Trial

NF1	neurofibromatosis type 1
NF-PPGLs	nonfunctioning pheochromocytomas and paragangliomas
NHS	National Health Service
OS	overall survival
PACS	picture archiving and communication system
PCC	pheochromocytoma
PD-1	programmed cell death protein 1
PD-L1	programmed cell death ligand 1
PET	positron emission tomography
PI3K	phosphoinositide 3-kinase
PKA	protein kinase A
PFS	progression-free survival
PGL	paraganglioma
PPGL	pheochromocytoma and paraganglioma
PRISMA	Preferred Reporting Items for Systematic Reviews and Meta-Analyses
PROSPERO	International Prospective Register of Systematic Reviews
PTH-rP	parathyroid hormone-related peptide
QUIPS	Quality in Prognostic Studies
RAF	“rapidly accelerated fibrosarcoma”
RAS	“rat sarcoma”
RCT	randomised controlled trial
RECIST	Response Evaluation Criteria in Solid Tumours

REML	restricted maximum-likelihood
RET	“rearranged during transfection”
RRGB	Renal/Endo Research Group Board
SD	standard deviation
SDH(<i>x</i>)	succinate dehydrogenase complex (subunit <i>x</i>)
SMD	standardised mean difference
SPECT	single-photon emission computed tomography
SUV	standardised uptake value
SUV _{max}	maximum standardised uptake value
SUV _{mean}	mean standardised uptake value
T ₃	triiodothyronine
T ₄	thyroxine
TR	thyroid hormone receptor
TRPV1	transient receptor potential vanilloid-1
Tyr	tyrosine
UCP1	uncoupling protein-1
UK	United Kingdom
ULN	upper limit of normal
VHL	Von Hippel-Lindau
vs	versus
WAT	white adipose tissue

1. Introduction

1.1. Pheochromocytoma and paraganglioma

Catecholamines are a group of sympathomimetic hormones derived from the amino acid tyrosine. They are synthesised mainly in the adrenal medulla and in sympathetic neurons through a series of enzymatic steps that convert tyrosine to dihydroxyphenylalanine (DOPA), dopamine, and subsequently to norepinephrine (noradrenaline) and epinephrine (adrenaline). These substances have crucial roles in mediating the body's response to stress by inducing positive chronotropy, positive inotropy, vasoconstriction in non-essential tissues (i.e., centralisation of blood circulation), increased oxygen intake (via bronchodilation), lipolysis and gluconeogenesis, diaphoresis, and reduced gastrointestinal motility. They exert their physiological effects via adrenergic receptors, which are broadly categorised into alpha (α) and beta (β) subtypes, each of which influences distinct pathways. While epinephrine and norepinephrine can activate both α - and β -adrenergic receptors, dopamine is primarily active at dopaminergic receptors, although at higher concentrations it can also stimulate adrenergic receptors. (1)

In adults, catecholamine-secreting neoplasms include pheochromocytomas and paragangliomas (PPGLs). Pheochromocytomas (PCCs) originate within the adrenal medulla, whereas paragangliomas (PGLs) develop outside the adrenal glands, commonly along the sympathetic chain or within parasympathetic tissues. (2) Although these tumours are uncommon, with an estimated incidence of approximately two to eight cases per million individuals per year, they are clinically significant due to their potential to overproduce catecholamines and, albeit even less frequently, to cause disseminated disease. (3, 4)

1.1.1. Pathogenesis

The pathogenesis of both pheochromocytomas and paragangliomas is closely related to both their embryological origins and specific genetic mutations that drive abnormal cell growth. These tumours originate from the neural crest, a population of pluripotent cells formed during early embryonic development. (5) Within the adrenal medulla, neural crest cells migrate and give rise to chromaffin cells, which represent the principal cell lineage involved in pheochromocytoma formation. (3-5) By contrast, paraganglia are extra-adrenal tissues derived from neural crest cells; they are located along the sympathetic chain and parasympathetic tissues (such as the carotid and jugular bodies), resulting in sympathetic and parasympathetic paragangliomas, respectively. Sympathetic paragangliomas typically secrete catecholamines, while parasympathetic paragangliomas are usually nonfunctioning. (2, 6)

Unregulated tumour expansion and catecholamine production in PPGLs result from multiple molecular-level abnormalities that affect cell proliferation and survival pathways. Two main molecular pathways are implicated in the pathogenesis of these tumours: the pseudohypoxic pathway and the kinase signalling pathway. (3, 7) Activation of these pathways shapes the overall tumour phenotype and determines factors such as oxygen-sensing mechanisms, the extent of angiogenesis, and the level of aberrant intracellular signalling.

In the upregulation of the pseudohypoxic pathway (i.e., “cluster 1”), mutations that alter cellular responses to oxygen availability (primarily hypoxia) are associated with tumour development. These mutations promote hypoxia-inducible factors (HIFs), transcription factors that promote cell survival, angiogenesis, and metabolic adaptation under low-oxygen conditions. Elevated HIF activity, even at normal oxygen levels, promotes tumour growth and catecholamine synthesis. (8, 9) Although HIFs are normally degraded under normoxic conditions (9), certain mutations cause them to persist, thereby simulating a hypoxic environment and promoting unchecked growth as well as byproduct synthesis. Mutations in the *VHL* gene interfere with the

normal degradation of HIFs, allowing for a persistent pseudohypoxic state facilitative to tumour initiation and progression, while *SDHx* gene mutations disrupt mitochondrial function by allowing succinate to accumulate, which also stabilises HIFs and perpetuates abnormal cellular proliferation. (3, 4) Through these mechanisms, the pseudohypoxic pathway establishes a metabolic milieu favourable to tumour evolution.

The kinase signalling pathway (i.e., “cluster 2”) involves mutations in genes that regulate intracellular signalling cascades, driving excessive cell replication and survival. Among the most common genetic contributors are the *RET* and *NF1* genes. (3, 4, 7) *RET* encodes a receptor tyrosine kinase that, when mutated to confer gain-of-function changes, activates downstream signalling modules, such as the PI3K/AKT/mTOR and RAS/RAF/MEK/ERK pathways, all of which enhance cellular growth and protect against apoptosis. (10) *NF1* mutations, on the other hand, eliminate or diminish the tumour-suppressive activity of neurofibromin, which serves as a negative regulator of the Ras oncoprotein. (4) The loss of neurofibromin-mediated Ras inactivation promotes continuous engagement of the MAPK/ERK signalling cascade, thereby sustaining proliferation and contributing to tumourigenesis.

1.1.2. Inherited syndromes

Due to their association with genetic disturbances, PPGLs may also arise as part of familial cases. In contrast to sporadic cases, it is estimated that up to 40% of PPGLs can be linked to inherited patterns of pathogenesis. (3, 4)

Multiple endocrine neoplasia type 2 (MEN2) is one of the primary syndromes associated with PPGLs. MEN2 is caused by germline mutations in the *RET* protooncogene. (11) MEN2 is subdivided into MEN2A, MEN2B, and familial medullary thyroid carcinoma (FMTC) syndromes. (6) The hallmark of all MEN2 syndromes is medullary thyroid carcinoma (MTC), which is present in nearly all patients and often manifests earlier than pheochromocytomas. (4, 6) PPGLs in

MEN2 are located within the adrenal medulla and are bilateral in around 2/3 of cases. (6) MEN2A is also characterised by parathyroid hyperplasia, whereas MEN2B is associated by marfanoid habitus and mucosal neurinomas.

Von Hippel-Lindau (VHL) disease is an autosomal dominant hereditary condition associated with PPGLs. This syndrome is caused by mutations in the *VHL* gene, a tumour suppressor that downregulates HIFs under normal conditions. In VHL, PPGLs occur in approximately 10–25% of cases, typically as adrenal phaeochromocytomas and tend to secrete demethylated (noradrenergic) catecholamines (i.e., norepinephrine and normetanephrine). (4, 6) These phaeochromocytomas are bilateral in 43.5% of the cases, while PGLs can be found in approximately 1/7 of patients. (6)

Neurofibromatosis type 1 (NF1) is an autosomal dominant inherited syndrome caused by a mutated *NF1* gene which upregulates the oncogenic MAPK/ERK pathway. NF1 primarily manifests with multiple cutaneous neurofibromas, café-au-lait spots, and optic pathway gliomas, while PPGLs occur in approximately 3% of patients with NF1, usually as unilateral adrenal phaeochromocytomas. (3, 6, 12, 13)

Hereditary paraganglioma-pheochromocytoma syndromes, caused by mutations in the succinate dehydrogenase (*SDHx*) genes, represent a group of syndromes with distinct patterns of tumour location and risk for malignancy. Mutations in genes encoding SDH subunits (*SDHA*, *SDHB*, *SDHC*, *SDHD*) and the SDH assembly factor *SDHAF2* lead to loss of mitochondrial complex II function, causing accumulation of succinate and activation of hypoxia pathways (3, 14). These tumours are in most cases extra-adrenal. *SDHB* mutations are associated with an increased risk of malignancy (6, 15–17) and typically involve functioning sympathetic paragangliomas. On the other hand, *SDHD*-associated tumours often occur in the head and neck and are commonly nonfunctioning. *SDHD* mutations are maternally imprinted, meaning that clinical disease typically manifests only if the mutation is inherited from the father (18). *SDHAF2*, *SDHC*, and *SDHA* mutations are rare and generally associated with benign head and neck PGLs (HNPG). (3, 6)

1.1.3. Clinical manifestations

Typical clinical manifestations of PPGLs result from the excessive production of catecholamines (predominantly norepinephrine and epinephrine), which promote a spectrum of symptoms associated with heightened sympathetic nervous system activity. Common symptoms include the classic triad: headache, excessive sweating (diaphoresis), and palpitations, each potentially occurring in isolation or concurrently. However, most patients do not present with all three symptoms of the triad. (19, 20) Various triggers for the increased catecholamine secretion from PPGLs have been identified, including physical exertion, acute psychological stress, postural changes, and minor activities which increase the intraabdominal pressure. (21) These typically present as paroxysmal episodes (“spells”), during which patients experience an abrupt onset of symptoms that can dissipate within minutes or persist for several hours before resolving spontaneously.

Among the most significant manifestations of PPGLs is hypertension, which may take multiple clinical forms. (19, 21) In approximately half of the patients, blood pressure elevations manifest episodically and may coincide with sympathetic spells or produce intermittent but possibly severe hypertensive crises. (19, 20) Certain patients exhibit chronic and sustained elevations in blood pressure that are often resistant to standard antihypertensive regimens. Less frequently, patients may occasionally experience orthostatic hypotension, arising from α -receptor downregulation that occurs secondary to prolonged exposure to elevated catecholamine levels, thereby leading to impaired vascular responsiveness upon standing. (22, 23) Cardiovascular complications extend beyond blood pressure malregulation, as tachycardia, arrhythmias, and in extreme instances, coronary vasospasm could be induced (19), as it has been shown that catecholamine-associated haemodynamic stressors can elevate myocardial oxygen demands and even precipitate stress-induced (takotsubo) cardiomyopathy. (24-27)

PPGLs may also exert their effects on a range of gastrointestinal, neurological, and psychiatric symptoms, likewise attributable to excessive sympathetic drive and

fluctuations in circulating catecholamines. Neurological manifestations may include anxiety, tremors, and restlessness and occasionally mimic panic attacks or generalised anxiety disorders, thus further complicating initial clinical evaluation, whereas the resulting insomnia and emotional lability can further impair quality of life. (19, 21, 28, 29) Therefore, a high index of suspicion should be maintained due to the overlap between PPGL-induced psychiatric presentations and primary psychiatric disorders, especially in individuals whose symptoms are coupled with the previously described autonomic findings.

It must be noted, however, that not all PPGLs secrete clinically relevant quantities of catecholamines. Tumours classified as nonfunctioning (NF-PPGLs) consist primarily of PGLs (located specifically in the head and neck region), although any type of these neuroendocrine tumours can present as either functioning or nonfunctioning. (20) NF-PPGLs may either produce negligible amounts of catecholamines or fail to synthesise them at all. Consequently, patients with NF-PPGLs usually lack the classic symptom constellation of catecholamine excess and, as such, these tumours are often diagnosed incidentally through imaging performed for unrelated indications or by exerting a mass effect on adjacent organs in the cases of large tumours. In these scenarios, the clinical presentation may centre on compressive symptoms (e.g., abdominal discomfort, urinary obstruction, or other site-specific complaints) rather than episodic autonomic disturbances. (20) As NF-PPGLs remain asymptomatic from a catecholamine perspective, they pose specific challenges in the diagnostic context and may be discovered at more advanced stages compared to their functioning counterparts. (30)

1.1.4. Diagnosis

The diagnostic approach to PPGLs involves biochemical testing and imaging with the aim of confirming excess catecholamine production and localising the tumour, respectively. Due to potential heredity, performing genetic assessment may influence further management.

The gold standard for diagnosing functioning PPGL is biochemical testing to detect elevated catecholamines or their metabolites. As catecholamine secretion can be episodic, specific measurement of their *stable* metabolites is essential for accurate diagnosis; therefore, measurement of plasma-free metanephrine and normetanephrine (with blood samples taken in supine position) is the most sensitive test (31), as these metabolites are continuously produced by the breakdown of catecholamines within the tumour. The high sensitivity of plasma-free (nor)metanephrines (approximately 99%) (32) makes it the preferred initial screening method, especially in cases where low-level catecholamine secretion is expected (e.g. asymptomatic disease, multiple/small tumours, positive family history). For patients where plasma testing is impractical or in cases where further confirmation is needed, 24-hour urinary measurements of fractionated catecholamines can be used. (19, 32) Mild elevations may be observed in other conditions (e.g., stress, blood sampling in seated position) and require careful clinical correlation. It must be noted that some medications (including tricyclic antidepressants, adrenergic agonists, and levodopa, among others) can interfere with assays.

3-methoxytyramine (3-MT) is a metabolite of dopamine formed through methylation by catechol-O-methyltransferase (COMT). Plasma 3-MT measurement is clinically useful for detecting rare dopamine-producing PPGLs by complementing standard catecholamine biochemical testing and increasing sensitivity from 22.1% to 50.0% and from 97.2% to 98.6% for HNPGL and PPGL detection, respectively. (33)

Computed tomography (CT) is used for proper localisation of both adrenal and extra-adrenal tumours. It has high sensitivity for detecting adrenal phaeochromocytomas, while its sensitivity decreases for small or extra-adrenal tumours (34). The protocol

for assessing adrenal masses includes a non-contrast (native) CT scan, followed by intravenous contrast administration if the benign nature of the mass cannot be confirmed. Magnetic resonance imaging (MRI) is an alternative to CT and is particularly useful for patients with allergy to intravenous contrast (iodine) agents or with contraindications to ionising radiation. Furthermore, MRI is most sensitive for imaging HNPGL due to its superior soft tissue resolution. (16, 35)

Positron emission tomography (PET) using ^{68}Ga -DOTATATE (DOTA-[Tyr³]-octreotate) and ^{18}F -FDG (fluorodeoxyglucose), as well as single-photon emission computed tomography (SPECT) using ^{123}I -MIBG (metaiodobenzylguanidine), are used for detecting PPGLs. Selection and performance of these imaging modalities is affected by tumour differentiation, catecholamine storage, expression of receptors, and tumour's metabolic activity. ^{68}Ga -DOTATATE PET targets somatostatin receptor expression and has recently shown excellent results in PPGL imaging. (36) It is particularly effective for detecting tumours with *SDHD/SDHC* mutations, i.e. well-differentiated, localised PPGLs and HNPGLs due to their high somatostatin receptor density, but also for metastatic disease. (19, 36, 37) ^{111}In -octreotide, another tracer which also targets somatostatin receptors, is occasionally used, but has moderate sensitivity (65–75% for PCCs, 94% for PGLs) and is generally inferior to ^{68}Ga -DOTATATE PET due to its lower resolution. (19, 38) ^{123}I -MIBG SPECT, which relies on catecholamine transport and vesicular storage, may be used as a method for functional adrenal pheochromocytomas, with 85–100% sensitivity in these tumours (38), although with variable performance in impaired catecholamine storage. Additionally, normal adrenal glands can take up ^{123}I and therefore lead to false-positive findings. (19, 38, 39) ^{18}F -FDG is a less specific tracer which reflects glucose metabolism via glycolysis, and is therefore superior for aggressive, metastatic or *SDHB*-mutated PPGLs (40), which show high glycolytic activity. It outperforms both MIBG and CT/MRI for metastatic disease detection (approximately 75–85% sensitivity for PGLs and malignant PCCs). (19, 38, 41, 42)

Due to the relatively high probability (approximately 40%) that a PPGL patient has a hereditary syndrome (3, 4), genetic testing for mutations in *RET*, *VHL*, and any of the *SDHx* genes is recommended for patients with PPGLs. (16, 43, 44)

1.1.5. Management

The only definitive treatment for PPGLs is surgical resection of the tumour. (2-4, 45) For patients with a confirmed diagnosis, preoperative medical management is initiated and should be based on sequential α - and β -adrenergic blockades.

At least one week prior to surgery, the α -blockade is initiated for blood pressure regulation. Selective α_1 -antiadrenergic drugs are preferred, such as doxazosin, but a nonspecific α -blocking agent such as phenoxybenzamine can also be used. Patients are also encouraged to start a high sodium diet to help with volume expansion and to prevent potential orthostatic side effects. Only after an adequate α -blockade has been achieved, the β -blockade can be started to control the tachycardia, commonly by using selective β_1 -antagonists such as metoprolol. (45, 46)

A laparoscopic or laparotomic approach is used for localised phaeochromocytomas and abdominal PGLs, while PGLs located in other regions require specialised approaches. In patients with hereditary phaeochromocytomas, a bilateral cortex-sparing adrenalectomy can be performed. (16, 40)

Metastatic disease can be cured only if all tumours are resectable; in all other cases, the management is oriented towards management of symptoms and systemic therapy (by ^{131}I -MIBG ablation or chemotherapeutic agents). (47) The assessment of immunotherapy, particularly therapies targeting programmed cell death protein 1 (PD-1) and its ligand (PD-L1) in the treatment of PPGLs is currently under investigation.

Postoperative follow-up surveillance should be individually based on multiple factors, including genetic background and biochemical activity of the disease. (45)

1.2. Brown adipose tissue

Adipose tissue in humans and other mammals can be categorised into two primary subtypes: white (WAT) and brown adipose tissue (BAT). WAT predominantly serves as an energy reservoir by sequestering surplus dietary calories in the form of triglycerides. (48) Beyond its storage capacity, WAT operates as an active endocrine organ, releasing cytokines and other signalling molecules that modulate energy metabolism and assist in maintaining overall physiological homeostasis. (49, 50) BAT, in contrast, is specialised for thermogenesis, with this activity being linked to elevated mitochondrial density and the expression of uncoupling protein-1 (UCP1), which facilitates heat production independent of adenosine triphosphate (ATP) synthesis. (49, 51) Although adult humans primarily produce heat via shivering mechanisms, the thermogenic role of BAT is vital in neonatal mammals (including human neonates), where heat production is necessary to counteract heat loss and preserve core body temperature in the context of underdeveloped muscular system. (52-54) Similarly, hibernating species rely on BAT's capacity for rapid heat generation to endure extended periods of reduced ambient temperatures. Notwithstanding its relevance in neonates and hibernators, BAT also persists in adult humans, albeit in smaller quantities. (55)

During the early stages of human development, BAT predominantly localises to specific anatomical regions, such as the neck, mediastinum, axilla, and retroperitoneum. (56) As individuals progress through childhood and into adolescence, the quantity of BAT in these depots tends to decrease and reflect reduced thermogenic demands and shifts in metabolic regulation. (56, 57) Nevertheless, residual BAT may remain dispersed in various sites with retained capacity to undergo thermogenic activation under particular physiological and pathological conditions. The regulation of BAT mass and function in later life appears to be influenced by various endocrine signals.

1.2.1. Catecholamine-mediated activation

Of all the potential stimuli for BAT activation, catecholamines are best described. Norepinephrine, which is released from sympathetic neurons, binds to the β_3 -adrenergic receptors on brown adipocytes. (58) This binding of norepinephrine with its receptor triggers a signalling pathway that activates adenylyl cyclase, leading to the production of cyclic adenosine monophosphate (cAMP). As cAMP levels increase, protein kinase A (PKA) is stimulated, which then phosphorylates hormone-sensitive lipase and perilipin. (52) Phosphorylation of these proteins enhances lipolysis by releasing free fatty acids that serve as substrates for thermogenesis, but also for activation of uncoupling protein-1. (52, 59, 60) Concurrently, PKA activation induces the transcription of thermogenic genes, upregulating *UCP1*.

Upon activation, *UCP1* acts as a proton channel, which enables protons to re-enter the mitochondrial matrix independently of ATP synthase. This process disrupts the coupling between oxidative phosphorylation and ATP production, which then dissipates the proton gradient as heat instead of utilising it for ATP production. (60, 61) This process is also known as non-shivering thermogenesis and is further augmented by an increased glucose uptake.

Beyond classical BAT activation, the process of “WAT browning”, which implies the conversion of white adipocytes into brown adipocyte-like cells, has recently gained attention. This process leads to the emergence of “beige” adipocytes within WAT, which exhibit key features usually associated with brown adipocytes, including multilocular lipid droplets and high mitochondrial content, and express *UCP1*. (62) Unlike classical brown adipocytes, however, beige adipocytes arise within WAT in response to external stimuli rather than being developmentally programmed as BAT. (3, 63, 64)

Moreover, while β_3 -adrenoreceptors are traditionally considered the primary subtype in BAT, recent *in vitro* studies suggest that β_2 -adrenoreceptors may also contribute significantly to increased BAT activity in humans. (65, 66)

1.2.2. *Regulatory factors*

A potent activator of human BAT is cold exposure via the sequence of the aforementioned, norepinephrine-mediated UCP1 upregulation. Upon sensing a drop in ambient temperature, thermoregulatory centres in the hypothalamus increase sympathetic stimulation to brown adipocytes. It has been shown that the extent of BAT activation is inversely correlated with outdoor temperature and body fat percentage, suggesting that individuals with lower body fat may rely more on BAT for thermoregulation. (67, 68)

However, beside the direct effects of circulating catecholamines, several physiological factors—including ambient temperature, dietary inputs, and overall energy status—as well as different hormone-associated signalling, can modulate BAT activity. This does not necessarily imply their *independent* ability to regulate BAT, but rather indicate a potential overlap with the catecholamine-signalling cascade.

Thyroid hormones, particularly triiodothyronine (T_3), synergise with adrenergic signalling to enhance BAT thermogenesis. T_3 acts through nuclear thyroid hormone receptors (TRs), with TR- α linking sympathetic nervous system with thyroid hormone signalling, while TR- β regulates UCP1 transcription. (69-71) Deiodinase type 2, expressed in brown adipocytes, converts thyroxine (T_4) to the more active T_3 , increasing local T_3 concentrations and amplifying the thermogenic response. (69)

Insulin signalling is also associated with BAT activation and thermogenesis. Cold exposure enhances insulin sensitivity in BAT, upregulating components of the insulin receptor signalling pathway. (72) As the increased insulin sensitivity facilitates glucose uptake and utilisation by brown adipocytes, it provides additional means for thermogenesis. (72, 73) Additionally, the PI3K/Akt pathway, when activated by insulin, intersects with adrenergic signalling to regulate BAT metabolism as cold exposure increases Akt phosphorylation, thereby also stimulating glucose uptake and promoting expression of thermogenic genes (72).

Capsaicin, which can be found in chili peppers, stimulating the sympathetic nervous system by activating the transient receptor potential vanilloid-1 (TRPV1) channels,

and consequently stimulates BAT thermogenesis. (74, 75) Other bioactive substances like resveratrol, curcumin, tea caffeine and catechins, menthol, and omega-3 fatty acids are being increasingly implied to be activating BAT. (75-78) Because of their tendency to stimulate sympathetic response, any of the mentioned dietary factors can work synergistically with catecholamine signalling and amplify the overall thermogenic response.

Furthermore, like WAT, BAT is also known to secrete cytokines (brown adipokines, “batokines”) that regulate energy expenditure via autocrine, paracrine, and endocrine mechanisms. (79) The brown adipocyte secretome includes both peptidic and non-peptidic molecules, including fibroblast growth factor 21 (FGF21), T_3 , and microRNAs (among others), which contribute to BAT remodelling and its ability to meet thermogenic needs. (79-81)

The central nervous system, particularly the hypothalamus, serves as an integration centre for multiple physiological signals affecting BAT activity. (82, 83) The hypothalamus processes information about ambient temperature and energy balance to coordinate an appropriate thermoregulatory response. (84) This integration can modulate sympathetic outflow to BAT and affect the catecholamine-driven activation. Leptin, an adipokine that signals energy sufficiency, acts on the hypothalamus by increasing sympathetic activity to BAT, effectively regulating BAT thermogenesis. (85)

Circadian rhythms have also shown association with BAT activation, with studies showing diurnal variations in BAT activity. BAT exhibits both circadian and circannual (seasonal) rhythms in its thermogenic activity, which are regulated by genetic and endocrine mechanisms. (86) In humans, non-shivering thermogenesis and fat oxidation in BAT are more pronounced in the morning than in the evening. (87)

1.2.3. Detection

FDG-PET imaging, as mentioned in the previous chapter, is commonly used for detecting abnormally metabolically active tissues, and can therefore incidentally reveal aBAT due to its high glucose uptake—often presenting as areas of intense FDG accumulation that may be mistaken for malignancy and lead to false-positive reporting of tumours. (88) This phenomenon has important diagnostic implications in patients with PPGLs as the adrenergic stimulation associated with PPGLs promotes BAT activation and subsequent FDG uptake, leading to aBAT as an incidental finding on PET imaging in these patients. This is particularly relevant as FDG-PET in these patients is typically used when aggressive disease is suspected. (40)

Research on FDG-PET imaging in patients with PPGL has reported aBAT detection, correlating with elevated plasma catecholamine levels. However, no clear association has been established between aBAT incidence and specific germline mutations within PPGL patients, though one study indicated that aBAT presence might be linked to poorer survival outcomes. (89) The propensity of aBAT to show up on FDG-PET, particularly in cases of catecholamine excess, emphasises the need for standardised imaging criteria and diagnostic cut-offs to differentiate between true tumour tissue and aBAT in clinical settings. Currently, the standardised uptake value (SUV) cut-off for aBAT identification varies, though it is often set between 1.0 and 2.0, with some PPGL studies employing a threshold of > 1.5 . (89, 90) Despite these guidelines, the relationship between aBAT and PPGL remains underexplored, and there is minimal consensus on its precise clinical significance.

In addition to diagnostic challenges, a deeper understanding of the aBAT and PPGL relationship could offer better understanding of the potential prognostic value of aBAT detection. However, not much is known from sources above primary research about the precise relationship of aBAT with PPGL and catecholamine levels. To the best of our knowledge, there has been only one brief narrative review (91) covering this area: it included 3 original research studies, with a conclusion that on FDG-PET, the aBAT detection rate was 27.4% in a pooled cohort of 146 patients (compared to

6.1% in patients with no evidence of PPGL) with no formal meta-analysis performed. The limited available research hints at a potential association between aBAT incidence and the severity of catecholamine excess, yet many questions remain about whether aBAT could serve as a marker for tumour burden, metabolic dysfunction, or adverse outcomes in patients with PPGL.

Our study aims to expand the current knowledge pool related to aBAT and its association with PPGLs, investigating its prevalence, biochemical associations, and clinical implications. By performing an observational cohort study, we hope to clarify how aBAT detection correlates with patient characteristics, biochemical markers, tumour characteristics, and survival outcomes. Afterwards, through analysing existing literature and performing a comprehensive systematic review of original research studies further quantified using meta-analysis, we aim to raise the evidence of these findings through the inclusion of previously conducted research along with our original research.

Ultimately, our goal is to determine whether aBAT could serve as a meaningful clinical indicator to aid in prognostication and potentially even guide therapeutic approaches for patients with PPGL.

2. Cohort study

2.1. Methods

We conducted a retrospective observational study across a single tertiary academic institution (King's College Hospital NHS Foundation Trust, London, United Kingdom), evaluating the presence of aBAT in patients who had undergone FDG-PET imaging for suspected PPGL. The selection criteria for FDG-PET included patients with presumed disseminated or extra-adrenal disease, or those with intermediate lesions based on strong clinical or radiological suspicion (e.g., findings on CT imaging). These cases were reviewed in adrenal multidisciplinary team meetings, where the indication for FDG-PET was determined. Guideline recommendations for imaging in PPGL were followed (40).

2.1.1. Patient characteristics and clinical assessment

The following data were collected for each included PPGL patient: demographics, baseline biochemistry (plasma metanephrine [pmol/L], normetanephrine [pmol/L], 3-methoxytyramine [pmol/L]), baseline imaging findings (anatomical location of aBAT, total number of lesions, size of largest lesion, presence of distant metastases), histology, mutational status, treatment modality, Response Evaluation Criteria in Solid Tumours (RECIST) v1.1 criteria response to treatment (92), and progression-free (PFS) and overall survival (OS).

The PPGL patients included had their baseline FDG-PET scans reviewed by two nuclear medicine consultant physicians experienced in FDG-PET CT reporting. Cases were independently scored for the presence of aBAT in predetermined locations (supraclavicular, paravertebral, perirenal). Any discrepant cases were mediated by a third such experienced nuclear medicine consultant physician. Images were transferred from the picture archiving and communication system (PACS) to the HERMES workstation to allow dedicated analysis with SUV quantification. In cases

with multiple scans, we included the first-ever FDG-PET scan that detected active brown adipose tissue in patients with PPGL for our analysis.

2.1.2. Statistical analysis

Continuous data were assessed for normality using the Shapiro–Wilk test. Normal data were expressed as the mean value with its respective standard deviation ($A_r \pm SD$). Non-normal data is presented as the median with interquartile range in square brackets (MED [IQR]). We reported categorical data using ratios and percentages. Missing data within the dataset were imputed using the *missRanger* package (version 2.4.0), employing a random forest algorithm for iterative imputation. The function was iterated 1,000 times, with each random forest consisting of 100 trees.

To investigate the potential association of covariates with the incidence of aBAT, we conducted a multivariate analysis using a logistic regression. The model was fitted with Firth’s bias reduction method to address issues of small sample sizes and rare events. The analysis incorporated pre-defined clinical covariates, while the results were presented as adjusted odds ratios (OR) for each covariate, with their respective 95% confidence intervals (95%–CI) and *P*-values ($\alpha = 0.05$), alongside non-adjusted (crude) ORs. The *logistf* package (version 1.26.0) was used for the multivariate logistic regression analysis. We defined statistically insignificant trends as $P < 0.2$.

To assess statistical significance in difference of observed numerical variables, we implemented an R function for non-parametric bootstrap *P*-value calculation (93) due to relatively small sample size. The function performed iterative resampling (10,000 iterations) to compute t-statistics for two-group comparisons, determining the *P*-value based on the proportion of resampled statistics. Statistical significance of independence of categorical data was tested using Fisher’s exact tests for count data.

We produced Kaplan–Meier plots to compare the OS and PFS times between the investigated and control group. Due to the sample size, the significance of survival differences was assessed using a univariate Cox model.

All analyses were performed in the R statistical software, version 4.4.0 (94).

2.1.3. Ethics

Ethical approval from a Regional Ethical Committee (REC) in the United Kingdom (UK) was not required as the data generated for the purposes of this project were fully anonymised, collected in line with the standard of care protocols for treating patients with PPGL at the King's College Hospital, and are processed and presented retrospectively. The study was discussed within Research Delivery Unit 6 (RDU6) meeting – Renal/Endo Research Group Board (RRGB) at King's College Hospital NHS Foundation Trust (Governance Arrangements for Research Ethics Committees [GafREC]: Endo203). The study is registered with ClinicalTrials.gov, with registration number NCT06440122.

2.2. Results

An initial list of 93 patients with suspected PPGL having undergone FDG-PET imaging was obtained from the nuclear medicine department covering the time period from 2013 to 2021. After exclusion of duplicate patients and reviewing electronic notes for the inclusion of only those with a PPGL diagnosis confirmed after discussion in multidisciplinary team meetings, this list was reduced to 62 patients (22 male, 40 female).

Three cases were excluded at the stage of dedicated analysis/SUV quantification (two cases had corrupted data, one case was not available) and were therefore also excluded from further analyses. Sixty-two cases were subsequently scored. Fifty-four cases (87%) were deemed not to have aBAT (53 initial agreement, one mediation) and 8 cases (13%) were deemed to have aBAT (7 initial agreement, one mediation) (Fig. 1). The cases without aBAT would form the basis of unmatched controls for further statistical analysis. Thus, the final cohort comprised 62 patients, of whom 8 were classified as aBAT-positive and 54 as aBAT-negative.

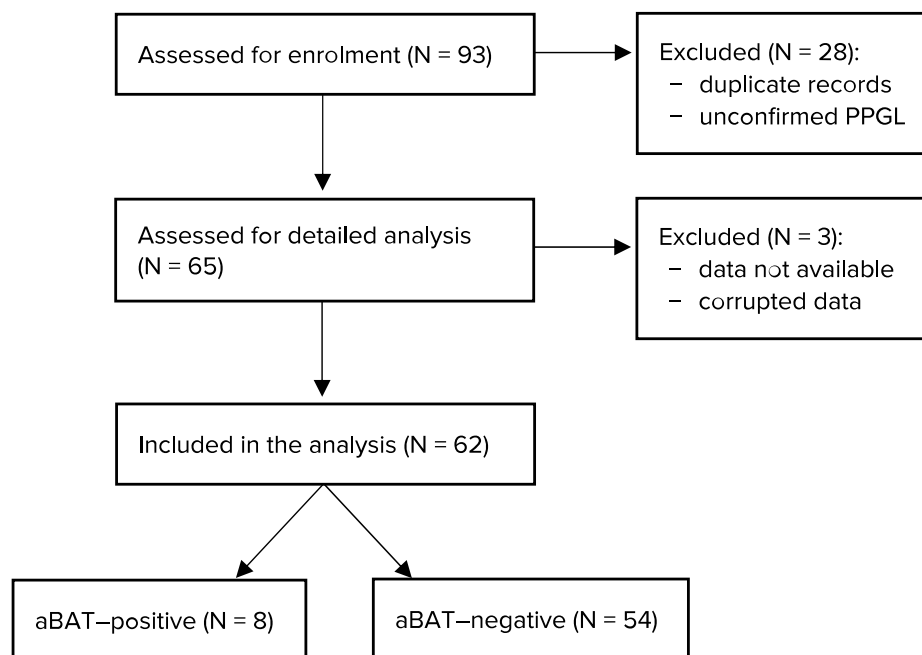


Figure 1. Enrolment and analysis flowchart

The median age was 46.0 years [29.8, 51.0] for aBAT-positive patients and 54.5 years [39.8, 60.8] for aBAT-negative patients ($P = 0.126$). The proportion of females was 87.5% in the aBAT-positive group and 61.1% in the aBAT-negative group, while males accounted for 12.5% and 38.9%, respectively ($P = 0.240$).

In clinical data, the mean body mass index (BMI) was 24.0 ± 6.64 kg/m² in aBAT-positive patients and 25.8 ± 4.82 kg/m² in aBAT-negative patients ($P = 0.548$). Among the aBAT-positive group, the Patient N° 4's BMI was recorded as 12.6 kg/m². Due to concerns about the reliability of this value, we initially included their anthropometric data but encountered difficulties in validating it, despite multiple attempts. While such a low BMI is clinically plausible, we were unable to confirm its accuracy through available clinical notes. To address this, we performed an imputation analysis to evaluate its plausibility in the context of other parameters for this patient and ultimately treated this value as missing data and excluded it from the analysis.

None of the aBAT-positive patients had a history of cardiovascular disease, compared to 24.1% in the aBAT-negative group ($P = 0.186$). Hypertension was observed in 25% of aBAT-positive patients and 53.7% of aBAT-negative patients ($P = 0.255$). The mean number of antihypertensives was 0.389 ± 0.737 for aBAT-positive patients and 0.903 ± 1.090 for aBAT-negative patients ($P = 0.083$). A positive family history was reported in 12.5% of aBAT-positive patients and 11.1% of aBAT-negative patients ($P = 1.000$).

Laboratory parameters revealed a median plasma metanephrine level of 279 pmol/L [202, 913] in aBAT-positive patients, statistically significantly different when compared to 505 pmol/L [169, 1920] in aBAT-negative patients ($P = 0.034$). Plasma normetanephrine levels were 7740 pmol/L [674, 14700] and 2320 pmol/L [1010, 10100] for aBAT-positive and negative patients, respectively ($P = 0.434$). The plasma normetanephrine-to-metanephrine ratio was 14.3 [3.66, 25.90] in aBAT-positive patients and 6.45 [3.03, 17.70] in aBAT-negative patients ($P = 0.472$). Plasma 3-methoxytyramine levels were 131 pmol/L [120, 231] and 120 pmol/L [120, 232] in aBAT-positive and negative patients, respectively ($P = 0.876$).

Regarding imaging and pathology, aBAT-positive patients had an average of 3.90 ± 2.78 aBAT locations, and the highest aBAT SUV_{max} was 5.69 [3.87, 12.70]. Tumour types were distributed as follows: pheochromocytoma in 62.5% of aBAT-positive patients and 63.0% of aBAT-negative patients, and paraganglioma in 37.5% and 37.0%, respectively ($P = 1.000$). The median size of the largest tumour was 57.5 mm [48.7, 70.3] in aBAT-positive patients and 49.5 mm [30.0, 64.3] in aBAT-negative patients ($P = 0.876$). Genetic mutation clusters were distributed as follows: no mutation (50.0% vs 31.5%), cluster 1 (12.5% vs 16.7%), cluster 2 (0% vs 3.7%), and unknown (37.5% vs 48.1%) ($P = 1.000$).

AJCC staging showed a comparable distribution across stages 1 to 4, although aBAT-positive patients had a higher proportion of advanced-stage disease. Specifically, 75% of aBAT-positive patients were classified as stage 3 or 4, compared to 44.4% of aBAT-negative patients, though this difference was not statistically significant ($P = 0.374$).

Treatment modalities included chemotherapy (12.5% in aBAT-positive vs 7.41% in aBAT-negative, $P = 0.511$), surgery (75% vs 85.2%, $P = 0.604$), radiotherapy (0% vs 5.56%, $P = 1.000$), and MIBG therapy (12.5% vs 14.8%, $P = 1.000$).

The results of demographic and clinical data analysis and laboratory, imaging, pathology, treatment, and follow-up information, are also presented in the patient characteristics table (Table 1) with respect to the presence or absence of aBAT. Except for the plasma metanephrine concentration, which was significantly negatively associated with aBAT, the differences in categorical and continuous data between the groups did not reach statistical significance in the univariate analysis.

Table 1. Patient characteristics table

	aBAT-positive (N = 8)	aBAT-negative (N = 54)	P-value
Demographic information			
Age [years]	46.0 [29.8, 51.0]	54.5 [39.8, 60.8]	0.126
Sex			0.240
— Female	7 (87.5%)	33 (61.1%)	
— Male	1 (12.5%)	21 (38.9%)	
Clinical data			
Body mass index [kg/m ²]	25.8 ± 4.82	26.9 ± 5.23	0.548
Prior cardiovascular disease	0 (0%)	13 (24.1%)	0.186
Hypertension	2 (25%)	29 (53.7%)	0.255
Number of antihypertensives	0.389 ± 0.737	0.903 ± 1.090	0.083
— Alpha blockade	0 (0%)	8 (14.81%)	0.581
— Beta blockade	0 (0%)	5 (9.26%)	1.000
Positive family history	1 (12.5%)	6 (11.1%)	1.000
Laboratory parameters			
Plasma metanephrine [pmol/L]	279 [202, 913]	505 [169, 1920]	0.034
Plasma normetanephrine [pmol/L]	7740 [674, 14700]	2320 [1010, 10100]	0.434
Ratio of plasma normetanephrine / metanephrine	14.3 [3.66, 25.90]	6.45 [3.03, 17.70]	0.472
Plasma 3-methoxytyramine [pmol/L]	131 [120, 231]	120 [120, 232]	0.876
Imaging and pathology			
Number of aBAT locations	3.90 ± 2.78	not applicable	
Highest aBAT SUV _{max}	5.69 [3.87, 12.70]	not applicable	
Tumour type			1.000
— Pheochromocytoma	5 (62.5%)	34 (63.0%)	
— Paraganglioma	3 (37.5%)	20 (37.0%)	
Size of largest tumour [mm]	57.5 [48.7, 70.3]	49.5 [30.0, 64.3]	0.876

	aBAT-positive (N = 8)	aBAT-negative (N = 54)	P-value
Cluster			1.000
— No mutation	4 (50.0%)	17 (31.5%)	
— Cluster 1 (<i>SDHx</i> , <i>VHL</i>)	1 (12.5%)	9 (16.7%)	
— Cluster 2 (<i>MEN</i> , <i>RET</i>)	0 (0%)	2 (3.7%)	
— Unknown	3 (37.5%)	26 (48.1%)	
AJCC staging			0.374
— 1	1 (12.5%)	16 (29.6%)	
— 2	1 (12.5%)	14 (25.9%)	
— 3	3 (37.5%)	8 (14.8%)	
— 4	3 (37.5%)	16 (29.6%)	
Metastatic disease	3 (37.5%)	16 (29.6%)	0.692
Treatment			
Chemotherapy	1 (12.5%)	4 (7.41%)	0.511
Surgery	6 (75%)	46 (85.2%)	0.604
Radiotherapy	0 (0%)	3 (5.56%)	1.000
MIBG therapy	1 (12.5%)	8 (14.8%)	1.000
Follow-up			
RECIST v1.1 criteria			0.292
— Complete response (CR)	1 (12.5%)	11 (20.4%)	
— Partial response (PR)	0 (0%)	6 (11.1%)	
— Stable disease (SD)	0 (0%)	2 (3.7%)	
— Progressive disease (PD)	3 (37.5%)	5 (9.3%)	
— No data	4 (50.0%)	30 (55.6%)	
Mortality	2 (25.0%)	12 (22.2%)	1.000
Progression-free survival [months]	41.0 [22.5, 60.0]	36.0 [24.3, 55.3]	0.913
Overall survival [months]	41.0 [23.3, 60.8]	47.5 [32.8, 95.3]	0.136

Legend: aBAT, active brown adipose tissue; SUV_{max} , maximum standardised uptake value; *SDH(x)*, succinate dehydrogenase complex (subunit x); *VHL*, Von Hippel-Lindau; *RET*, “rearranged during transfection”; *MEN*, multiple endocrine neoplasia; *RECIST*, Response Evaluation Criteria in Solid Tumours; *MIBG*, metaiodobenzylguanidine.

Penalised multivariate analysis with multiple clinical covariates indicated that male sex (adjusted OR 0.1; CI 0.00, 1.05), tumour type (adjusted OR 2.10; CI 0.37, 16.41), hypertension (adjusted OR 0.26; CI 0.03, 1.42), and increased plasma metanephrine levels (adjusted OR 0.00; CI 0.00, 1.06) were not significantly associated with the presence of aBAT. In contrast, increased plasma normetanephrine levels (adjusted OR 2.85; CI 1.11, 10.35) showed a statistically significant trend towards aBAT presence, as shown in Fig. 2.

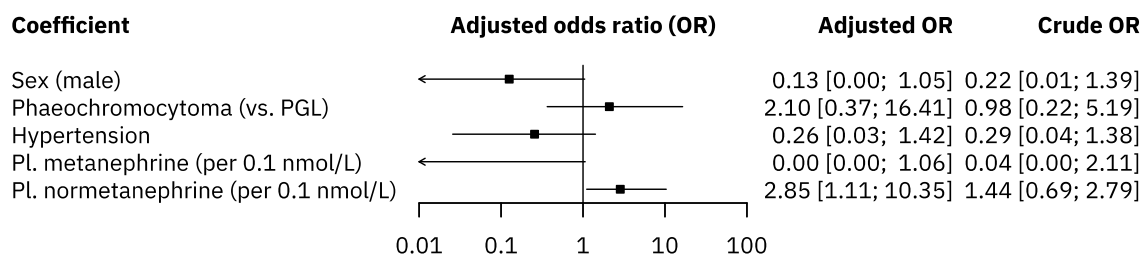


Figure 2. Forest plot showing multivariate adjusted and unadjusted odds ratios of aBAT presence associated with multiple covariates.

During follow-up, RECIST v1.1 criteria outcomes in aBAT-positive versus aBAT-negative patients were complete response (12.5% vs 20.4%), partial response (0% vs 11.1%), stable disease (0% vs 3.7%), progressive disease (37.5% vs 9.3%), and no data (50.0% vs 55.6%) ($P = 0.292$). Overall, mortality rates were 25.0% in aBAT-positive patients and 22.2% in aBAT-negative patients ($P = 1.000$). The median progression-free survival was 41.0 months [22.5, 60.0] in aBAT-positive patients and 36.0 months [24.3, 55.3] in aBAT-negative patients ($P = 0.913$). Overall survival medians were 41.0 months [23.3, 60.8] for aBAT-positive patients and 47.5 months [32.8, 95.3] for aBAT-negative patients ($P = 0.136$).

The univariate Cox proportional hazards model indicated hazard ratios of 1.77 (CI 0.38, 8.18) and 1.38 (CI 0.30, 6.34) for overall and progression-free survival probabilities, respectively. The survival data for both overall and progression-free survival are visually represented using Kaplan–Meier survival curves in Fig. 3.

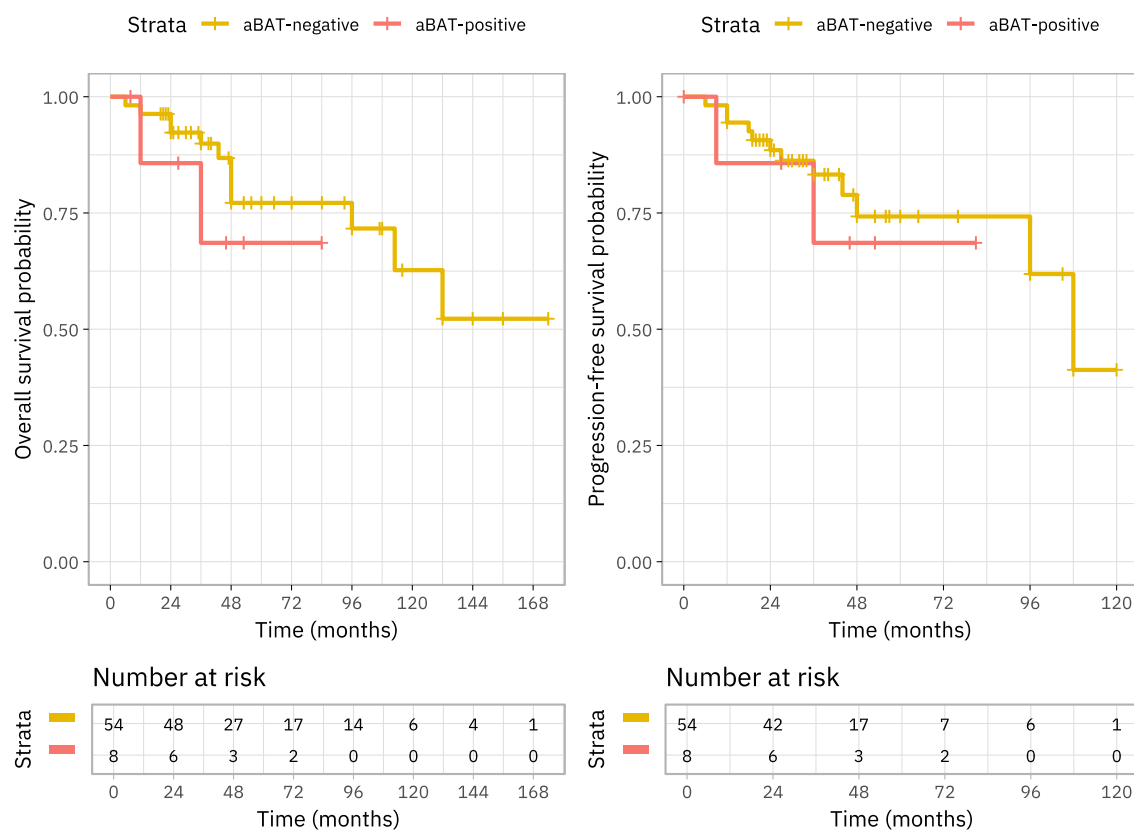


Figure 3. Kaplan–Meier survival plots: (a) Overall survival, (b) Progression-free survival.

While statistically insignificant, the aBAT-positive group showed trends (defined as $P < 0.2$) in association with lower age, absence of prior cardiovascular disease, lower number of antihypertensive medications, and lower overall survival. In our study, although no patients with detectable aBAT were taking adrenoreceptor blockade, we found no statistical association between aBAT and either alpha- or beta-blocking medication ($P = 0.581$ and $P = 1.000$, respectively).

Detailed per-patient data for the aBAT-positive group are reported separately in Table 2.

Table 2. Individual characteristics of patients with aBAT

Patient	1	2	3	4	5	6	7	8
Age	45	29	61	49	28	47	57	30
Sex	F	M	F	F	F	F	F	F
BMI [kg/m ²]	26.2	24.6	28.6	N/A	22.1	35.5	20.8	21.4
Pl. metanephrine [pmol/L]	56	1766	134	224	1966	314	243	629
Pl. normetanephrine [pmol/L]	337	>40000	<109	14476	7945	786	7544	15227
Pl. 3-MT [pmol/L]	142	235	<120	677	<120	<120	<120	229
Hypertension	–	–	–	+	–	+	–	–
Highest SUV _{max}	3.88	10.6	3.39	4.09	23.4	7.29	3.83	18.81
Tumour type	PCC	PCC	PGL	PCC	PCC	PCC	PGL	PGL
Size of largest tumour [mm]	49	71	70	65	46	49	50	86
Family history	–	–	–	–	–	–	–	+
Mutational status	N/A	W/T	N/A	W/T	W/T	N/A	W/T	SDHB
Metastatic disease	–	–	+	+	–	–	–	+
Mortality	–	–	+	+	–	–	–	–
RECIST v1.1	ND	ND	PD	PD	CR	ND	ND	PD

Legend: M, male; F, female; BMI, body mass index; Pl., plasma; 3-MT, 3-methoxytyramine; SUV_{max}, maximum standardised uptake value; PCC, pheochromocytoma; PGL, paraganglioma; N/A, not available; W/T, wild type; SDHB, succinate dehydrogenase complex subunit B; RECIST, Response Evaluation Criteria in Solid Tumours; ND, no data; PD, progressive disease; CR, complete response.

One of our patients in the aBAT-positive cohort had a confirmed diagnosis of MEN2A proceeding to a right adrenalectomy for pheochromocytoma and total thyroidectomy for medullary thyroid carcinoma (MTC); both in 2014 with satisfactory surgical clearance. Areas of aBAT uptake on FDG-PET were retrospectively confirmed (in supraclavicular, paravertebral, perirenal and ‘other’ locations with highest SUV_{max} of 10.6) and correlated with brown adipose tissue on histology specimens (Figures 4, 5, & 6).

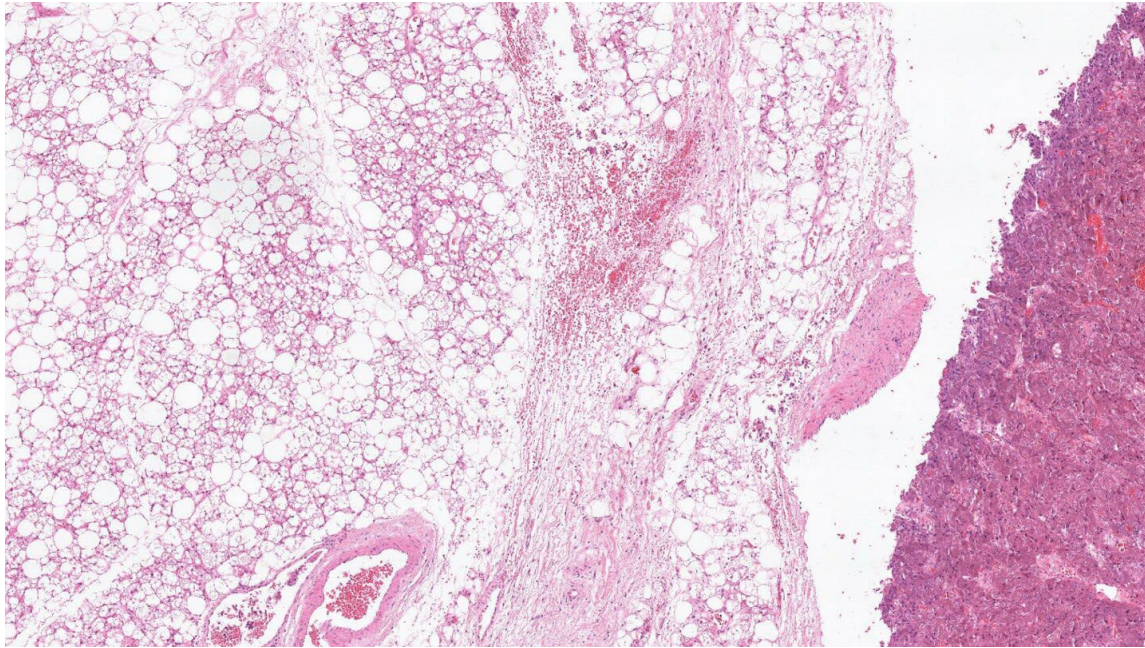


Figure 4. Low magnification image shows phaeochromocytoma to the far right of the image in an aBAT patient from our cohort in a retrospective post-surgical specimen. Brown adipose tissue adjacent to the phaeochromocytoma is seen occupying the left two thirds of the field.

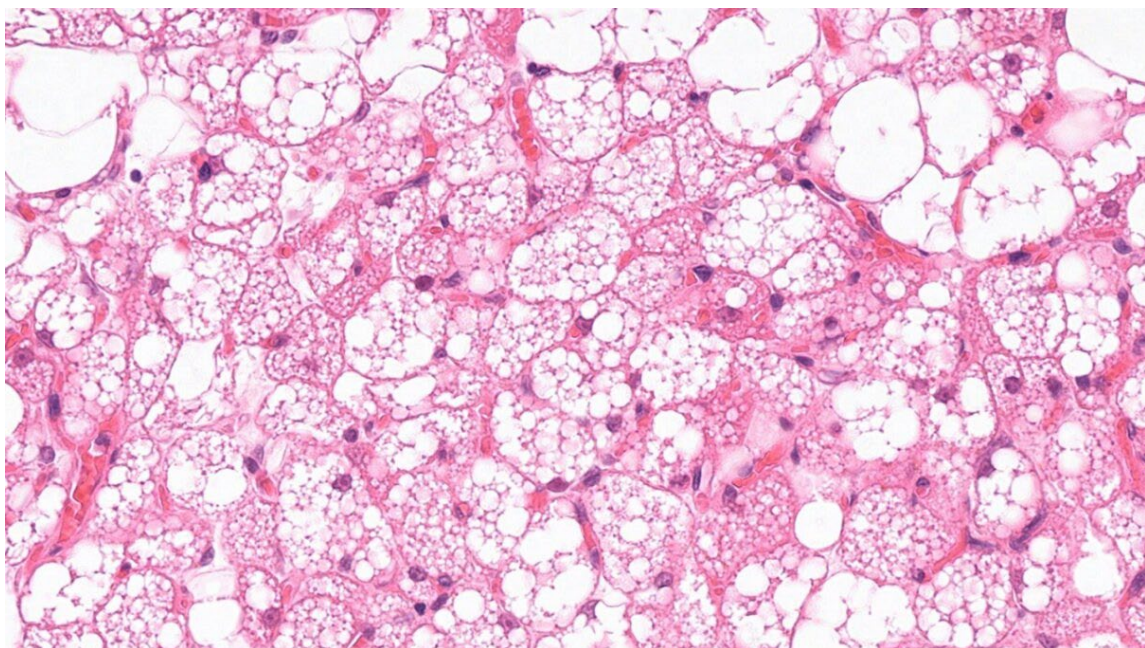


Figure 5. At higher magnification (from Fig. 2), the adipocytes in brown fat show multivacuolated cytoplasm resulting from numerous small lipid droplets. The cytoplasm is acidophilic and granular due to large number of mitochondria. (95) A small number of white fat adipocytes are present in this field for comparison. These have a single intracytoplasmic large fat droplet only.

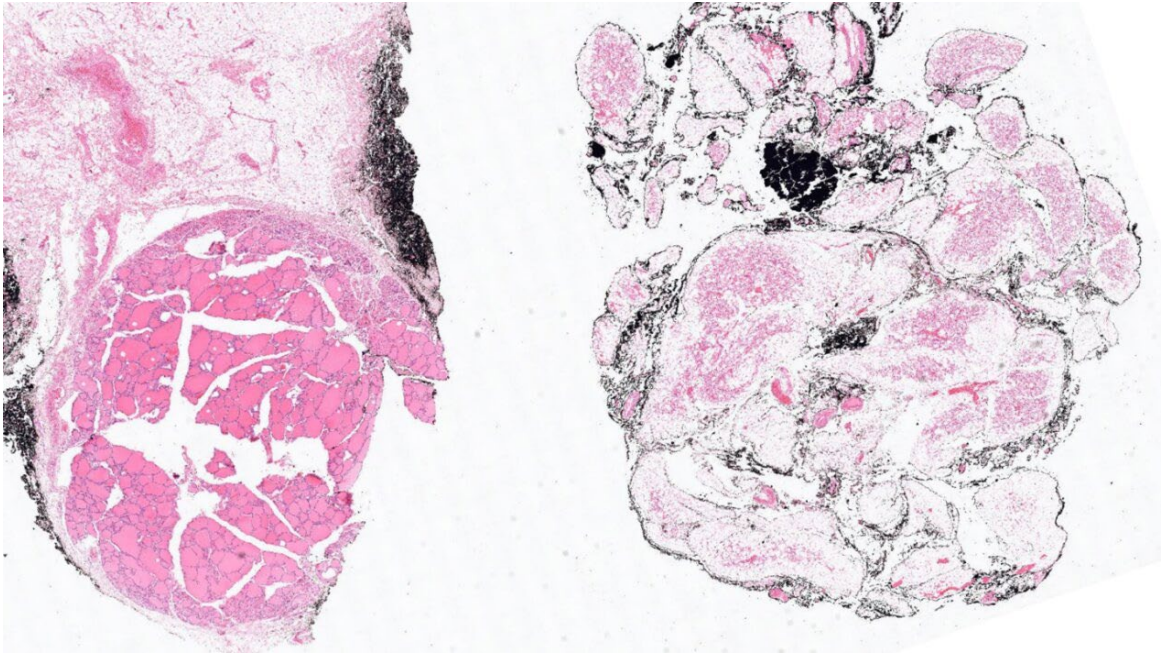


Figure 6. Low magnification shows thyroid tissue on the left-hand side of the field and brown fat in the adjacent right-hand side of the field.

3. Systematic review of literature

3.1. Methods

The design of this study was set as a systematic review and meta-analysis of original research studies. A protocol was created using PICO (population, intervention, control, outcomes) framework and registered in the International Prospective Register of Systematic Reviews (PROSPERO) under the number CRD42021276073 and was conducted based on the Preferred Reporting Items for Systematic Reviews and Meta-Analyses (PRISMA) 2020.

3.1.1. Study eligibility

The review assessed only peer-reviewed publications in English. We used all of the following inclusion criteria:

- All prospective and retrospective studies examining BAT in patients with PPGL (randomised controlled trials [RCTs], observational, cohort, and other).
- Diagnosis of PPGL based on biochemistry, pathognomonic imaging, and/or histology.
- Patients to have completed FDG-PET imaging.

In line with the Cochrane Collaboration's recommendations (96), case reports and case series were excluded from the quantitative synthesis as these reports do not provide denominator data.

3.1.2. Search strategy

The following search key was utilised, with Medical Subject Headings (MeSH) terms in mind:

((brown adipose) OR (brown fat) OR BAT) AND (paragangliom OR phaeo* OR pheo* OR pheochromocytoma OR paraganglioma) AND (fdg OR pet OR (pet ct) OR positron OR (positron emission tomography computed tomography))*

We searched for publications in the following databases: MEDLINE/PubMed, Embase, and SCOPUS. The time frame was set as all studies published from inception until 26 November 2022, with an update check performed on 2 July 2024 in MEDLINE/PubMed, Embase, and SCOPUS. No language filter or any other filters were selected.

3.1.3. Data collection

Afterward, we imported the abstracts extracted from the search into Covidence Systematic Review Software (Veritas Health Innovation, Melbourne, Australia; <https://www.covidence.org>), a systematic review management tool. Two reviewers then independently performed parallel reviews of all selected abstracts for relevance according to our protocol requirements. From these relevant abstracts, full-text reviews were subsequently performed to select the final appropriate eligible studies for inclusion in the systematic review. Any conflicts between reviewers regarding the inclusion or exclusion of any particular study would be decided from the ultimate decision of an assigned third reviewer.

If an article was unavailable, an email was sent to the study authors to request the full text. Additionally, results from our group's own cohort study from a single-centre experience are included in the statistical analysis. The results, however, for the purposes of ensuring transparency and minimise potential bias, the findings will be presented both with and without it, with the excluding subset available in the supplementary material of the systematic review.

3.1.4. Risk of bias assessment

A qualitative assessment using the Quality in Prognostic Studies (QUIPS) tool was performed on all selected studies by two reviewers for the potential risk of bias (RoB) and to help understand the validity of the presented findings. The following 6 domains were assessed and tabulated for each study: study participation, study attrition, prognostic factor measurement, outcome measurement, study confounding, and statistical analysis and reporting. Each domain was discussed and mutually agreed between reviewers as either low, moderate, or high risk of bias, or N/A if not applicable. Any disputes were ultimately decided by an assigned third reviewer.

3.1.5. Statistical analysis

The collected continuous data were initially retrieved into a pre-defined spreadsheet and subsequently pooled into combined groups of metabolites, i.e. normetanephrine with metanephrine, and norepinephrine with epinephrine, using the equations for combining groups described in the Cochrane Handbook for Systematic Reviews of Interventions (96). We used the random-effects model with the inverse variance method and restricted maximum-likelihood (REML) tau-estimation to pool such quantitative data and calculate the summary results based on effect sizes. Subsequently, the results were expressed using forest plots as standardised mean differences (SMD) with respective 95%-confidence intervals (CI). Afterwards, a cumulative meta-analysis, using the chronological criterion, was also performed in order to assess the evolution and trends in the data over time, with results plotted on a cumulative forest plot.

Studies were also analysed using a meta-analysis of proportions with respective 95%-CIs, both as standard and cumulative meta-analytical methods, after each of which a forest plot was generated.

We assessed the statistical heterogeneity using the I^2 statistic for its quantification and the chi-square for the presence of heterogeneity. The heterogeneity

quantification statistic was interpreted as low ($< 30\%$), moderate (30–50%), substantial (50–90%), or considerable (75–100%), according to the Cochrane guidelines. Publication bias was to be assessed using Egger's test of intercept and by visual inspection of funnel plots should the number of selected studies per plot exceed $k = 10$.

All analyses were performed using *R* statistical software (version 4.4.0) (94) and *meta* package (version 7.0.0) (97).

3.2. Results

3.2.1. Search and selection

A total of 145 records were identified through database searches, including MEDLINE (35 records), Embase (59 records), and Scopus (51 records). After the removal of 83 duplicate records, 62 records remained for screening ($\kappa = 1.00$). During the screening phase, 53 records were excluded: 34 were case reports, 12 were reviews, and 7 were excluded for other reasons. Consequently, 9 reports were sought for retrieval, and all 9 reports were successfully retrieved for assessment.

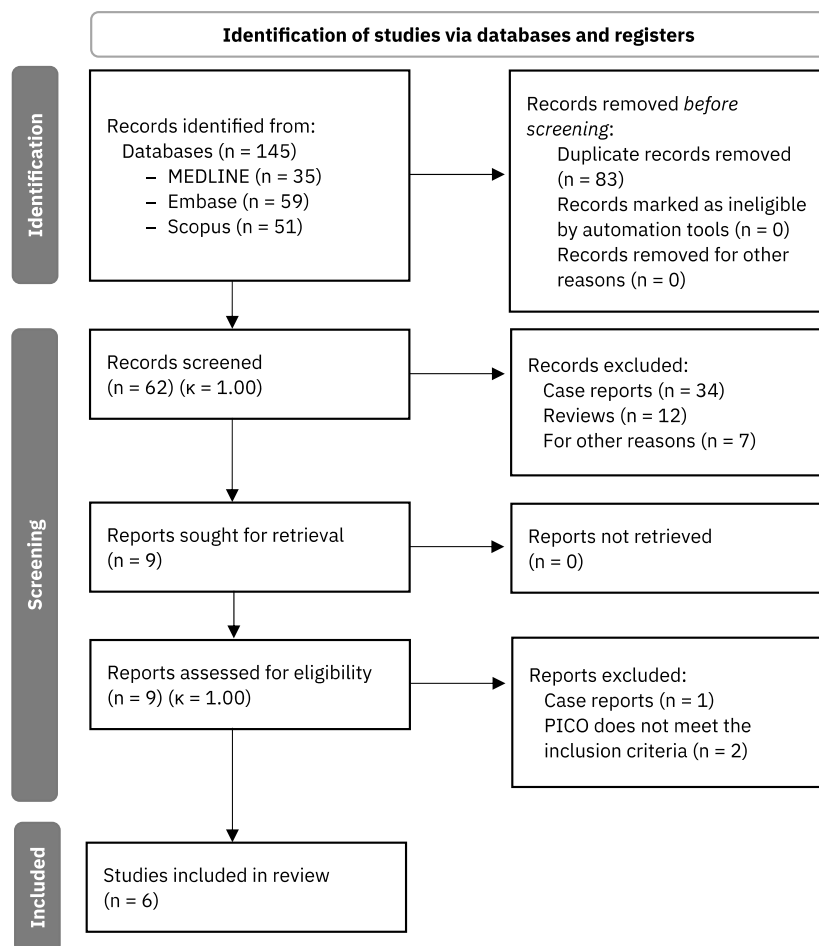


Figure 7. Study selection flowchart

The eligibility assessment included all 9 reports ($\kappa = 1.00$), resulting in the exclusion of 3 reports. Of these, 1 report was excluded as it was a case report, and 2 reports were

excluded because they did not meet the inclusion criteria based on PICO parameters. Ultimately, six studies were included in the review. A flowchart of the process is outlined in Fig. 7.

3.2.2. Risk of bias assessment

At the RoB assessment, we found all studies to be eligible for inclusion in this systematic review. Detailed results of RoB analysis can be found in Table 3 and an overview by QUIPS domains is shown in Fig. 8.

Table 3. Risk of bias assessment of the identified studies

Study	Study participation	Study attrition	Prognostic factor measurement	Outcome measurement	Study confounding	Statistical analysis reporting	Overall risk of bias	Included in the review
Hadi 2007		N/A						Yes
Wang 2011		N/A						Yes
Nagano 2015		N/A						Yes
Puar 2016		N/A						Yes
Sater 2020		N/A						Yes
Mubeen 2022	N/A	N/A	N/A	N/A	N/A	N/A		Yes

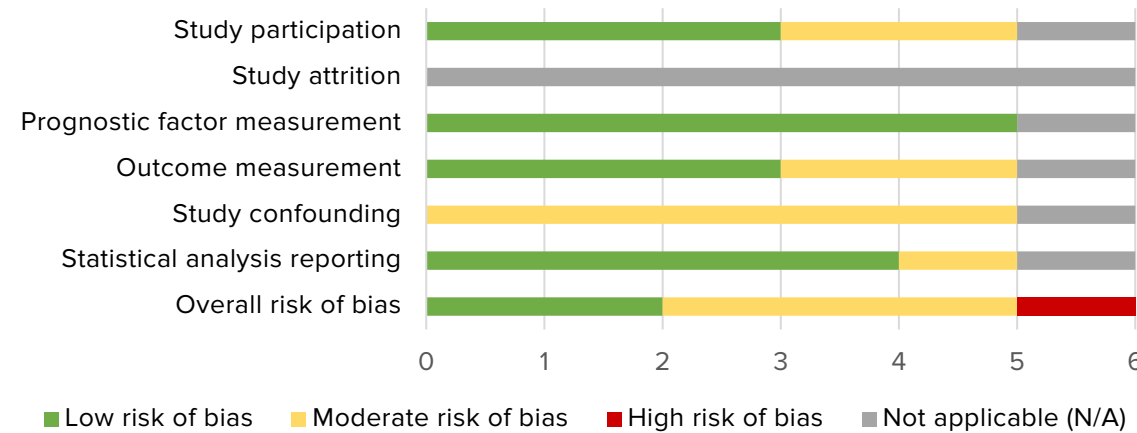


Figure 8. Overview of the risk of bias assessment

3.2.3. Quantitative synthesis

The meta-analysis of pooled data showed a statistically significant positive difference in isolated normetanephrine/norepinephrine (SMD = 0.70; CI 0.37, 1.03) catecholamine levels between the aBAT-positive ($N = 69$) and negative ($N = 210$) groups, with a low level of heterogeneity ($I^2 = 20\%$, $P = 0.29$). Isolated metanephrine/epinephrine levels indicated a negative, albeit statistically insignificant, mean difference between the groups (SMD -0.15; CI -0.47, 0.16). When combined, however, normetanephrine/norepinephrine and metanephrine/epinephrine levels also showed statistically significant positive difference between the aBAT-positive ($N = 67$) and negative ($N = 188$) groups (SMD 0.51; CI 0.18, 0.85) with low, statistically insignificant heterogeneity ($I^2 = 24\%$, $P = 0.26$). Overall, the random-effects meta-analysis indicated a moderate but statistically significant pooled effect size (SMD = 0.40; 95% CI: 0.15, 0.65; $P = 0.0018$). The detailed results are reported in a forest plot (Fig. 9).

The test for overall heterogeneity was statistically significant ($Q = 26.65$, $df = 13$, $P = 0.0139$), indicating a non-negligible inter-study variability that should be accounted for when interpreting the findings. Despite these variations, the directionality of the effect remained consistent across most studies.

After performing a cumulative meta-analysis on the combined groups of metabolites in chronological order, the SMD showed notable variation as new studies were added, with an initial large effect size decreasing and stabilising over time, with initially substantial heterogeneity ($I^2 = 57\%$) reducing over time to low ($I^2 = 24\%$). The addition of data from our study led to a pooled estimate of SMD = 0.51 (95% CI: 0.18, 0.85), with a further reduction in heterogeneity to $I^2 = 24.1\%$. Over time, the confidence interval of the effect size narrowed, and the P -value decreased, despite only one study in isolation reached statistical significance (Figures 9, 10).

The proportion of pheochromocytoma patients who also had aBAT was 26% (CI 20%, 32%), with moderate, albeit statistically insignificant heterogeneity ($I^2 = 32\%$, $P = 0.18$) (Fig. 11). The cumulative meta-analysis showed that inclusion of our study in

assessing the proportion of PPGL patients who also had BAT increased the heterogeneity to low-to-moderate, while the pooled proportion of patients reduced from 28% to 26% (Fig. 12).

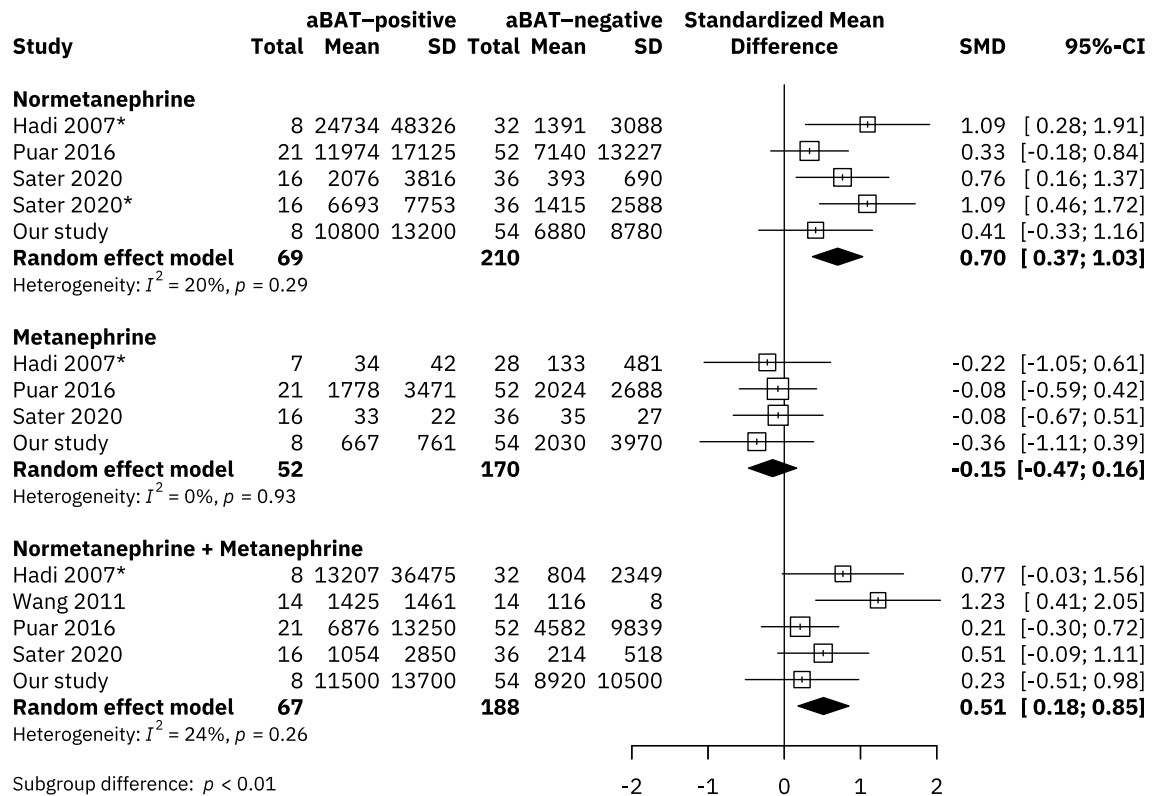


Figure 9. Forest plot showing mean differences in levels of different catecholamines.

* asterisk indicates (nor)epinephrine instead of (nor)metanephrine.

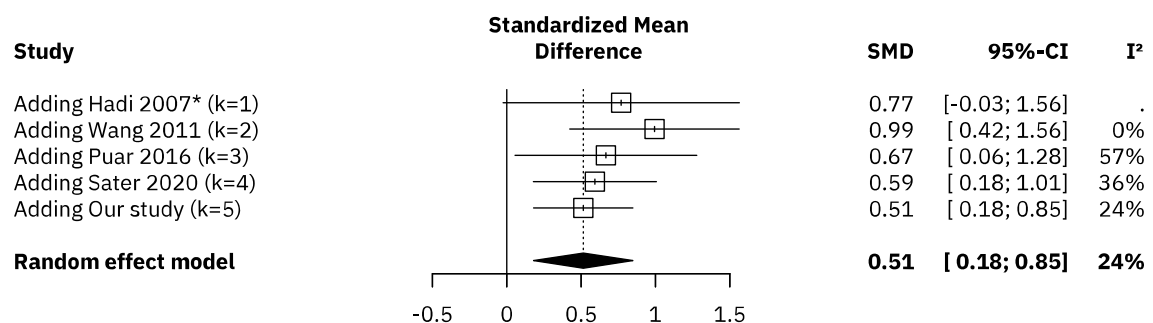


Figure 10. Forest plot of cumulative meta-analysis of catecholamine level means

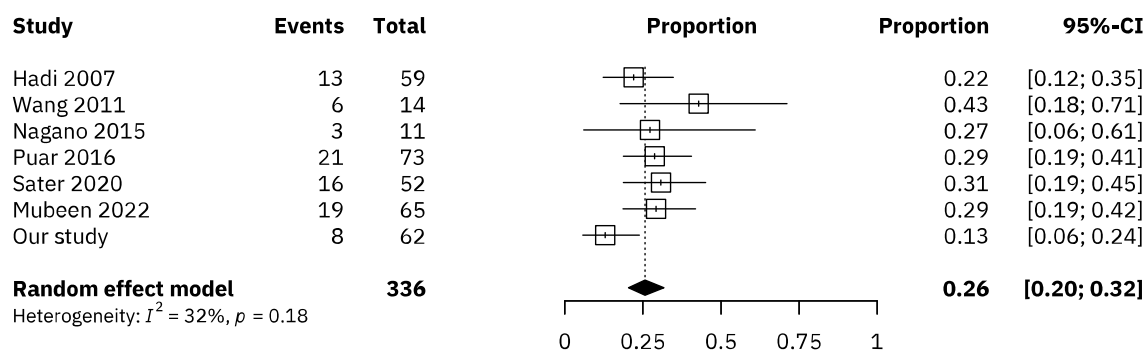


Figure 11. Forest plot showing proportions of patients with PPGL presenting with aBAT

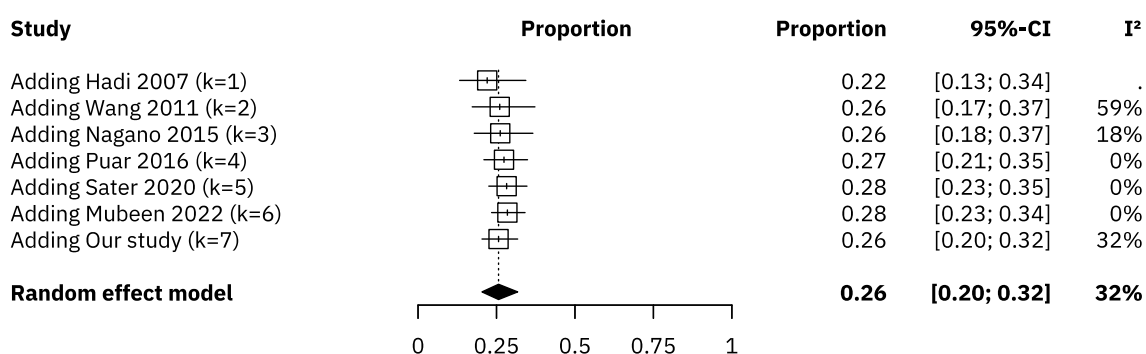


Figure 12. Forest plot of cumulative meta-analysis showing proportions of patients with PPGL presenting with aBAT

3.2.4. Qualitative synthesis

The included studies were primarily conducted on a retrospective basis, with a PPGL diagnosis being made multi-modally. Cohort samples analysed ranged from 28 to 205 patients. The included studies revealed a clear correlation between the elevation of catecholamine tracers and the predisposition to increased BAT activity. For 12 out of 12 patients with non-secreting PPGLs (normal catecholamine assessment) across two studies, BAT activation was absent. (68, 98)

In the study by *Puar et al.* (90), aBAT on FDG-PET was identified by an SUV_{max} value > 1.5 . Three studies analysed SUV_{max} values in their PPGL cohorts displaying aBAT with mean values of 6.7, 4.0 and 4.91, respectively (68, 90, 99). In the study by *Puar et al.*, a subgroup analysis showed that the highest mean SUV_{max} values belonged to those with cluster 1 germline mutations (*VHL*, *SDHx*) compared to cluster 2 (*RET*, *NF1*,

MAX), and sporadic tumours. Nevertheless, this study demonstrated no statistically significant association between germline mutations and the prevalence of BAT activation.

In the study by *Sater et al.* (89), 16 patients were identified with PPGL and concurrent aBAT. Approximately 70% of patients from this cohort were found to have combined cluster 1 or cluster 2 mutations. Kaplan–Meier survival analysis revealed that presence of activated BAT was linked to decreased overall survival when compared to the control group, not expressing aBAT (HRz 5.80, 95% CI, 1.05–32.05; $P = 0.02$) with an associated 5.8-fold increased chance of death attributed to tumour progression. Of note, all deaths (4/4) in the aBAT group from this study were in those with succinate dehydrogenase mutations. Death in the aBAT group was noted to occur at a younger age with markedly higher norepinephrine levels (22.10 ± 8.00 vs $0.48 \pm 0.27 \times ULN$). No other study which was included performed an analysis of mortality in aBAT cohorts.

The studies included in our synthesis revealed a trend toward a lower age at diagnosis in aBAT cohorts as well as an observed inverse relationship between aBAT presence and waist circumference/body mass index (BMI). In comparisons of patients with PPGL and aBAT vs patients with PPGL without aBAT, no significant differences were found in multiple domains, including tumour size, tumour burden, or tumour location. There were also no significant differences found in systolic and diastolic blood pressure, lipid profiles, thyroid function, fasting blood glucose, or gender.

In the study by *Hadi et al.* (99), alternative imaging for activated BAT was reviewed, the only study to do so. They concluded that of 83 patients with PPGL imaged with ^{18}F FDG-PET, 19.2% had aBAT. With those imaged with ^{18}F -6-fluorodopamine (F-DA) PET (67 patients with PPGL), 17.9% had aBAT. F-DA PET images BAT through localisation of sympathetic innervations in these areas in a similar manner to ^{123}I -MIBG.

4. Discussion

The interplay between PPGLs and brown adipose tissue (BAT) represents a complex and evolving area of research, linked together in the context of catecholamine excess. Given that BAT is primarily activated by sympathetic stimulation, its incidental detection on FDG-PET imaging in patients with PPGLs has raised questions about its underlying metabolic interactions, clinical significance, and potential prognostic value. To comprehensively investigate this relationship, we used a dual approach: (1) conducting a retrospective cohort study to assess the prevalence and clinical correlates of BAT activation in PPGL patients, and (2) performing a systematic review with meta-analysis (SR/MA) to integrate our findings with existing literature and previously available data. Our cohort study provided a deeper insight into the association between aBAT and specific biochemical markers (particularly plasma normetanephrine), while the SR/MA allowed us to contextualise these findings within a broader evidence base.

Previous studies reviewing PPGLs have reported on probable BAT activity in patients with PPGL. Specifically, an aBAT prevalence of 7.8% to 42.8% was observed on FDG-PET imaging using less stringent criteria of maximum standardised uptake value (SUV_{max}) cut-offs for aBAT between 1.0 and 2.0; in other cases, activity of BAT was quantified by mean standardised uptake values (SUV_{mean}). (68, 99) We found that 13% of PPGL patients had aBAT positivity on FDG-PET imaging ($N = 8/62$) using a stricter criterion of SUV_{max} cut-off value of 1.5 in line with more recent findings. (89, 90)

However, FDG-PET analysis alone does not confirm BAT, but only suggests its presence due to its correlation with anatomical area of specific metabolic activity. One of our patients in the aBAT-positive cohort with a confirmed diagnosis of MEN2A underwent right adrenalectomy for pheochromocytoma and total thyroidectomy for MTC. BAT adjacent to the pheochromocytoma and MTC was histopathologically confirmed in line with the FDG-PET findings, providing a direct validation of BAT activation.

Regarding the clinical characteristics of patients and BAT activation, several observed differences between the aBAT-positive and aBAT-negative groups in our cohort study did not reach statistical significance but showed trends (defined as $P < 0.2$) suggestive of potentially relevant differences. The lower age (median 46.0 years vs 54.5 years, $P = 0.126$), absence of prior cardiovascular disease (0% vs 24.1%, $P = 0.186$), and lower number of antihypertensive medications (0.389 vs 0.903, $P = 0.083$) in the aBAT-positive group, as well as the higher proportion of advanced AJCC staging (stages 3–4: 75% vs 44.4%, $P = 0.374$) and the lower observed overall survival (median 41.0 months vs 47.5 months, $P = 0.136$), should nevertheless be considered suggestive findings requiring further investigation rather than established associations.

Although age is often considered the strongest determinant of BAT activation (90, 100), it is possible that the limited age range for these patients may not have identified this. In other cohorts with PPGL, multiple domains of patient characteristics were assessed, with no statistically significant differences noted in aBAT patients, including tumour size, burden, and location. Notably, aBAT has been shown to be visualised on other imaging modalities, including F-DA PET (99), due to the likely localisation of sympathetic innervations.

The observed higher proportion of females in the aBAT-positive group (87.5% compared to 61.1% in the aBAT-negative group), although not statistically significant, raises the question of whether sex hormones could play a role in BAT activation in patients with PPGL. Previous research has established that sex hormones significantly influence BAT function and thermogenesis, with energy homeostasis differing between sexes and impacting the development of pathological conditions. (101) Sex hormones may modulate the responsiveness of BAT to adrenergic stimulation, with evidence indicating they play a relevant role in the regulation of BAT activity in both males and females. (101, 102) This sex-based difference in BAT regulation could potentially contribute to the varying presentation of aBAT in PPGL patients and may partially explain the higher prevalence in females observed in our cohort.

It was noticed that the inclusion of our cohort's proportions of patients with PPGL and aBAT in the meta-analysis tends to be on the low side compared to other studies, increasing the heterogeneity of the pooled result. Nevertheless, the cumulative result is changed by only 2 percentage points after its inclusion, indicating that the proportion of patients with PPGL who present with aBAT is stable at around one quarter. Additionally, despite our efforts, we were unable to obtain the *full text* of the study performed by *Mubeen et al.* (103); still, we have included their result because it showed accordance with other reviewed papers.

Our systematic review showed that the average concentrations of demethylated metabolites, prefixed with nor- (i.e., normetanephrine and norepinephrine), were statistically significantly higher in the aBAT-positive groups compared to the aBAT-negative ones, suggesting its potential use in predicting the presence of active brown adipose tissue in patients with PPGLs. Preclinical studies have shown that norepinephrine stimulation of BAT via β_3 -receptors leads to an increased number of brown adipose tissue cells, lipolysis, glucose transportation, UCP1 expression, and ultimately thermogenesis. (90, 104) Significant BAT activation in patients with PPGLs is likely to be due to the systemic effects of catecholamine excess, as reported in previous studies. (90) In our study, average normetanephrine concentration was higher in the aBAT-positive group, which was statistically significant in the multivariate analysis, although this difference did not reach the limit of significance in the univariate analysis of the differences in medians. Plasma metanephrine levels, however, showed statistical significance in the univariate analysis, inversely proportional to the presence of aBAT, indicating a potentially strong preference for increased normetanephrine-to-metanephrine ratio's association with BAT activation. Although norepinephrine is typically associated with both pheochromocytomas and paragangliomas (unlike epinephrine, which is produced only in pheochromocytomas) (105), our study had comparable numbers of patients with pheochromocytomas and paragangliomas associated with activated BAT.

Since aBAT is a highly vascularised and metabolically active tissue, it could facilitate the clearance of circulating catecholamines. It may uptake and metabolise

catecholamines as part of its thermogenic activity, potentially reducing the demethylated catecholamine pool available for conversion into metanephrines. In addition, the aBAT-positive group might represent a subgroup with a distinct hormonal or tumour phenotype leading to an altered catecholamine production or metabolism. In our study, 86% of our patients were deemed to not have aBAT. This raises the question of whether there are other mechanisms of BAT activation beyond sympathetic stimulation and what are the other “browning” factors in PPGL. BAT activation has previously been linked to malignancies (106), and clinical studies have reported characteristic alterations in BAT in patients with cancer. (107) Evidence regarding the role of catecholamine excess in BAT activation in these patients is controversial. The mechanisms underlying dynamic interactions between cancer cells and stromal adipocytes remain unclear. (108) It is generally believed that BAT predominantly expresses β_3 -adrenoreceptors and exhibits enhanced norepinephrine responsiveness compared to WAT. (58) However, *in vitro* experiments indicate that thermogenesis in BAT might primarily be mediated through the stimulation of β_2 -adrenoreceptors. (65) Although no patients with detectable aBAT in our study were taking adrenoreceptor blockade, the lack of statistical association between aBAT and either alpha- or beta-blocking medication ($P = 0.581$, $P = 1.000$, respectively) suggests that these medications were unlikely to confound our findings. However, the possibility of an undetected influence cannot be completely excluded.

The role of catecholamines in tumour progression remains intriguing. Earlier studies have suggested that catecholamines directly affect tumour cell behaviour and gene expression by growth-promoting effects and possible chemotactic activity of norepinephrine-producing organs to recruit tumour cells (adrenal gland and brain are the common sites of metastasis for several sites of malignancies). In addition, catecholamines have been shown to have anti-apoptotic effects on cancer cells and may render tumour cells resistant to chemotherapeutic drugs. (109) The variable effects of catecholamines could be explained by nine adrenergic receptor isoforms but also catecholamine effects on cancer cells. (110)

Similarly, BAT activation, including browning of WAT to form beige adipocytes, can be induced by a variety of other factors, including thyroxine, bile acids, and factors overexpressed in certain malignant tumours, including interleukin 6 (IL-6), parathyroid hormone-related peptide (PTH-rP), fibroblast growth factor 21, and natriuretic peptides. (89, 111) PPGLs, whilst principally being known for secretion of catecholamines, can also secrete various growth factors responsible for autocrine or paracrine functions. (89, 112) Adrenomedullin (ADM), a vasodilator peptide hormone induced by hypoxia, was initially isolated in 1993 from a pheochromocytoma. (113) In a 3D mammosphere model, breast cancer cells secrete adrenomedullin to promote lipolysis and browning of adjacent mature adipocytes, which highly express the adrenomedullin receptors. (107, 108) However, further studies are needed to investigate the association between PPGLs and browning factors other than (nor)metanephrine.

As mentioned above, our cohort study found that increased plasma normetanephrine concentrations were associated with active BAT. In contrast, we did not find that BAT activation was significantly associated with any assessed imaging findings, other pathological findings, or treatment modalities. BAT activation was also not associated with specific germline mutations, which is consistent with previous findings. (90) In our study, we observed a greater proportion in advanced AJCC staging in aBAT-positive patients. Specifically, 75% of aBAT-positive patients were classified as stage 3 or 4, compared to only 44.4% of aBAT-negative patients, although this difference did not reach statistical significance. This disparity in tumour stage may possibly contribute to shorter survival rates observed in aBAT-positive patients. Hence, we aimed to account for tumour stage in the multivariate analysis or compare the eight aBAT-positive subjects to a matched control cohort, but the small sample size limited the statistical power and interpretability of such comparisons.

Anatomically, many types of solid tumours (e.g., breast cancer, prostate cancer, and renal cancer) grow in either direct contact or close proximity to adipose tissue (AT), which provides a suitable model for studies investigating the direct interactions between cancer cells and adipocytes. (107) Tumour cells interact with the cells that

compose their environment to promote tumour growth and invasion. Among them, adipocytes provide lipids that are used as a source of energy and adipokines that contribute to tumour expansion. (107, 108) Although beneficial in some other circumstances, such as obesity and diabetes prevention, BAT was found to contribute to the development of complications, such as cancer-induced cachexia (CAC). (114, 115) It was hypothesised as early as 1981 that BAT activation induces a hypermetabolic state and contributes to weight loss in cancer patients (115, 116). Recent studies have emphasised the potential implication of BAT activity in the weight status of oncological patients and demonstrated that localisation, along with the amount of activated BAT, could influence its effects on BMI (115). Moreover, a recently published case report described a patient with pheochromocytoma and BAT activation, evidenced by significant FDG uptake that resolved postoperatively, alongside normalisation of plasma catecholamine levels. (117)

From the studies assessed in our systematic review, an inverse relationship between aBAT and weight / BMI has been noted. It is postulated that BAT activation and expansion in various forms of cancer may be a relevant contributor to cancer-associated cachexia associated with the cancer hypermetabolic state, mediated through increased energy expenditure via UCP1 activity. (118) However, recent large retrospective case control studies have failed to demonstrate significant links between aBAT and CAC or increased mortality. (119, 120) Preclinical models suggest a greater association between aBAT and CAC than comparable results in human studies. (121) Whilst data presented in this synthesis indicated increased all-cause mortality in patients with PPGLs and aBAT, there is insufficient evidence of such an association in patients with other cancer types from retrospective clinical studies. Subsequently, the hypothesis that aBAT confers poorer outcomes in cancer patients cannot be generalised but requires further investigation in prospective clinical studies. This is already an established area of interest as it is acknowledged that BAT in humans may have a pivotal role in weight regulation and, by contrast, even form the basis of a therapeutic target in obesity. (106)

In our cohort study, Kaplan–Meier survival plots indicated trends towards reduced overall survival and progression-free survival in the aBAT-positive group; however, due to the stricter SUV_{max} cut-off used in our study and the resulting smaller sample size, this information was statistically underpowered in the performed univariate survival analysis, making multivariate survival analysis even less feasible. Previous Recent research has indicated that heightened norepinephrine levels and FDG-PET-detected brown adipose tissue (BAT) activity in individuals with PPGL correlate with reduced overall survival, norepinephrine possibly being an independent predictor of mortality. (89)

There is a growing interest in prognostic biomarkers that can predict the outcomes in PPGL, including metastatic disease and survival. (89) Mechanistically, there is evidence suggesting that aBAT may confer poorer outcomes due to its contribution to a hypermetabolic state, which has been linked to cancer cachexia, malnutrition, and metabolic derangements (121, 122). It is well established that severe catecholamine excess can exacerbate metabolic instability and increase cardiovascular disease risk. It has been shown that elevated catecholamine levels can lead to a catecholamine-induced cardiomyopathy in patients with pheochromocytoma. (24-26) However, preclinical evidence indicates that aBAT activity may contribute to weight loss and cancer cachexia, a condition characterised by profound malnutrition and systemic metabolic disruption. (123) These factors could compromise patient resilience, potentially leading to lower performance scores, reduced ability to tolerate treatments, and to a diminished likelihood of surgical interventions, eventually leading to poorer survivability.

In the context of PPGL, severe catecholamine excess and its systemic effects may not only activate BAT, but also further exacerbate the negative impact of aBAT activity. The mechanistic pathways involving hypermetabolism, cancer cachexia, malnutrition, and cardiovascular risks support the plausibility of aBAT being an independent determinant of survival. However, further research (both preclinical and clinical) based on prospective studies is required to delineate these pathways more clearly in the context of aBAT in patients with PPGL.

4.1. Integration of findings

The synthesis of our cohort study with the broader literature examined in our systematic review and meta-analysis provides a more comprehensive understanding of the relationship between PPGL, catecholamine excess, and BAT activation. Both approaches independently support the association between elevated catecholamine levels, particularly increased levels of normetanephrine, and the presence of activated BAT in PPGL patients. Our cohort study demonstrated a significant association between normetanephrine levels and aBAT in multivariate analysis (adjusted OR 2.85; CI 1.11, 10.35), while the meta-analysis also revealed a moderate but statistically significant standardized mean difference in demethylated catecholamine levels between aBAT-positive and aBAT-negative patients (SMD = 0.70; CI 0.37, 1.03).

The prevalence of aBAT in our cohort (13%) was somewhat lower than the pooled estimate from the meta-analysis (26%), potentially due to our stricter SUV_{max} criteria or differences in patient populations. However, the contribution of our data to the cumulative meta-analysis strengthened the overall findings by reducing heterogeneity and narrowing confidence intervals.

The combined evidence supports the biological plausibility of this association through mechanisms related to hypermetabolism, catecholamine excess, and potential contributions to cancer-associated metabolic derangements.

4.2. Strengths and limitations

To the best of our knowledge, this cohort study is the first *clinical* study assessing BAT activation on FDG-PET and its clinical implications in PPGL patients with histopathological confirmation of brown adipose tissue. Albeit on a single patient, the pathological confirmation supports the correlation between imaging findings and true aBAT in our study. Furthermore, unlike other clinical cohort papers assessing

aBAT in PPGL patients, our study incorporates a robust multivariate statistical approach, additionally contributing to the generalisability of its implications.

From a methodological and statistical standpoint, the main limitations of our cohort study arise from its retrospective nature and the relatively small number of cases. While we histopathologically confirmed aBAT in one patient, consistent histological correlation across multiple cases was not feasible due to the ethical and practical constraints of obtaining multiple biopsies from patients in clinical and surgical practice. In addition, the retrospective observational design of our study limited the ability to systematically perform such analyses. As with all cohort studies, it is also possible that transient or persistent confounding factors that could have affected the results were overlooked. Despite having access to electronic records, the information was not always comprehensive for some out-of-region cases, leading to known or unknown missing data points. However, to ensure robust imputation, we employed a random forest algorithm for iterative imputing using 1,000× iterations with each random forest consisting of 100 trees. Nevertheless, because of relatively low sample size given the rarity of this group of neoplasms and the less common use of FDG-PET imaging to characterise them, the implied trends in our study should be interpreted with caution.

During the analysis of cumulative meta-analytical results, it was noticed that the pattern of increased catecholamine levels is consistent over studies, concomitant with a decrease in heterogeneity, which resulted in shortening of the confidence intervals and an increased statistical significance. While the meta-analysis revealed a statistically significant positive association between increased demethylated catecholamine levels and the presence of aBAT, the inclusion of our study lowered the *P*-value to 0.0025 of pooled data and reduced overall heterogeneity by 12%, specifically in terms of catecholamine level variability. Sensitivity analyses, conducted with and without our data, demonstrably reinforced the observed trends, thereby further validating our findings. This confirms the reliability of our results across different analytical scenarios, despite the initial non-significance of plasma normetanephrine levels in the univariate analysis of our cohort, demonstrating their

importance in contributing to overall results and predicting equivalent results in further studies.

It must be noted that pooling comparable data for our meta-analysis proved challenging because not all studies had measured the same parameters for catecholamine assessment, depending on assay availability in their laboratories. Furthermore, some studies combined the measured variables while others did not. For all these reasons, we had to assess the retrieved information by combining all the values prior to their analysis and standardising the data. However, as previously noted, this meta-analysis is based on only six eligible studies and given the variability in study designs, their observational nature, sample sizes, and measurement parameters, the conclusions thus may not be fully generalisable and should be interpreted cautiously. Further analysis of aBAT in patients with PPGL with imaging methods alternative to FDG-PET may add more valuable information to a growing knowledge base. By contributing to a larger evidence pool, our study enhanced the statistical robustness of the meta-analysis, providing a clearer perspective on aBAT prevalence and its biochemical correlates.

5. Future perspectives

The exploration of catecholamine-secreting tumours in association with BAT activation opens several areas for future research, particularly given the potential prognostic implications of activated BAT in these patients. This study has established the foundation for univariately and multivariately identifying the biochemical markers—most notably normetanephrine—that correlate with aBAT presence. However, the association between aBAT and patient outcomes, specifically in terms of disease progression and survival, requires further investigation.

Expanding our understanding of the molecular pathways involved in BAT activation within the PPGL population could provide significant insights into this field. Although catecholamine excess is likely a primary driver of BAT activation, other factors may also contribute. Investigating these “browning” factors—such as inflammatory cytokines, adrenomedullin, and parathyroid hormone-related peptide (PTH-rP)—could clarify whether BAT activation in patients with PPGL reflects broader metabolic dysregulation. Future studies might benefit from employing high-throughput “omics” approaches (i.e., genomics, proteomics, metabolomics) to identify novel biomarkers and pathways involved in BAT activation.

Another potential area for future research is to refine imaging criteria for aBAT detection. Given that FDG-PET imaging can reveal intense BAT activity, which may mimic malignancy, establishing robust diagnostic criteria (including SUV cut-offs) for aBAT would enhance the accuracy of aBAT identification. Additional insights may be obtained by assessing alternative imaging options which directly target sympathetic innervation (e.g., F-DA PET). Integrating multimodal imaging strategies could also provide a more nuanced understanding of BAT activity and potentially aid in differential diagnosis and risk stratification.

The prognostic role of aBAT in patients with PPGLs requires further investigation. Although preliminary data suggest that the presence of aBAT may correlate with more advanced disease stages, larger prospective studies are needed to confirm whether

aBAT serves as a reliable marker of tumour burden and adverse clinical outcomes. Moreover, investigating whether interventions targeting BAT (e.g., β_3 -adrenergic antagonists) could modulate disease progression presents a promising yet untested therapeutic approach.

Finally, it would be valuable to explore BAT activation's role in broader oncologic and metabolic contexts, particularly given the hypothesised link between BAT activation and cancer-associated cachexia (CAC). Future studies should investigate whether BAT contributes to the hypermetabolic state observed in CAC and whether the aBAT prevalence varies across different cancer types to identify tailored therapeutic strategies for metabolic management in oncology.

Advancing our understanding of BAT activation in PPGLs requires a multifaceted approach involving multiple dimensions. Future research should prioritise large-scale, prospective cohort studies to validate the current findings and investigate BAT's role as a potential prognostic biomarker. Additionally, mechanistic studies exploring non-sympathetic pathways of BAT activation and intervention trials targeting BAT modulation may offer new perspectives for managing PPGLs and other metabolically influenced cancers.

6. Summary of findings

This study provides insights into the relationship between activated brown adipose tissue and clinical and biochemical factors in patients with pheochromocytomas and paragangliomas. The key findings of this research are as follows:

1. In contrast to prior studies that univariately linked general catecholamine levels or single catecholamines with aBAT, our results revealed a statistically significant association between elevated plasma normetanephrine levels and aBAT presence in a *multivariate* analysis. This confirms plasma normetanephrine as a specific biomarker for aBAT presence in PPGL.
2. Our study identified an inverse relationship between plasma metanephrine levels and aBAT presence, as observed in the univariate analysis, which implies a possible association with a higher normetanephrine-to-metanephrine ratio suggesting the presence of aBAT.
3. This study is the first *clinical* study to provide histopathological confirmation of brown adipose tissue adjacent to pheochromocytoma, thereby further validating FDG-PET imaging as a reliable method for identifying BAT in this patient group.
4. Our study showed that aBAT-positive patients more frequently presented with advanced stage (3–4) disease, implying that this association might suggest the potential of aBAT as a marker of disease burden or progression in PPGL.
5. Our meta-analytical synthesis of catecholamine data, both before and after the inclusion of our study's results, indicated a consistent positive association between combined catecholamine levels and aBAT, with a reduction in heterogeneity across studies. This analysis strengthens the reliability of currently available but limited evidence for catecholamine excess as a key factor for the presence of aBAT in PPGL.

7. Acknowledgments

I want to express my deepest gratitude to Professor Silvija Canecki-Varžić and Dr Georgios K. Dimitriadis for their immense and invaluable support through this journey of crossing initial milestones in clinical medical research. The opportunities they have provided to me throughout my thus far brief but productive academic career have left a lasting mark, whereas the mentorship they have offered is nothing short of exemplary—just as true mentorship should be.

I am also grateful to my research colleagues from Pécs, including Dr Noémi Zádori, Dr Fanni Dembrovszky, Mr Leonardo Kelava, and many others, whose support helped me push forward when the finish line felt out of reach. Likewise, I owe my sincere appreciation to the London team—Professor Ashley B. Grossman, Dr Michael C. Onyema, Dr Zoulikha M. Zaïr, Dr Fannie Lajeunesse-Trempe, and the rest of the group—for their dedication and contributions to this project.

Furthermore, I am grateful for having had the privilege of meeting and collaborating with other professors outside of this project, including Professor Elmir Omerovic and Professor Ines Bilić-Ćurčić, among others.

And from Croatia, I am fortunate to have had Professor Tamara Braut and Dr Antonia Ferenčaba in my life, whose unwavering encouragement has shaped me into the person I am today.

8. References

1. De Backer D, Biston P, Devriendt J, Madl C, Chochrad D, Aldecoa C, et al. Comparison of dopamine and norepinephrine in the treatment of shock. *N Engl J Med*. 2010;362(9):779-89.
2. Lloyd RV, Osamura RY, Klöppel Gn, Rosai J, World Health O, International Agency for Research on C. WHO classification of tumours of endocrine organs. 4th edition ed. Lyon, France: International Agency for Research on Cancer (IARC); 2017.
3. Wass JAH, Arlt W, Semple R. Oxford textbook of endocrinology and diabetes. Third edition ed. Oxford, United Kingdom: Oxford University Press; 2022.
4. Melmed S, Auchus RJ, Goldfine AB, Rosen CJ, Kopp PA. Williams textbook of endocrinology. 15th edition ed. Philadelphia, PA: Elsevier; 2025.
5. Sadler TW. Langman's medical embryology. Fifteenth edition ed. Philadelphia: Wolters Kluwer; 2024.
6. Welander J, Soderkvist P, Gimm O. Genetics and clinical characteristics of hereditary pheochromocytomas and paragangliomas. *Endocr Relat Cancer*. 2011;18(6):R253-76.
7. Cascon A, Calsina B, Monteagudo M, Mellid S, Diaz-Talavera A, Curras-Freixes M, et al. Genetic bases of pheochromocytoma and paraganglioma. *J Mol Endocrinol*. 2023;70(3).
8. Jochmanova I, Yang C, Zhuang Z, Pacak K. Hypoxia-inducible factor signaling in pheochromocytoma: turning the rudder in the right direction. *J Natl Cancer Inst*. 2013;105(17):1270-83.
9. Smith TG, Robbins PA, Ratcliffe PJ. The human side of hypoxia-inducible factor. *Br J Haematol*. 2008;141(3):325-34.
10. Chappell WH, Steelman LS, Long JM, Kempf RC, Abrams SL, Franklin RA, et al. Ras/Raf/MEK/ERK and PI3K/PTEN/Akt/mTOR inhibitors: rationale and importance to inhibiting these pathways in human health. *Oncotarget*. 2011;2(3):135-64.

11. Mulligan LM, Kwok JB, Healey CS, Elsdon MJ, Eng C, Gardner E, et al. Germ-line mutations of the RET proto-oncogene in multiple endocrine neoplasia type 2A. *Nature*. 1993;363(6428):458-60.
12. Landsberg L. Pheochromocytomas, paragangliomas and disorders of the sympathoadrenal system : clinical features, diagnosis and management. Cham, Switzerland: Humana Press; 2018.
13. Gruber LM, Erickson D, Babovic-Vuksanovic D, Thompson GB, Young WF, Jr., Bancos I. Pheochromocytoma and paraganglioma in patients with neurofibromatosis type 1. *Clin Endocrinol (Oxf)*. 2017;86(1):141-9.
14. Castro-Vega LJ, Buffet A, De Cubas AA, Cascon A, Menara M, Khalifa E, et al. Germline mutations in FH confer predisposition to malignant pheochromocytomas and paragangliomas. *Hum Mol Genet*. 2014;23(9):2440-6.
15. Brouwers FM, Eisenhofer G, Tao JJ, Kant JA, Adams KT, Linehan WM, et al. High frequency of SDHB germline mutations in patients with malignant catecholamine-producing paragangliomas: implications for genetic testing. *J Clin Endocrinol Metab*. 2006;91(11):4505-9.
16. Lenders JW, Duh QY, Eisenhofer G, Gimenez-Roqueplo AP, Grebe SK, Murad MH, et al. Pheochromocytoma and paraganglioma: an endocrine society clinical practice guideline. *J Clin Endocrinol Metab*. 2014;99(6):1915-42.
17. Gimenez-Roqueplo AP, Favier J, Rustin P, Rieubland C, Crespin M, Nau V, et al. Mutations in the SDHB gene are associated with extra-adrenal and/or malignant pheochromocytomas. *Cancer Res*. 2003;63(17):5615-21.
18. Peixoto JCAdC. Inherited genetic alterations in pheochromocytomas and paragangliomas: Universidade de Aveiro; 2012.
19. Young WF, Jr. Clinical presentation and diagnosis of pheochromocytoma. 2025. In: UpToDate [Internet]. Wolters Kluwer.
20. Young WF, Jr. Epidemiology, clinical presentation, and diagnosis of paragangliomas. 2025. In: UpToDate [Internet]. Wolters Kluwer.
21. Kannan CR. Pheochromocytoma. In: Kannan CR, editor. *The Adrenal Gland*. Boston, MA: Springer US; 1988. p. 465-95.

22. Malindretos PM, Sarafidis PA, Geropoulou EZ, Kapoulas S, Paramythiotis DD, Lasaridis AN. Sustained hypotension complicating an extra-adrenal pheochromocytoma. *Am J Hypertens*. 2008;21(7):840-2.
23. Streeten DH, Anderson GH, Jr. Mechanisms of orthostatic hypotension and tachycardia in patients with pheochromocytoma. *Am J Hypertens*. 1996;9(8):760-9.
24. Wilkenfeld C, Cohen M, Lansman SL, Courtney M, Dische MR, Pertsemlidis D, et al. Heart transplantation for end-stage cardiomyopathy caused by an occult pheochromocytoma. *J Heart Lung Transplant*. 1992;11(2 Pt 1):363-6.
25. Zhang R, Gupta D, Albert SG. Pheochromocytoma as a reversible cause of cardiomyopathy: Analysis and review of the literature. *Int J Cardiol*. 2017;249:319-23.
26. Szatko A, Glinicki P, Gietka-Czernel M. Pheochromocytoma/paraganglioma-associated cardiomyopathy. *Front Endocrinol (Lausanne)*. 2023;14:1204851.
27. Kassim TA, Clarke DD, Mai VQ, Clyde PW, Mohamed Shakir KM. Catecholamine-induced cardiomyopathy. *Endocr Pract*. 2008;14(9):1137-49.
28. Kantorovich V, Eisenhofer G, Pacak K. Pheochromocytoma: an endocrine stress mimicking disorder. *Ann N Y Acad Sci*. 2008;1148:462-8.
29. Alguire C, Chbat J, Forest I, Godbout A, Bourdeau I. Unusual presentation of pheochromocytoma: thirteen years of anxiety requiring psychiatric treatment. *Endocrinol Diabetes Metab Case Rep*. 2018;2018.
30. Constantinescu G, Preda C, Constantinescu V, Siepmann T, Bornstein SR, Lenders JWM, et al. Silent pheochromocytoma and paraganglioma: Systematic review and proposed definitions for standardized terminology. *Front Endocrinol (Lausanne)*. 2022;13:1021420.
31. Eisenhofer G. Screening for pheochromocytomas and paragangliomas. *Curr Hypertens Rep*. 2012;14(2):130-7.
32. Eisenhofer G, Pamporaki C, Lenders JWM. Biochemical Assessment of Pheochromocytoma and Paraganglioma. *Endocr Rev*. 2023;44(5):862-909.
33. Rao D, Peitzsch M, Prejbisz A, Hanus K, Fassnacht M, Beuschlein F, et al. Plasma methoxytyramine: clinical utility with metanephrines for diagnosis

- of pheochromocytoma and paraganglioma. *Eur J Endocrinol.* 2017;177(2):103-13.
34. Pacak K, Eisenhofer G, Ilias I. Diagnostic imaging of pheochromocytoma. *Front Horm Res.* 2004;31:107-20.
 35. Thelen J, Bhatt AA. Multimodality imaging of paragangliomas of the head and neck. *Insights Imaging.* 2019;10(1):29.
 36. Taieb D, Hicks RJ, Hindie E, Guillet BA, Avram A, Ghedini P, et al. European Association of Nuclear Medicine Practice Guideline/Society of Nuclear Medicine and Molecular Imaging Procedure Standard 2019 for radionuclide imaging of phaeochromocytoma and paraganglioma. *Eur J Nucl Med Mol Imaging.* 2019;46(10):2112-37.
 37. Janssen I, Chen CC, Millo CM, Ling A, Taieb D, Lin FI, et al. PET/CT comparing (68)Ga-DOTATATE and other radiopharmaceuticals and in comparison with CT/MRI for the localization of sporadic metastatic pheochromocytoma and paraganglioma. *Eur J Nucl Med Mol Imaging.* 2016;43(10):1784-91.
 38. Mettler FA, Guiberteau MJ. 11 - Hybrid PET/CT Neoplasm Imaging. In: Mettler FA, Guiberteau MJ, editors. *Essentials of Nuclear Medicine and Molecular Imaging (Seventh Edition)*. Philadelphia: Elsevier; 2019. p. 328-61.
 39. Wiseman GA, Pacak K, O'Dorisio MS, Neumann DR, Waxman AD, Mankoff DA, et al. Usefulness of ¹²³I-MIBG scintigraphy in the evaluation of patients with known or suspected primary or metastatic pheochromocytoma or paraganglioma: results from a prospective multicenter trial. *J Nucl Med.* 2009;50(9):1448-54.
 40. Fassnacht M, Arlt W, Bancos I, Dralle H, Newell-Price J, Sahdev A, et al. Management of adrenal incidentalomas: European Society of Endocrinology Clinical Practice Guideline in collaboration with the European Network for the Study of Adrenal Tumors. *Eur J Endocrinol.* 2016;175(2):G1-G34.
 41. Timmers HJ, Chen CC, Carrasquillo JA, Whatley M, Ling A, Eisenhofer G, et al. Staging and functional characterization of pheochromocytoma and

- paraganglioma by 18F-fluorodeoxyglucose (18F-FDG) positron emission tomography. *J Natl Cancer Inst.* 2012;104(9):700-8.
42. Nockel P, El Lakis M, Gaitanidis A, Merkel R, Patel D, Nilubol N, et al. Preoperative 18F-FDG PET/CT in Pheochromocytomas and Paragangliomas Allows for Precision Surgery. *Ann Surg.* 2019;269(4):741-7.
 43. Young WF, Jr. Pheochromocytoma in genetic disorders. 2025. In: UpToDate [Internet]. Wolters Kluwer.
 44. Plouin PF, Amar L, Dekkers OM, Fassnacht M, Gimenez-Roqueplo AP, Lenders JW, et al. European Society of Endocrinology Clinical Practice Guideline for long-term follow-up of patients operated on for a phaeochromocytoma or a paraganglioma. *Eur J Endocrinol.* 2016;174(5):G1-G10.
 45. Young WF, Jr., Kebebew E. Treatment of pheochromocytoma in adults. 2025. In: UpToDate [Internet]. Wolters Kluwer.
 46. Bakris GL, Sorrentino MJ. Hypertension : a companion to Braunwald's heart disease. Philadelphia, PA: Elsevier; 2018.
 47. Young WF, Jr. Management of malignant (metastatic) paraganglioma and pheochromocytoma. 2025. In: UpToDate [Internet]. Wolters Kluwer.
 48. Trayhurn P, Beattie JH. Physiological role of adipose tissue: white adipose tissue as an endocrine and secretory organ. *Proc Nutr Soc.* 2001;60(3):329-39.
 49. Heyde I, Begemann K, Oster H. Contributions of white and brown adipose tissues to the circadian regulation of energy metabolism. *Endocrinology.* 2021;162(3).
 50. Large V, Peroni O, Letexier D, Ray H, Beylot M. Metabolism of lipids in human white adipocyte. *Diabetes Metab.* 2004;30(4):294-309.
 51. Fenzl A, Kiefer FW. Brown adipose tissue and thermogenesis. *Horm Mol Biol Clin Investig.* 2014;19(1):25-37.
 52. Jung SM, Sanchez-Gurmaches J, Guertin DA. Brown Adipose Tissue Development and Metabolism. *Handb Exp Pharmacol.* 2019;251:3-36.

53. Lidell ME. Brown Adipose Tissue in Human Infants. *Handb Exp Pharmacol*. 2019;251:107-23.
54. Saha U. Changes in the Newborn at Birth: Fetal-to-Newborn Transition. In: Saha U, editor. *Clinical Anesthesia for the Newborn and the Neonate*. Singapore: Springer Nature Singapore; 2023. p. 29-47.
55. Boon MR, van Marken Lichtenbelt WD. Brown Adipose Tissue: A Human Perspective. *Handb Exp Pharmacol*. 2016;233:301-19.
56. Sacks H, Symonds ME. Anatomical locations of human brown adipose tissue: functional relevance and implications in obesity and type 2 diabetes. *Diabetes*. 2013;62(6):1783-90.
57. Gilsanz V, Hu HH, Kajimura S. Relevance of brown adipose tissue in infancy and adolescence. *Pediatr Res*. 2013;73(1):3-9.
58. Cero C, Lea HJ, Zhu KY, Shamsi F, Tseng YH, Cypess AM. beta3-Adrenergic receptors regulate human brown/beige adipocyte lipolysis and thermogenesis. *JCI Insight*. 2021;6(11).
59. Han JS, Jeon YG, Oh M, Lee G, Nahmgoong H, Han SM, et al. Adipocyte HIF2alpha functions as a thermostat via PKA Calpha regulation in beige adipocytes. *Nat Commun*. 2022;13(1):3268.
60. Fedorenko A, Lishko PV, Kirichok Y. Mechanism of fatty-acid-dependent UCP1 uncoupling in brown fat mitochondria. *Cell*. 2012;151(2):400-13.
61. Jastroch M. Uncoupling protein 1 controls reactive oxygen species in brown adipose tissue. *Proc Natl Acad Sci U S A*. 2017;114(30):7744-6.
62. Weber BZC, Arabaci DH, Kir S. Metabolic Reprogramming in Adipose Tissue During Cancer Cachexia. *Front Oncol*. 2022;12:848394.
63. Nedergaard J, Cannon B. The browning of white adipose tissue: some burning issues. *Cell Metab*. 2014;20(3):396-407.
64. Montanari T, Poscic N, Colitti M. Factors involved in white-to-brown adipose tissue conversion and in thermogenesis: a review. *Obes Rev*. 2017;18(5):495-513.

65. Blondin DP, Nielsen S, Kuipers EN, Severinsen MC, Jensen VH, Miard S, et al. Human Brown Adipocyte Thermogenesis Is Driven by beta2-AR Stimulation. *Cell Metab.* 2020;32(2):287-300 e7.
66. Ishida Y, Matsushita M, Yoneshiro T, Saito M, Fuse S, Hamaoka T, et al. Genetic evidence for involvement of beta2-adrenergic receptor in brown adipose tissue thermogenesis in humans. *Int J Obes (Lond).* 2024;48(8):1110-7.
67. Huo C, Song Z, Yin J, Zhu Y, Miao X, Qian H, et al. Effect of Acute Cold Exposure on Energy Metabolism and Activity of Brown Adipose Tissue in Humans: A Systematic Review and Meta-Analysis. *Front Physiol.* 2022;13:917084.
68. Wang Q, Zhang M, Ning G, Gu W, Su T, Xu M, et al. Brown adipose tissue in humans is activated by elevated plasma catecholamines levels and is inversely related to central obesity. *PLoS One.* 2011;6(6):e21006.
69. Cioffi F, Gentile A, Silvestri E, Goglia F, Lombardi A. Effect of Iodothyronines on Thermogenesis: Focus on Brown Adipose Tissue. *Front Endocrinol (Lausanne).* 2018;9:254.
70. Pelletier P, Gauthier K, Sideleva O, Samarut J, Silva JE. Mice lacking the thyroid hormone receptor-alpha gene spend more energy in thermogenesis, burn more fat, and are less sensitive to high-fat diet-induced obesity. *Endocrinology.* 2008;149(12):6471-86.
71. Ribeiro MO, Bianco SD, Kaneshige M, Schultz JJ, Cheng SY, Bianco AC, et al. Expression of uncoupling protein 1 in mouse brown adipose tissue is thyroid hormone receptor-beta isoform specific and required for adaptive thermogenesis. *Endocrinology.* 2010;151(1):432-40.
72. Wang X, Wahl R. Responses of the insulin signaling pathways in the brown adipose tissue of rats following cold exposure. *PLoS One.* 2014;9(6):e99772.
73. Gasparetti AL, de Souza CT, Pereira-da-Silva M, Oliveira RL, Saad MJ, Carneiro EM, et al. Cold exposure induces tissue-specific modulation of the insulin-signalling pathway in *Rattus norvegicus*. *J Physiol.* 2003;552(Pt 1):149-62.

74. Sun W, Luo Y, Zhang F, Tang S, Zhu T. Involvement of TRP Channels in Adipocyte Thermogenesis: An Update. *Front Cell Dev Biol.* 2021;9:686173.
75. Saito M, Matsushita M, Yoneshiro T, Okamatsu-Ogura Y. Brown Adipose Tissue, Diet-Induced Thermogenesis, and Thermogenic Food Ingredients: From Mice to Men. *Front Endocrinol (Lausanne).* 2020;11:222.
76. Dulloo AG, Duret C, Rohrer D, Girardier L, Mensi N, Fathi M, et al. Efficacy of a green tea extract rich in catechin polyphenols and caffeine in increasing 24-h energy expenditure and fat oxidation in humans. *Am J Clin Nutr.* 1999;70(6):1040-5.
77. El Hadi H, Di Vincenzo A, Vettor R, Rossato M. Food Ingredients Involved in White-to-Brown Adipose Tissue Conversion and in Calorie Burning. *Front Physiol.* 2018;9:1954.
78. Zhou L, Xiao X, Zhang Q, Zheng J, Deng M. Deciphering the Anti-obesity Benefits of Resveratrol: The "Gut Microbiota-Adipose Tissue" Axis. *Front Endocrinol (Lausanne).* 2019;10:413.
79. Villarroya F, Gavaldà-Navarro A, Peyrou M, Villarroya J, Giralt M. Brown Adipokines. In: Pfeifer A, Klingenspor M, Herzig S, editors. *Brown Adipose Tissue*. Cham: Springer International Publishing; 2019. p. 239-56.
80. Clemente-Suarez VJ, Redondo-Florez L, Beltran-Velasco AI, Martin-Rodriguez A, Martinez-Guardado I, Navarro-Jimenez E, et al. The Role of Adipokines in Health and Disease. *Biomedicines.* 2023;11(5).
81. Villarroya J, Cereijo R, Villarroya F. An endocrine role for brown adipose tissue? *Am J Physiol Endocrinol Metab.* 2013;305(5):E567-72.
82. Fang R, Yan L, Liao Z. Abnormal lipid metabolism in cancer-associated cachexia and potential therapy strategy. *Front Oncol.* 2023;13:1123567.
83. Cao L, Choi EY, Liu X, Martin A, Wang C, Xu X, et al. White to brown fat phenotypic switch induced by genetic and environmental activation of a hypothalamic-adipocyte axis. *Cell Metab.* 2011;14(3):324-38.
84. Zhang W, Bi S. Hypothalamic Regulation of Brown Adipose Tissue Thermogenesis and Energy Homeostasis. *Front Endocrinol (Lausanne).* 2015;6:136.

85. Pandit R, Beerens S, Adan RAH. Role of leptin in energy expenditure: the hypothalamic perspective. *Am J Physiol Regul Integr Comp Physiol*. 2017;312(6):R938-R47.
86. Straat ME, Hogenboom R, Boon MR, Rensen PCN, Kooijman S. Circadian control of brown adipose tissue. *Biochim Biophys Acta Mol Cell Biol Lipids*. 2021;1866(8):158961.
87. Matsushita M, Nirengi S, Hibi M, Wakabayashi H, Lee SI, Domichi M, et al. Diurnal variations of brown fat thermogenesis and fat oxidation in humans. *Int J Obes (Lond)*. 2021;45(11):2499-505.
88. Nedergaard J, Bengtsson T, Cannon B. Unexpected evidence for active brown adipose tissue in adult humans. *Am J Physiol Endocrinol Metab*. 2007;293(2):E444-52.
89. Abdul Sater Z, Jha A, Hamimi A, Mandl A, Hartley IR, Gubbi S, et al. Pheochromocytoma and paraganglioma patients with poor survival often show brown adipose tissue activation. *J Clin Endocrinol Metab*. 2020;105(4):1176-85.
90. Puar T, van Berkel A, Gotthardt M, Havekes B, Hermus ARMM, Lenders JWM, et al. Genotype-dependent brown adipose tissue activation in patients with pheochromocytoma and paraganglioma. *J Clin Endocrinol Metab*. 2016;101(1):224-32.
91. Santhanam P, Treglia G, Ahima RS. Detection of brown adipose tissue by (18) F-FDG PET/CT in pheochromocytoma/paraganglioma: A systematic review. *J Clin Hypertens (Greenwich)*. 2018;20(3):615.
92. Eisenhauer EA, Therasse P, Bogaerts J, Schwartz LH, Sargent D, Ford R, et al. New response evaluation criteria in solid tumours: revised RECIST guideline (version 1.1). *Eur J Cancer*. 2009;45(2):228-47.
93. Dwivedi AK, Mallawaarachchi I, Alvarado LA. Analysis of small sample size studies using nonparametric bootstrap test with pooled resampling method. *Stat Med*. 2017;36(14):2187-205.
94. R Core Team. R: A Language and Environment for Statistical Computing. Vienna, Austria 2024.

95. Sule N. Histology-brown and white adipose 2021 [Available from: <https://www.pathologyoutlines.com/topic/softtissueadiposewhitefat.html>].
96. Higgins JPT TJ, Chandler J, Cumpston M, Li T, Page MJ, Welch VA (editors). Cochrane Handbook for Systematic Reviews of Interventions. 2nd edition. Chichester (UK): John Wiley & Sons; 2019.
97. Balduzzi S RG, Schwarzer G. How to perform a meta-analysis with R: a practical tutorial.22(4):153-60.
98. Terada E, Ashida K, Ohe K, Sakamoto S, Hasuzawa N, Nomura M. Brown adipose activation and reversible beige coloration in adipose tissue with multiple accumulations of 18F-fluorodeoxyglucose in sporadic paraganglioma: A case report. Clin Case Rep. 2019;7(7):1399-403.
99. Hadi M, Chen CC, Whatley M, Pacak K, Carrasquillo JA. Brown fat imaging with (18)F-6-fluorodopamine PET/CT, (18)F-FDG PET/CT, and (123)I-MIBG SPECT: a study of patients being evaluated for pheochromocytoma. J Nucl Med. 2007;48(7):1077-83.
100. Pfannenbergh C, Werner MK, Ripkens S, Stef I, Deckert A, Schmadl M, et al. Impact of age on the relationships of brown adipose tissue with sex and adiposity in humans. Diabetes. 2010;59(7):1789-93.
101. Kaikaew K, Grefhorst A, Visser JA. Sex Differences in Brown Adipose Tissue Function: Sex Hormones, Glucocorticoids, and Their Crosstalk. Front Endocrinol (Lausanne). 2021;12:652444.
102. Quarta C, Mazza R, Pasquali R, Pagotto U. Role of sex hormones in modulation of brown adipose tissue activity. J Mol Endocrinol. 2012;49(1):R1-7.
103. Mubeen A, Canete-Portillo S, Galgano S, Rais-Bahrami S, Magi-Galluzzi C. The Enigmatic Association of Brown Adipose Tissue with Pheochromocytoma. Modern Pathology. 2022;35(SUPPL 2):395-6.
104. Cannon B, Nedergaard J. Brown adipose tissue: function and physiological significance. Physiol Rev. 2004;84(1):277-359.
105. Al-Harthy M, Al-Harthy S, Al-Otieschan A, Velagapudi S, Alzahrani AS. Comparison of pheochromocytomas and abdominal and pelvic

- paragangliomas with head and neck paragangliomas. *Endocr Pract.* 2009;15(3):194-202.
106. Santhanam P, Solnes L, Hannukainen JC, Taïeb D. Adiposity-related cancer and functional imaging of brown adipose tissue. *Endocr Pract.* 2015;21(11):1282-90.
 107. Dong K, Wei G, Sun H, Gu D, Liu J, Wang L. Metabolic crosstalk between thermogenic adipocyte and cancer cell: Dysfunction and therapeutics. *Curr Opin Pharmacol.* 2023;68:102322.
 108. Paré M, Darini CY, Yao X, Chignon-Sicard B, Rekima S, Lachambre S, et al. Breast cancer mammospheres secrete Adrenomedullin to induce lipolysis and browning of adjacent adipocytes. *BMC Cancer.* 2020;20(1):784.
 109. Yang EV. Role for catecholamines in tumor progression: possible use for beta-blockers in the treatment of cancer. *Cancer Biol Ther.* 2010;10(1):30-2.
 110. Wackerhage H, Christensen JF, Ilmer M, von Lüttichau I, Renz BW, Schönfelder M. Cancer catecholamine conundrum. *Trends Cancer.* 2022;8(2):110-22.
 111. Villarroja F, Vidal-Puig A. Beyond the sympathetic tone: the new brown fat activators. *Cell Metab.* 2013;17(5):638-43.
 112. Kontogeorgos G, Scheithauer BW, Kovacs K, Horvath E, Melmed S. Growth factors and cytokines in paragangliomas and pheochromocytomas, with special reference to sustentacular cells. *Endocr Pathol.* 2002;13(3):197-206.
 113. Kitamura K, Kangawa K, Kawamoto M, Ichiki Y, Nakamura S, Matsuo H, et al. Adrenomedullin: a novel hypotensive peptide isolated from human pheochromocytoma. *Biochem Biophys Res Commun.* 1993;192(2):553-60.
 114. Nishio M, Saeki K. The remaining mysteries about brown adipose tissues. *Cells.* 2020;9(11):2449.
 115. Jalloul W, Moscalu M, Moscalu R, Jalloul D, Grierosu IC, Ionescu T, et al. Off the beaten path in oncology: Active brown Adipose Tissue by virtue of molecular imaging. *Curr Issues Mol Biol.* 2023;45(10):7891-914.

116. Ma J, Huang M, Wang L, Ye W, Tong Y, Wang H. Obesity and risk of thyroid cancer: evidence from a meta-analysis of 21 observational studies. *Med Sci Monit.* 2015;21:283-91.
117. Md Nor MN, Healy K, Feeney J, Garrahy A. Brown Adipose Tissue Activation on (18-)F-FDG-PET/CT Manifesting as Cachexia in a Patient With Pheochromocytoma. *JCEM Case Rep.* 2024;2(5):luaeo82.
118. Vaitkus JA, Celi FS. The role of adipose tissue in cancer-associated cachexia. *Exp Biol Med (Maywood).* 2017;242(5):473-81.
119. Becker AS, Zellweger C, Bacanovic S, Franckenberg S, Nagel HW, Frick L, et al. Brown fat does not cause cachexia in cancer patients: A large retrospective longitudinal FDG-PET/CT cohort study. *PLoS One.* 2020;15(10):e0239990.
120. Eljalby M, Huang X, Becher T, Wibmer AG, Jiang CS, Vaughan R, et al. Brown adipose tissue is not associated with cachexia or increased mortality in a retrospective study of patients with cancer. *Am J Physiol Endocrinol Metab.* 2023;324(2):E144-E53.
121. Beijer E, Schoenmakers J, Vijgen G, Kessels F, Dingemans AM, Schrauwen P, et al. A role of active brown adipose tissue in cancer cachexia? *Oncol Rev.* 2012;6(1):e11.
122. Sherlock FG, Riedinger MS, Fishbein MC. Brown adipose tissue in cancer patients: possible cause of cancer-induced cachexia. *J Cancer Res Clin Oncol.* 1986;111(1):82-5.
123. Brooks SL, Neville AM, Rothwell NJ, Stock MJ, Wilson S. Sympathetic activation of brown-adipose-tissue thermogenesis in cachexia. *Biosci Rep.* 1981;1(6):509-17.

9. Publications & author-level research metrics

9.1. Author metrics

as of 7 May 2025

Journal ranking	Number of full-text publications
Q1	13
(D1)	(5)
Q2	4
Q3	2
Q4	3
Cumulative impact factor (IF)	84.696
<i>h</i> -index	8

9.2. Publications related to the dissertation

1. **Oštarijaš E**, Onyema M, Zair Z, Taylor DR, Lajeunesse-Trempe F, Reynolds S, Mullholland N, Corcoran B, Halim M, Drakou EE, Grossman A, Vincent RP, Aylwin S, Dimitriadis GK, Canecki-Varžić S. *Metabolically active brown adipose tissue in PPGL: an observational cohort study*. Endocr Relat Cancer. 2025 Mar 07;32(4):e240200. doi: 10.1530/ERC-24-0200. (2023 Q1, IF 4.1)
2. Onyema MC, **Oštarijaš E**, Zair Z, Roy A, Minhas R, Lajeunesse-Trempe F, Kearney J, Drakou EE, Grossman AB, Aylwin SJ, Canecki-Varžić S, Dimitriadis GK. *The Role of Active Brown Adipose Tissue in Patients With Pheochromocytoma or Paraganglioma*. Endocr Pract. 2024 Nov 16:S1530-891X(24)00828-0. doi: 10.1016/j.eprac.2024.11.003. (2023 Q1, IF 3.7)

9.3. Publications unrelated to the dissertation

1. Llewellyn D, Nuamek T, **Ostarijas E**, Logan Ellis H, Drakou EE, Aylwin SJ, Dimitriadis GK. Low-dose tolvaptan for the treatment of SIADH-associated hyponatremia: a systematic review, meta-analysis, and meta-regression analysis of clinical effectiveness and safety. *Endocr Pract.* 2025 Apr 25:S1530-891X(25)00131-4. doi: 10.1016/j.eprac.2025.04.012. (2023 Q1, IF 3.7)
2. Llewellyn DC, **Oštarijaš E**, Sahadevan S, Nuamek T, Byrne C, Taylor DR, Vincent RP, Dimitriadis GK, Aylwin SJ. *Efficacy and safety of low-dose tolvaptan (7.5mg) in the treatment of inpatient hyponatraemia: a retrospective study.* *Endocr Pract.* 2025 Apr;31(4):419-425. doi: 10.1016/j.eprac.2024.12.019. (2023 Q1, IF 3.7)
3. Lajeunesse-Trempe F, Okroj D, **Ostarijas E**, Ramalho A, Tremblay EJ, Llewellyn D, Harlow C, Chandhyoke N, Chew NWS, Vincent RP, Tchernof A, Piché ME, Poirier P, Biertho L, Morin MP, Copeland CS, Dimitriadis GK. *Medication and Supplement Pharmacokinetic Changes Following Bariatric Surgery: A Systematic Review And Meta-Analysis.* *Obesity Reviews.* 2024. doi: 10.1111/obr.13759. (2023 Q1/D1, IF 8.0)
4. Samarasinghe SNS, **Ostarijas E**, Long MJ, Erridge S, Purkayastha S, Dimitriadis GK, Miras AD. *Impact of insulin sensitization on metabolic and fertility outcomes in women with polycystic ovary syndrome and overweight or obesity—A systematic review, meta-analysis, and meta-regression.* *Obesity Reviews.* 2024;e13744. doi:10.1111/obr.13744 (2023 Q1/D1, IF 8.0)
5. Petursson P, **Oštarijaš E**, Redfors B, Råmunddal T, Angerås O, Völz S, Rawshani A, Hambræus K, Koul S, Alfredsson J, Hagström H, Loghman H, Hofmann R, Fröbert O, Jernberg T, James S, Erlinge D, Omerovic E. *Effects of pharmacological interventions on short- and long-term mortality in patients with*

- takotsubo syndrome: a report from the SWEDEHEART registry*. ESC Heart Failure. 2024. doi: 10.1002/ehf2.14713. (2023 Q1, IF 3.2)
6. Kukuljan M, Mršić E, **Oštarijaš E**. *CT-guided transthoracic core needle biopsies of focal pleural lesions smaller than 10 mm: a retrospective study*. Cancer Imaging. 23, 48 (2023). doi: 10.1186/s40644-023-00569-4. (2023 Q1, IF 3.5)
 7. Palčevski D, Belančić A, Mikuličić I, **Oštarijaš E**, Likić R, Dyar O, Vlahović-Palčevski V. *Antimicrobial Prescribing Preparedness of Croatian Medical Students-Did It Change between 2015 and 2019?* Medicines (Basel). 2023 Jun 29;10(7):39. doi: 10.3390/medicines10070039. (2023 Q4)
 8. Llewellyn DC, Logan Ellis H, Aylwin SJB, **Oštarijaš E**, Green S, Sheridan W, Chew NWS, le Roux CW, Miras AD, Patel AG, Vincent RP, Dimitriadis GK. *The efficacy of GLP-1RAs for the management of postprandial hypoglycemia following bariatric surgery: a systematic review*. Obesity. 2023 Jan;31(1):20-30. doi: 10.1002/oby.23600. (2022 Q1/D1, IF 6.9)
 9. Zombori-Tóth N, Kiss S, **Oštarijaš E**, Alizadeh H, Zombori T. *Adjuvant chemotherapy could improve the survival of pulmonary sarcomatoid carcinoma: A systematic review and meta-analysis*. Surg Oncol. 2022 Sep;44:101824. doi: 10.1016/j.suronc.2022.101824. (2022 Q2, IF 2.3)
 10. Martonosi AR, Pázmány P, Kiss Sz, Dembrovszky F, **Oštarijaš E**, Szabó L. *Urodynamics in Early Diagnosis of Diabetic Bladder Dysfunction in Women: A Systematic Review and Meta-Analysis*. Medical Science Monitor. 2022. doi: 10.12659/MSM.937166. (2022 Q2, IF 3.1)
 11. Simon O, Görbe A, Hegyi P, Szakó L, **Oštarijaš E**, Dembrovszky F, Kiss Sz, Czopf L, Erőss B, Szabó I. *Helicobacter pylori Infection is Associated with Carotid Intima and Media Thickening. A Systematic Review and Meta-Analysis*. Journal of the American Heart Association. 2022 Feb;11(3). doi: 10.1161/JAHA.121.022919 (2022 Q1/D1, 2021 IF 6.106).

12. Omran A, Leca BM, **Oštarijaš E**, Graham N, Dasilva A, Zair Z, Miras A, le Roux C, Vincent RP, Cardozo L, Dimitriadis GK. *Metabolic syndrome is associated with prostate hyperplasia in patients with lower urinary tract symptoms: a systematic review, meta-analysis and meta-regression analysis*. Ther Adv Endocrinol Metab. 2021 Dec 8;12. doi: 10.1177/20420188211066210. (2021 Q2, IF 4.435)
13. Zádori N, Szakó L, Váncsa Sz, Vörhendi N, **Oštarijaš E**, Kiss Sz, Frim L, Hegyi P, Czimmer J. *Six autoimmune disorders are associated with increased incidence of gastric cancer: A systematic review and meta-analysis of half a million patients*. Front Immunol. 2021 Nov 23;12:750533. doi: 10.3389/fimmu.2021.750533. (2021 Q1, IF 8.786)
14. Borodavkin P, Sheridan W, Coehlo C, **Oštarijaš E**, Zaïr ZM, Miras AD, McGowan B, le Roux CW, Vincent RP, Dimitriadis GK. *Effects of glucagon-like peptide-1 receptor agonists on histopathological and secondary biomarkers of non-alcoholic steatohepatitis: A systematic review and meta-analysis*. Diabetes Obes Metab. 2021 Oct 4; 1-6. doi: 10.1111/dom.14565. (2020 Q1/D1, IF 6.577)
15. Boros E, Sipos Z, Hegyi P, Teutsch B, Frim L, Váncsa Sz, Kiss Sz, Dembrovszky F, **Oštarijaš E**, Shawyer A, Erőss B. *Prophylactic transcatheter arterial embolization reduces rebleeding in non-variceal upper gastrointestinal bleeding: A meta-analysis*. World J Gastroenterol. 2021 Oct; 27(40). doi: 10.3748/wjg.v27.i40.0000. (2020 Q1, IF 5.742)
16. Sheridan W, Da Silva AS, Leca BM, **Oštarijaš E**, Patel AG, Aylwin SJ, Vincent RP, Panagiotopoulos S, El-Hasani S, le Roux CW, Miras AD, Cardozo L, Dimitriadis GK. *Weight loss with bariatric surgery or behaviour modification and the impact on female obesity-related urine incontinence: A comprehensive systematic review and meta-analysis*. Clin Obes. 2021:e12450. doi: 10.1111/cob.12450. (2020 Q3)
17. Braut T, Krstulja M, Marijić B, Maržić D, Kujundžić M, Zamolo G, Vučinić D, **Oštarijaš E**. *Tip of the iceberg: Immunohistochemical markers reveal malignant*

- transformation underneath a vocal polyp surface. Medicina fluminensis. 2021;57(2):171-176. doi: 10.21860/medflum2021_371640. (2021 Q4)*
18. Franjić K, **Oštarijaš E**, Kaštelan A. *Adolescent compliance in psychiatric treatment. Medicina fluminensis. 2020;56(1):26-34. doi: 10.21860/medflum2020_232815. Croatian. (2020 Q4)*
 19. Kukuljan M, Šoša I, Mršić E, **Oštarijaš E**, Mršić A, Miletić D. *Diagnostic Accuracy of Computed Tomography-Guided Noncoaxial Cutting Needle: Transthoracic Lung Biopsies and the Associated Pneumothorax. J Biol Regul Homeost Agents. 2019 Nov 21;33(6). doi: 10.23812/19-358-L. (2019 Q3, IF 1.506)*
 20. Braut T, Krstulja M, Marijić B, Maržić D, Kujundžić M, Brumini G, Vučinić D, **Oštarijaš E**. *Immunohistochemical analysis of vocal cord polyps applying markers of squamous cell carcinogenesis. Pathol Res Pract. 2019;215(1):144-50. doi: 10.1016/j.prp.2018.11.001. (2019 Q2, IF 2.050)*

9.4. Abstracts and other publications

1. Marušić R, Bilić-Ćurčić I, Schönberger E, Steiner K, Ormanac K, **Oštarijaš E**, Canecki-Varžić S. *A thousand faces of pheochromocytoma: Insights from a case series. Endocrine Abstracts. 2024;99(EP632). In: 26th European Congress of Endocrinology. doi: 10.1530/endoabs.99.EP632.*
2. Marušić R, Bilić-Ćurčić I, Schönberger E, Steiner K, Ormanac K, **Oštarijaš E**, Canecki-Varžić S. *Symptomatic diversity in Cushing's disease: A complex case report on diagnosis challenges. 2024 Feb. 2nd Regional Symposium of Young Endocrinologists and Diabetologists. Croatian.*
3. Lajeunesse-Trempe F, Okroj D, Llewellyn D, Harlow C, Chandhyoke N, Ramalho A, Tremblay EJ, **Ostarijas E**, Tchernof A, Copeland C, Dimitriadis GK. *The impact of bariatric surgery on drug and supplement absorption: A meta-*

- analysis*. Obesity Surgery. 2023 Jul;33(S1):S125. Springer New York. doi: 10.1007/s11695-023-06662-8. (2022 D1, IF 2.921)
4. Canecki-Varžić S, **Oštarijaš E**. *The most common malignant diseases in the population of war veterans*. 2023 Apr. Na prvoj crti zdravlja. Croatian.
 5. Onyema M, **Ostarijas E**, Minhas R, Roy A, Kearney J, Omran A, Zair Z, Reynolds S, Mulholland N, Corcoran B, Mohammad H, Simon A, Dimitriadis GK. *The incidence and clinical significance of metabolically active brown adipose tissue in patients with pheochromocytomas and paragangliomas: A retrospective cohort study, systematic review and meta-analysis*. Endocrine Abstracts. 2022: Bioscientifica. doi: 10.1530/endoabs.86.P194.
 6. **Oštarijaš E**, Dembrovszky F, Simon OA, Teutsch B, Boros E, Szakó L, Szabó I, Hegyi P, Erőss B. *Comorbidities and rebleeding are associated with significant mortality in non-variceal upper gastrointestinal bleeding (NVUGIB): a systematic review and meta-analysis (MP064)*. In: Tilg H, editor. Proceedings of the 29th United European Gastroenterology Week Virtual 2021. United European Gastroenterology Journal. 2021 Oct;9(S8):204. Vienna, Austria. doi: 10.1002/ueg2.12139. (2021 Q1, IF 6.866)
 7. Boros E, Sipos Z, Hegyi P, Teutsch B, Frim L, Váncsa Sz, Kiss Sz, Dembrovszky F, **Oštarijaš E**, Shawyer A, Erőss B. *Prophylactic transcatheter arterial embolization is associated with lower odds of rebleeding in non-variceal upper gastrointestinal bleeding: a systematic review and meta-analysis (P1058)*. In: Tilg H, editor. Proceedings of the 29th United European Gastroenterology Week Virtual 2021. United European Gastroenterology Journal. 2021 Oct;9(S8):869. Vienna, Austria. doi: 10.1002/ueg2.12139. (2021 Q1, IF 6.866)
 8. Simon OA, Görbe A, Hegyi P, Szakó L, **Oštarijaš E**, Dembrovszky F, Kiss Sz, Czopf L, Erőss B, Szabó I. *Helicobacter pylori infection is associated with carotid intima and media thickening. A systematic review and meta-analysis (P0094)*. In: Tilg H, editor. Proceedings of the 29th United European Gastroenterology

Week Virtual 2021. United European Gastroenterology Journal. 2021 Oct;9(S8):315. Vienna, Austria. doi: 10.1002/ueg2.12139. (2021 Q1, IF 6.866)

9. Mršić E, Mršić A, **Oštarijaš E**, Kukuljan M. *Computed tomography-guided biopsy of pulmonary lesions: diagnostic yield and complication rate*. Bulletin: Newsletter of the Society of Radiographers of Slovenia & the Chamber of Radiographers of Slovenia. 2019;36(2):29-34.
10. **Oštarijaš E**. *A Myth about Vaccination?*. 17. riječki dani bioetike: Profesionalizam u medicini i zdravstvu. 2015. Croatian.
11. **Oštarijaš E**. *Impact of Acetylsalicylic Acid on Abundance of Drosophila melanogaster*. MedRi Znanstveni piknik 2013. 2013. Croatian.

RESEARCH

Metabolically active brown adipose tissue in PPGL: an observational cohort study

Eduard Oštarijaš¹, Michael C Onyema², Zoulikha Zair², David R Taylor³, Fannie Lajeunesse-Trempe^{2,4}, Saira Reynolds⁵, Nicola Mulholland⁵, Ben Corcoran⁵, Mohamed Halim⁵, Eftychia E Drakou⁶, Ashley B Grossman^{7,8,9}, Royce P Vincent³, Simon J B Aylwin², Georgios K Dimitriadis^{2,10} and Silvija Caneck-Varžić^{1,11}

¹Doctoral School of Clinical Medical Sciences, Medical School, University of Pécs, Pécs, Hungary

²Department of Endocrinology ASO/EASO COM, King's College Hospital NHS Foundation Trust, London, UK

³Department of Clinical Biochemistry (Synnovis), King's College Hospital NHS Foundation Trust, London, UK

⁴Quebec Heart and Lung Institute, Quebec City, Canada

⁵Department of Nuclear Medicine, King's College Hospital NHS Foundation Trust, London, UK

⁶Department of Clinical Oncology, Guy's Cancer Centre – Guy's and St Thomas' NHS Foundation Trust, London, UK

⁷Green Templeton College, University of Oxford, Oxford, UK

⁸Centre for Endocrinology, William Harvey Institute, Barts and The London School of Medicine and Dentistry, London, UK

⁹Neuroendocrine Tumour Unit, Royal Free Hospital, London, UK

¹⁰Faculty of Life Sciences and Medicine, School of Cardiovascular and Metabolic Medicine & Sciences, King's College London, London, UK

¹¹Department of Pathophysiology, Josip Juraj Strossmayer University of Osijek School of Medicine, Osijek, Croatia

Correspondence should be addressed to G K Dimitriadis: georgios.dimitriadis@kcl.ac.uk

Abstract

Brown adipose tissue (BAT) activity, identifiable through fluorodeoxyglucose positron emission tomography (FDG-PET), has gained interest due to its potential link with metabolic disorders and tumour pathophysiology. This study aims to explore the activation of BAT in patients with pheochromocytoma/paraganglioma (PPGL) and its clinical relevance. This retrospective observational study, conducted in a large academic centre in London, reviewed FDG-PET images of 62 confirmed PPGL patients, collected between 2013 and 2021. We assessed patient demographics, biochemistry, radiological features, mutational status and outcomes, focussing on activated BAT detection. Of the 62 patients, 13% demonstrated active brown adipose tissue (aBAT) on FDG-PET imaging. Histopathological confirmation of BAT from one patient was used to validate BAT activation observed during imaging. Multivariate analysis indicated that elevated plasma normetanephrine concentrations were directly proportional to aBAT presence, suggesting their strong association with BAT activation. Despite identifying aBAT, no significant differences were found in BMI, sex, age or mutational status between aBAT-positive and aBAT-negative groups. Kaplan–Meier survival plots assessing overall and progression-free survival did not reach statistical significance. This study underscores the complex interaction between catecholamine excess and BAT activation in patients with PPGLs. The findings suggest that aBAT activity might be an indicator of severe catecholamine excess (especially normetanephrine), potentially influencing patient outcomes. Our study adds to the limited pool of knowledge and offers novel insights into BAT activation in patients with PPGLs, highlighting its potential link with metabolic derangements and patient outcomes.

Keywords: brown adipose tissue; BAT; pheochromocytoma; paraganglioma; PPGL; FDG-PET; catecholamines

Introduction

White adipose tissue (WAT) and brown adipose tissue (BAT) form the main adipose tissue subtypes in humans and several animal species. Recently BAT, owing to its unique metabolic function, has been of increased focus and interest in metabolic research (Santhanam *et al.* 2015). BAT is the major organ of non-shivering thermogenesis in the body, with this activity being dependent on the large number of mitochondria and increased expression of uncoupling protein-1 (UCP-1) activity present within this type of tissue (Fenzl & Kiefer 2014). There are numerous triggers for the metabolic activation of BAT, including cold temperature, low body mass index (BMI), adrenergic agonists and elevated concentration of thyroid hormones (Marlatt & Ravussin 2017).

Clinical research suggests that activation and thermogenesis in BAT is mediated by norepinephrine release from the sympathetic nervous system (Bartness *et al.* 2010). BAT has traditionally been considered to mainly express β_3 -adrenoreceptors; however, *in vitro* studies have indicated that activated β_2 -adrenoreceptors may be the main driving force behind thermogenesis (Blondin *et al.* 2020). Active brown adipocytes take up glucose from the circulation, which they use to synthesise free fatty acids (Jung *et al.* 2019). Due to this aspect of BAT metabolism and the increasing use of fluorodeoxyglucose positron emission tomography (^{18}F FDG-PET) imaging, there has been an increased detection rate of activated brown adipose tissue (aBAT); this may affect diagnoses by leading to false-positive reporting of tumours (Nedergaard *et al.* 2007).

BAT is most abundant in fetuses and infants, with significant regression of levels into adulthood. In newborn infants, BAT is located in large interscapular and perirenal depots, while in adults, BAT is mainly located in the neck, mediastinum, axilla, retroperitoneum and abdominal wall (Iyer *et al.* 2009).

Phaeochromocytomas/paragangliomas (PPGLs) are catecholamine-producing endocrine tumours that emerge from the adrenal medulla or extra-adrenal ganglia. High FDG accumulation in aBAT has been frequently noted in patients with PPGL, with subsequent resolution of these findings after PPGL resection (Terada *et al.* 2019). This finding is likely related to the increased glucose transport related to norepinephrine excess (Iyer *et al.* 2009).

Studies reviewing PPGLs have shown an aBAT detection rate of 7.8–42.8% on FDG-PET imaging, correlating with elevated catecholamine levels but without clear correlation to germline mutations (Hadi *et al.* 2007, Wang *et al.* 2011, Puar *et al.* 2016, Abdul Sater *et al.* 2020). In one study, this imaging finding was associated with a statistically significant reduction in overall survival (OS) (Abdul Sater *et al.* 2020). Standardisation for standardised uptake value (SUV) cut-offs for aBAT

on FDG-PET are lacking, but these are often reported between 1.0 and 2.0 (Sampath *et al.* 2016); in previous studies of PPGL, a cut-off value of >1.5 has been employed (Puar *et al.* 2016, Abdul Sater *et al.* 2020).

Research on the clinical implications of aBAT in patients with PPGL remains scarce. The main objectives of this study were to gain further insights into BAT activation rates in patients with PPGLs and how this may relate to patient demographics, biochemistry, radiological features, mutational status and outcomes. The main hypotheses were that aBAT rates would be significantly linked to the severity of catecholamine excess and could be considered a poor prognostic feature.

Methods

Study design

This is a retrospective observational study across a single tertiary academic institution (King's College Hospital NHS Foundation Trust, UK) evaluating the presence of aBAT in patients who had undergone FDG-PET imaging for suspected PPGL. The selection criteria for FDG-PET included patients with presumed disseminated or extra-adrenal disease or those with intermediate lesions based on strong clinical or radiological suspicion (e.g., findings on CT imaging). These cases were reviewed in adrenal multidisciplinary team meetings, where the indication for FDG-PET was determined. Guideline recommendations for imaging in PPGL were followed (Fassnacht *et al.* 2016).

Patient characteristics and clinical assessment

The following data were collected for each PPGL patient: demographics, baseline biochemistry (plasma metanephrine (pmol/L), normetanephrine (pmol/L) and 3-methoxytyramine (pmol/L)), baseline imaging findings (anatomical location of aBAT, total number of lesions, size of largest lesion and presence of distant metastases), histology, mutational status, treatment modality, response evaluation criteria in solid tumours (RECIST) v1.1 criteria response to treatment (Eisenhauer *et al.* 2009), progression-free survival (PFS) and OS.

The PPGL patients included had their baseline FDG-PET scans reviewed by two nuclear medicine consultant physicians experienced in FDG-PET CT reporting. Cases were independently scored for the presence of aBAT in predetermined locations (supraclavicular, paravertebral or perirenal). Any discrepant cases were mediated by a third such experienced nuclear medicine consultant physician. Images were transferred from the picture archiving and communication system to the HERMES workstation to allow dedicated analysis/SUV quantification. In cases with multiple scans,

we included the first-ever FDG-PET scan that detected aBAT in patients with PPGL for our analysis.

Statistical analysis

Continuous data were assessed for normality using the Shapiro–Wilk test. Normal data were expressed as the mean value with its respective standard deviation ($A_r \pm SD$). Non-normal data were presented as the median with interquartile range (MED (IQR)). We reported categorical data using ratios and percentages. Missing data within the dataset were imputed using the *missRanger* package (version 2.4.0), employing a random forest algorithm for iterative imputation. The function was iterated 1,000 times, with each random forest consisting of 100 trees.

To investigate the potential association of covariates with the incidence of aBAT, we conducted a multivariate analysis using a logistic regression. The model was fitted with Firth's bias reduction method to address issues of small sample sizes and rare events. The analysis incorporated pre-defined clinical covariates, while the results were presented as adjusted odds ratios for each covariate, with their respective 95% confidence intervals (95%–CI) and *P*-values ($\alpha = 0.05$) alongside non-adjusted (crude) ORs. The *logistf* package (version 1.26.0) was used for the multivariate logistic regression analysis.

To assess statistical significance in difference of observed numerical variables, we implemented an R function for non-parametric bootstrap *P*-value calculation (Dwivedi *et al.* 2017) due to relatively small sample size. The function performed iterative resampling (10,000 iterations) to compute *t*-statistics for two-group comparisons, determining the *P*-value based on the proportion of resampled statistics. Statistical significance of independence of categorical data was tested using Fisher's exact tests for count data.

We produced Kaplan–Meier plots to compare the OS and PFS times between the investigated and control group. Due to the sample size, the significance of survival differences was assessed using a univariate Cox model.

All analyses were performed in the R version 4.4.0.

Ethics

Ethical approval from a Regional Ethical Committee (REC) in the United Kingdom (UK) was not required as the data generated for the purposes of this project were fully anonymised, collected in line with the standard of care protocols for treating patients with PPGL at the King's College Hospital, and are processed and presented retrospectively. The study was discussed within research delivery unit 6 (RDU6) meeting – Renal/Endo Research Group Board (RRGB) at the King's College Hospital NHS Foundation Trust

(Governance Arrangements for Research Ethics Committees (GafREC): Endo203). The study is registered with clinicaltrials.gov, with registration number NCT06440122.

Results

An initial list of 93 patients with suspected PPGL having undergone FDG-PET imaging was obtained from the nuclear medicine department covering the time period from 2013 to 2021. After exclusion of duplicate patients and reviewing electronic notes for the inclusion of only those with a PPGL diagnosis confirmed after discussion in multidisciplinary team meetings, this list was reduced to 62 patients (22 male, 40 female).

Three cases were excluded at the stage of dedicated analysis/SUV quantification (two cases had corrupted data and one case was not available) and were excluded from subsequent analyses. Sixty-two cases were subsequently scored. Fifty-four cases (87%) were deemed not to have aBAT (53 initial agreement and one mediation) and eight cases (13%) were deemed to have aBAT (seven initial agreement and one mediation) (Fig. 1). The cases without aBAT would form the basis of unmatched controls for further statistical analysis.

One of our patients in the aBAT-positive cohort had a confirmed diagnosis of MEN 2A proceeding to a right adrenalectomy for pheochromocytoma and total thyroidectomy for medullary thyroid carcinoma (MTC), both in 2014 with satisfactory surgical clearance. Areas of aBAT uptake on FDG-PET were retrospectively confirmed (in supraclavicular, paravertebral, perirenal and 'other' locations with highest maximum standardised uptake value (SUV_{max}) of 10.6) and correlated with BAT on histology specimens (Figs 2, 3, 4).

The results of demographic and clinical data analysis and laboratory, imaging, pathology, treatment and follow-up information are presented in

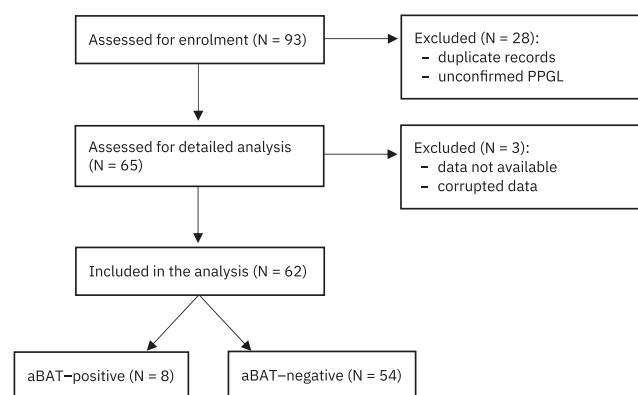
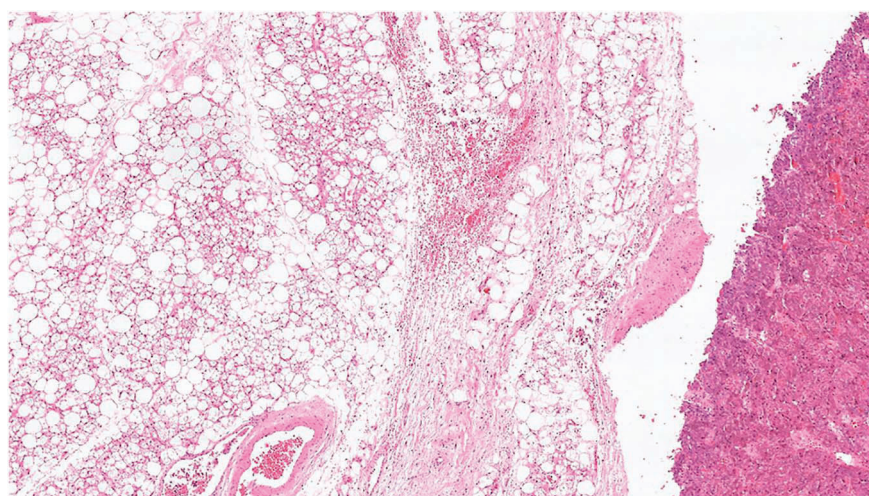


Figure 1
Enrolment and analysis flowchart.

**Figure 2**

Low magnification image shows phaeochromocytoma to the far right of the image in an aBAT patient from our cohort in a retrospective post-surgical specimen. BAT adjacent to the phaeochromocytoma is seen occupying the left two-thirds of the field.

the patient characteristics table (Table 1) with respect to the presence or absence of aBAT. Except for the plasma metanephrine concentration, which was significantly negatively associated with aBAT, the differences in categorical and continuous data between the groups did not reach statistical significance in the univariate analysis. While statistically insignificant, the aBAT-positive group showed trends (defined as $P < 0.2$) in association with lower age, female sex, lower BMI, absence of prior cardiovascular disease, lower number of antihypertensive medication and lower OS. In our study, although no patients with detectable aBAT were taking adrenoreceptor blockade, we found no statistical association between aBAT and either alpha- or beta-blocking medication ($P = 0.581$ and $P = 1.000$, respectively). Detailed per-patient data for the aBAT-positive group are available separately in Table 2.

Penalised multivariate analysis with multiple clinical covariates indicated that male sex (adjusted OR 0.1; CI 0.00, 1.05), tumour type (adjusted OR 2.10; CI 0.37, 16.41), hypertension (adjusted OR 0.26; CI 0.03, 1.42) and increased plasma metanephrine levels (adjusted OR 0.00; CI 0.00, 1.06) were not significantly associated

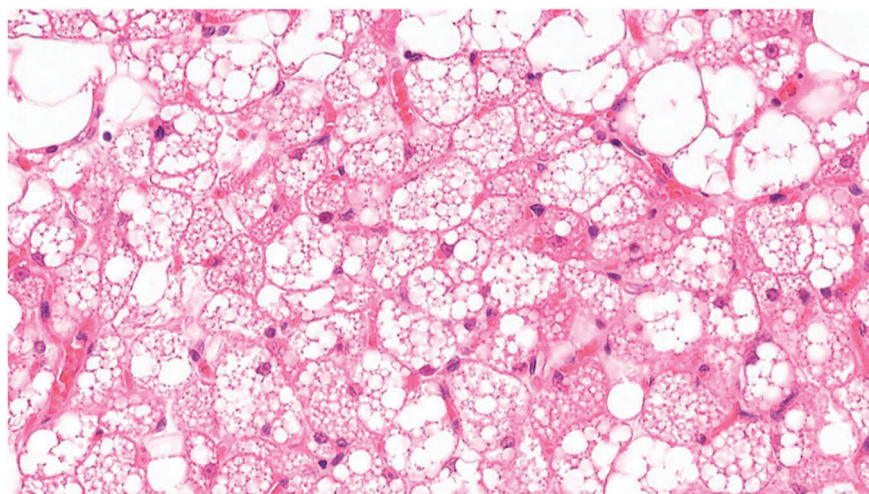
with the presence of aBAT. In contrast, increased plasma normetanephrine levels (adjusted OR 2.85; CI 1.11, 10.35) showed a statistically significant trend towards aBAT presence, as shown in Fig. 5.

The univariate Cox proportional hazards model indicated hazard ratios of 1.77 (CI 0.38, 8.18) and 1.38 (CI 0.30, 6.34) for overall and PFS probabilities, respectively. The survival data for both overall and PFS are visually represented using Kaplan–Meier survival curves in Fig. 6.

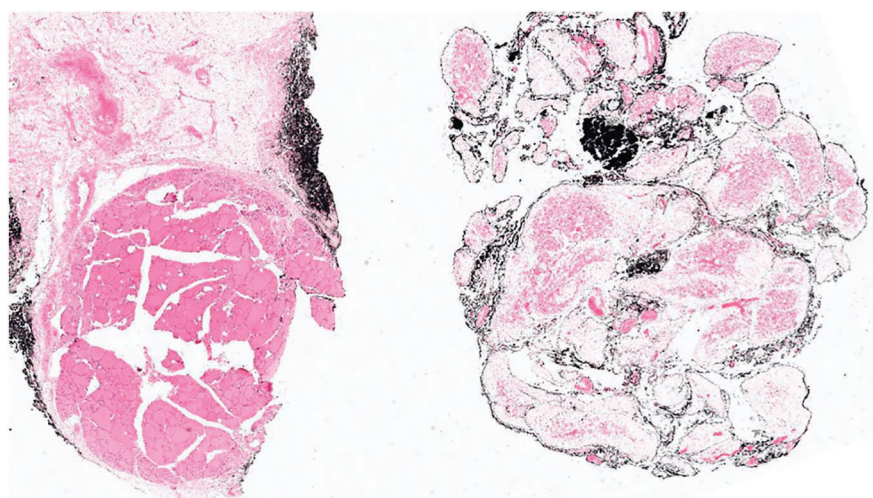
Discussion

The main objectives of our study were to investigate BAT activation rates detected by FDG-PET and its relationship with patients' characteristics, biochemistry, radiological features, mutational status and outcomes in patients with PPGLs.

Previous studies reviewing PPGLs have reported on probable BAT activity in patients with PPGL. Specifically, an aBAT prevalence of 7.8–42.8% was observed on FDG-PET imaging using less stringent

**Figure 3**

At higher magnification (from Fig. 2), the adipocytes in brown fat show multivacuolated cytoplasm resulting from numerous small lipid droplets. The cytoplasm is acidophilic and granular due to large number of mitochondria. Small number of white fat adipocytes are present in this field for comparison. These have a single intracytoplasmic large fat droplet only.

**Figure 4**

Low magnification shows thyroid tissue on the left-hand side of the field and brown fat in the adjacent right-hand side of the field.

criteria of SUV_{max} cut-offs for aBAT between 1.0 and 2.0; in other cases, activity of BAT was quantified by mean standardised uptake values (SUV_{mean}) (Hadi *et al.* 2007, Wang *et al.* 2011). We found that 13% of PPGL patients had aBAT positivity on FDG-PET imaging ($n = 8/62$) using a stricter criterion of SUV_{max} cut-off value of 1.5 in line with more recent findings (Puar *et al.* 2016, Abdul Sater *et al.* 2020).

However, FDG-PET analysis alone does not confirm BAT, but only suggests its presence due to its correlation with anatomical area of specific metabolic activity. One of our patients in the aBAT-positive cohort with a confirmed diagnosis of MEN 2A underwent right adrenalectomy for phaeochromocytoma and total thyroidectomy for MTC. BAT adjacent to the phaeochromocytoma and MTC was histopathologically confirmed in line with the FDG-PET findings, providing a direct validation of BAT activation.

To the best of our knowledge, this is the first clinical study assessing BAT activation on FDG-PET and its clinical implications in PPGL patients with histopathological confirmation of BAT. Albeit on a single patient, the pathological confirmation supports the correlation between imaging findings and true aBAT in our study. Furthermore, unlike other clinical cohort papers assessing aBAT in PPGL patients, our study incorporates a robust multivariate statistical approach, additionally contributing to the generalisability of implications.

From a methodological and statistical standpoint, the main limitations of this study arise from its retrospective nature and the relatively small number of cases. While we histopathologically confirmed aBAT in one patient, consistent histological correlation across multiple cases was not feasible due to the ethical and practical constraints of obtaining multiple biopsies from patients in clinical and surgical practice. In addition, the retrospective observational design of our study limited

the ability to systematically perform such analyses. As with all cohort studies, it is also possible that transient or persistent confounding factors that could have affected the results were overlooked. Despite having access to electronic records, the information was not always comprehensive for some out-of-region cases, leading to known or unknown missing data points. However, to ensure robust imputation, we employed a random forest algorithm for iterative imputing using 1,000× iterations, with each random forest consisting of 100 trees. Nevertheless, because of relatively low sample size given the rarity of this group of neoplasms and the less common use of FDG-PET imaging to characterise them, the implied trends in our study should be interpreted with caution.

Regarding the clinical characteristics of patients and BAT activation, our study did not reveal significant differences between the aBAT-positive and aBAT-negative groups in terms of BMI, sex or age; although age is often considered the strongest determinant of BAT activation (Pfannenberger *et al.* 2010, Puar *et al.* 2016), the limited age range for these patients may not have identified this.

The inclusion of our study's results in a recently performed cumulative meta-analysis has further validated our findings (Onyema *et al.* 2024). The meta-analysis revealed a statistically significant positive association between demethylated catecholamine levels and the presence of aBAT, while the inclusion of our study reduced overall heterogeneity in the pooled data, particularly in terms of catecholamine level variability. Sensitivity analyses, conducted with and without our data, demonstrated that our findings reduced heterogeneity and reinforced the observed trends. This confirms the reliability of our results across analytical scenarios, despite the initial non-significance of normetanephrine levels in our univariate analysis. By contributing to a larger evidence pool, our study enhanced the statistical robustness of

Table 1 Patient characteristics table.

	aBAT-positive (n = 8)	aBAT-negative (n = 54)	Pre-imputation data availability	P-value
Demographic information				
Age (years)	46.0 (29.8, 51.0)	54.5 (39.8, 60.8)	61/62 (98.4%)	0.126
Sex			62/62 (100%)	0.240
Female	7 (87.5%)	33 (61.1%)		
Male	1 (12.5%)	21 (38.9%)		
Clinical data				
BMI (kg/m ²)	25.8 ± 4.82	26.9 ± 5.23	51/62 (82.3%)	0.548
Prior cardiovascular disease	0 (0%)	13 (24.1%)	59/62 (95.2%)	0.186
Hypertension	2 (25%)	29 (53.7%)	59/62 (95.2%)	0.255
Number of antihypertensives	0.389 ± 0.737	0.903 ± 1.090	57/62 (91.9%)	0.083
Alpha-blockade	0 (0%)	8 (14.81%)	59/62 (95.2%)	0.581
Beta-blockade	0 (0%)	5 (9.26%)	59/62 (95.2%)	1.000
Positive family history	1 (12.5%)	6 (11.1%)	56/62 (90.3%)	1.000
Laboratory parameters				
Plasma metanephrine (pmol/L)	279 (202, 913)	505 (169, 1,920)	57/62 (91.9%)	0.034
Plasma normetanephrine (pmol/L)	7,740 (674, 14,700)	2,320 (1,010, 10,100)	58/62 (93.6%)	0.434
Ratio of plasma normetanephrine/metanephrine	14.3 (3.66, 25.90)	6.45 (3.03, 17.70)		0.472
Plasma 3-methoxytyramine (pmol/L)	131 (120, 231)	120 (120, 232)	56/62 (90.3%)	0.876
Imaging and pathology				
Number of aBAT locations	3.90 ± 2.78	Not applicable	8/8 (100%)	
Highest aBAT SUV _{max}	5.69 (3.87, 12.70)	Not applicable	8/8 (100%)	
Tumour type			58/62 (93.6%)	1.000
Pheochromocytoma	5 (62.5%)	34 (63.0%)		
Paraganglioma	3 (37.5%)	20 (37.0%)		
Size of largest tumour (mm)	57.5 (48.7, 70.3)	49.5 (30.0, 64.3)	54/62 (87.1%)	0.876
Cluster			62/62 (100%)	1.000
No mutation	4 (50.0%)	17 (31.5%)		
Cluster 1 (SDHx, VHL)	1 (12.5%)	9 (16.7%)		
Cluster 2 (MEN, RET)	0 (0%)	2 (3.7%)		
Unknown	3 (37.5%)	26 (48.1%)		
AJCC staging			57/62 (91.9%)	0.374
1	1 (12.5%)	16 (29.6%)		
2	1 (12.5%)	14 (25.9%)		
3	3 (37.5%)	8 (14.8%)		
4	3 (37.5%)	16 (29.6%)		
Metastatic disease	3 (37.5%)	16 (29.6%)	57/62 (91.9%)	0.692
Treatment				
Chemotherapy	1 (12.5%)	4 (7.41%)	59/62 (95.2%)	0.511
Surgery	6 (75%)	46 (85.2%)	60/62 (96.8%)	0.604
Radiotherapy	0 (0%)	3 (5.56%)	60/62 (96.8%)	1.000
MIBG therapy	1 (12.5%)	8 (14.8%)	59/62 (95.2%)	1.000
Follow-up				
RECIST v1.1 criteria			62/62 (100%)	0.292
CR	1 (12.5%)	11 (20.4%)		
PR	0 (0%)	6 (11.1%)		
SD	0 (0%)	2 (3.7%)		
PD	3 (37.5%)	5 (9.3%)		
No data	4 (50.0%)	30 (55.6%)		
Mortality	2 (25.0%)	12 (22.2%)	62/62 (100%)	1.000
PFS (months)	41.0 (22.5, 60.0)	36.0 (24.3, 55.3)	62/62 (100%)	0.913
OS (months)	41.0 (23.3, 60.8)	47.5 (32.8, 95.3)	62/62 (100%)	0.136

Non-normal data presented as median with interquartile range (MED (IQR)). BMI, body mass index; PFS, progression-free survival; OS, overall survival; aBAT, active brown adipose tissue; SUV_{max}, maximum standardised uptake value; RECIST, response evaluation criteria in solid tumours; CR, complete response; PR, partial response; SD, stable disease; PD, progressive disease.

the meta-analysis, offering a more robust perspective on aBAT prevalence and its biochemical correlates. Animal studies have shown that norepinephrine stimulation of BAT via β_3 -receptors leads to an increased number of

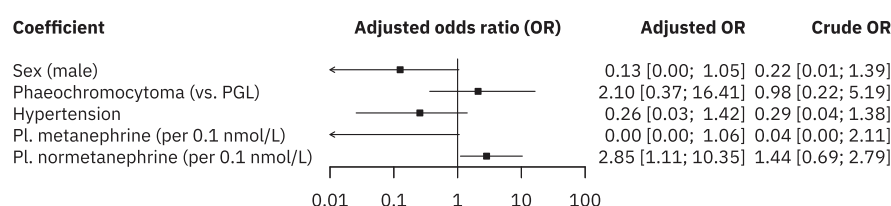
BAT cells, lipolysis, glucose transportation, uncoupling protein-1 (UCP1) expression, and ultimately, thermogenesis (Cannon & Nedergaard 2004, Puar *et al.* 2016). Significant BAT activation in patients with PPGLs is

Table 2 Individual characteristics of patients with aBAT.

Patient	Age	Sex	BMI (kg/ m ²)	PI. metanephrine (pmol/L)	PI. normetanephrine (pmol/L)	PI. 3- methoxytyramine (pmol/L)	Hypertension	Highest SUV _{max}	Tumour type	Size of largest tumour (mm)	Mutational status	Metastatic disease	Family history	No mortality	RECIST v1.1
1	45	F	26.2	56	337	142	No	3.88	PCC	49	N/A	No	–	Yes	ND
2	29	M	24.6	1,766	>40,000	235	No	10.60	PCC	71	W/T	No	–	Yes	ND
3	61	F	28.6	134	<109	<120	No	3.39	PGL	70	N/A	Yes	–	No	PD
4	49	F	N/A*	224	14,476	677	Yes	4.09	PCC	65	W/T	Yes	–	No	PD
5	28	F	22.1	1,966	7,945	<120	No	23.40	PCC	46	W/T	No	–	No	CR
6	47	F	35.5	314	786	<120	Yes	7.29	PCC	49	N/A	No	–	–	ND
7	57	F	20.8	243	7,544	<120	No	3.83	PGL	50	W/T	No	–	–	ND
8	30	F	21.4	629	15,227	229	No	18.81	PGL	86	SDHB	Yes	+	No	PD

BMI, body mass index; M, male; F, female; SUV_{max}, maximum standardised uptake value; PCC, pheochromocytoma; PGL, paraganglioma; N/A, not available; W/T, wild-type; SDHB, succinate dehydrogenase complex subunit B; RECIST, response evaluation criteria in solid tumours; ND, no data; PD, progressive disease; CR, complete response; aBAT, active brown adipose tissue.

*Patient no. 4's BMI was recorded as 12.6 kg/m². Due to concerns about the reliability of this value, we initially included their anthropometric data, but encountered difficulties in validating it, despite multiple attempts. While such a low BMI is clinically plausible, we were unable to confirm its accuracy through available clinical notes. To address this, we performed an imputation analysis to evaluate its plausibility in the context of other parameters for this patient. Ultimately, we treated this value as missing data and excluded it from the analysis. This adjustment did not affect the statistical significance in BMI difference between the groups.

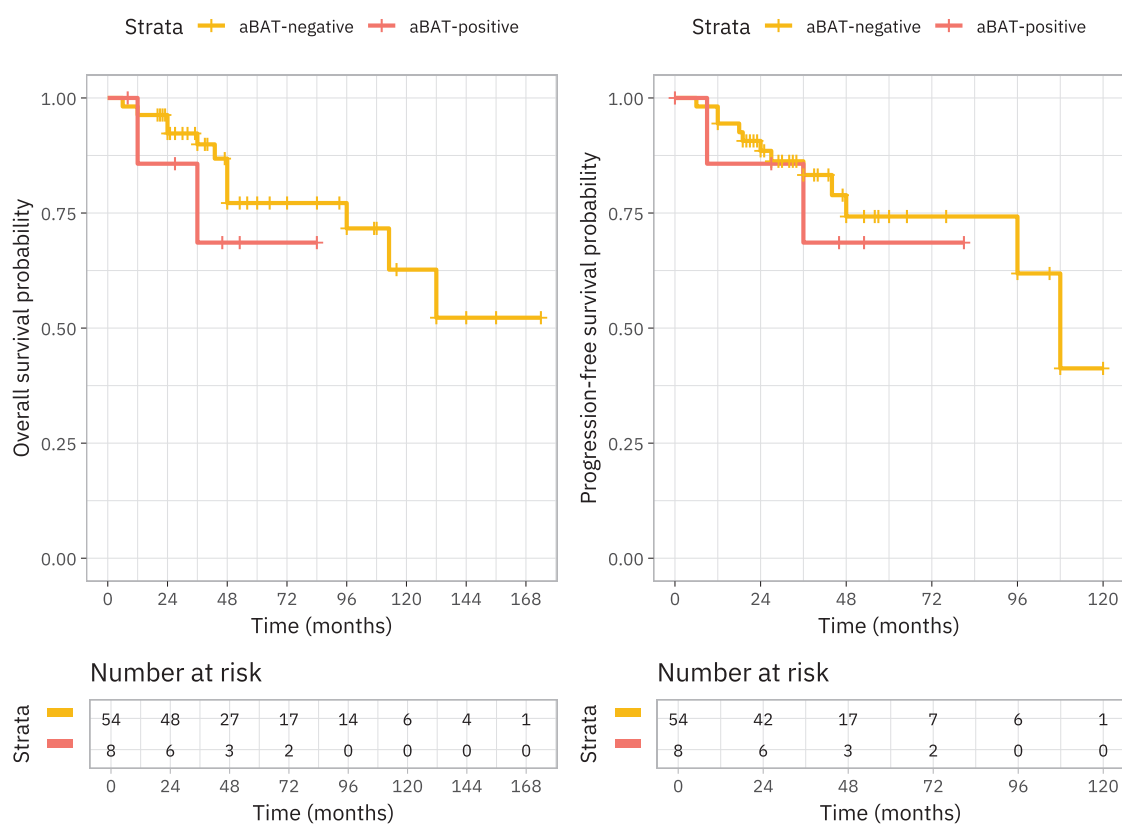
**Figure 5**

Forest plot showing multivariate adjusted and unadjusted odds ratios of aBAT presence associated with multiple covariates.

likely to be due to the systemic effects of catecholamine excess, as reported in previous studies (Puar *et al.* 2016). In our study, average normetanephrine concentration was higher in the aBAT-positive group, which was statistically significant in the multivariate analysis, although this difference did not reach the limit of significance in the univariate analysis of the differences in medians. Plasma metanephrine levels, however, showed statistical significance in the univariate analysis, inversely proportional to the presence of aBAT, indicating a potentially strong preference for increased normetanephrine/metanephrine ratio's association with BAT activation. Although norepinephrine is typically associated with both phaeochromocytomas and paragangliomas (unlike epinephrine, which is produced only in phaeochromocytomas) (Al-Harthy *et al.* 2009),

our study had comparable numbers of patients with phaeochromocytomas and paragangliomas associated with activated BAT. Since aBAT is a highly vascularised and metabolically active tissue, it could facilitate the clearance of circulating catecholamines. It may uptake and metabolise catecholamines as part of its thermogenic activity, potentially reducing the demethylated catecholamine pool available for conversion into metanephrines. In addition, the aBAT-positive group might represent a subgroup with a distinct hormonal or tumour phenotype leading to an altered catecholamine production or metabolism.

In addition, 86% of our patients were deemed to not have aBAT. This raises the question of whether there are other mechanisms of BAT activation beyond sympathetic stimulation and what are the other 'browning' factors

**Figure 6**

Kaplan-Meier survival plots: (A) OS, (B) PFS.

in PPGL. BAT activation has previously been linked to malignancies (Santhanam *et al.* 2015), and clinical studies have reported characteristic alterations in BAT in patients with cancer (Dong *et al.* 2023). Evidence regarding the role of catecholamine excess in BAT activation in these patients is controversial. The mechanisms underlying dynamic interactions between cancer cells and stromal adipocytes remain unclear (Paré *et al.* 2020). It is generally believed that BAT predominantly expresses β_3 -adrenoreceptors and exhibits enhanced norepinephrine responsiveness compared to WAT (Cero *et al.* 2021). However, *in vitro* experiments indicate that thermogenesis in BAT might primarily be mediated through the stimulation of β_2 -adrenoreceptors (Blondin *et al.* 2020). Although no patients with detectable aBAT in our study were taking adrenoreceptor blockade, the lack of statistical association between aBAT and either alpha- or beta-blocking medication ($P = 0.581$, $P = 1.000$, respectively) suggests that these medications were unlikely to confound our findings. However, the possibility of an undetected influence cannot be completely excluded.

BAT activation, including browning of WAT to form beige adipocytes, can be induced by multiple factors including thyroxine, bile acids and factors overexpressed in certain malignant tumours, including interleukin 6 (IL-6), parathyroid hormone-related peptide (PTH-rP), fibroblast growth factor 21 and natriuretic peptides (Villarroya & Vidal-Puig 2013, Abdul Sater *et al.* 2020). PPGLs, while principally being known for secretion of catecholamines, can also secrete various growth factors responsible for autocrine or paracrine functions (Kontogeorgos *et al.* 2002, Abdul Sater *et al.* 2020). Adrenomedullin (ADM), a vasodilator peptide hormone induced by hypoxia, was initially isolated in 1993 from a pheochromocytoma (Kitamura *et al.* 1993). In a three-dimensional mammosphere model, breast cancer cells secrete adrenomedullin to promote lipolysis and browning of adjacent mature adipocytes, which highly express the adrenomedullin receptors (Paré *et al.* 2020, Dong *et al.* 2023). Further studies are needed to investigate the association between PPGLs and browning factors other than catecholamines.

Anatomically, many types of solid tumours (e.g., breast cancer, prostate cancer and renal cancer) grow in either direct contact or close proximity to adipose tissue, which provides a suitable model for studies investigating the direct interactions between cancer cells and adipocytes (Dong *et al.* 2023). Tumour cells interact with the cells that compose their environment to promote tumour growth and invasion. Among them, adipocytes provide lipids that are used as a source of energy and adipokines that contribute to tumour expansion (Paré *et al.* 2020, Dong *et al.* 2023). Although beneficial in some other circumstances, such as obesity and diabetes prevention, BAT was found to contribute to the development of complications, such as cancer-induced cachexia (Nishio & Saeki 2020, Jalloul *et al.* 2023). It was hypothesised as

early as 1981 that BAT activation induces a hypermetabolic state and contributes to weight loss in cancer patients (Ma *et al.* 2015, Jalloul *et al.* 2023). Recent studies have emphasised the potential implication of BAT activity in the weight status of oncological patients and demonstrated that localisation, along with the amount of activated BAT, could influence its effects on BMI (Jalloul *et al.* 2023). Moreover, a recently published case report described a patient with pheochromocytoma and BAT activation, evidenced by significant FDG uptake that resolved postoperatively alongside normalisation of plasma catecholamine levels (Md Nor *et al.* 2024).

In our study, we found that increased plasma normetanephrine concentration were associated with active BAT. We did not find that BAT activation was significantly associated with any assessed imaging findings, other pathological findings or treatment modalities. BAT activation was also not associated with specific germline mutations, which is consistent with previous findings (Puar *et al.* 2016). In our study, we observed a greater proportion in advanced AJCC staging in aBAT-positive patients. Specifically, 75% of aBAT-positive patients were classified as stage 3 or 4, compared to only 44.4% of aBAT-negative patients, although this difference did not reach statistical significance. This disparity in tumour stage is possible to contribute to the shorter survival rates observed in aBAT positive patients. Hence, we aimed to account for tumour stage in the multivariate analysis or compare the eight aBAT-positive subjects to a matched control cohort, but the small sample size limits the statistical power and interpretability of such comparisons in the context of survival analysis.

There is growing interest in prognostic biomarkers that can predict metastatic disease and survival in patients with PPGL. In our study, Kaplan–Meier survival plots indicated trends towards reduced OS and PFS in the aBAT-positive group; however, due to the stricter SUV_{max} cut-off used in our study and small sample size, this information was statistically underpowered. Previous studies have shown that elevated levels of norepinephrine and the detection of BAT activity by FDG-PET in patients with PPGL were associated with decreased OS, with norepinephrine as an independent risk factor for mortality, likely unrelated to cardiovascular complications (Abdul Sater *et al.* 2020). Mechanistically, there is evidence suggesting that aBAT may confer poorer outcomes due to its contribution to a hypermetabolic state, which has been linked to cancer cachexia, malnutrition and metabolic derangements (Shellock *et al.* 1986, Beijer *et al.* 2012). It is well-established that severe catecholamine excess can exacerbate metabolic instability and increase cardiovascular disease risk – e.g., elevated catecholamine levels can lead to a catecholamine-induced cardiomyopathy in patients with pheochromocytoma (Wilkenfeld *et al.* 1992, Zhang *et al.* 2017, Szatko *et al.* 2023).

However, preclinical evidence indicates that aBAT activity may contribute to weight loss and cancer cachexia, a condition characterised by profound malnutrition and systemic metabolic disruption (Brooks *et al.* 1981). These factors could compromise patient resilience, potentially leading to lower performance scores, reduced ability to tolerate treatments and a diminished likelihood of surgical interventions leading to poorer survivability.

The role of catecholamines in tumour progression remains intriguing. Earlier studies have suggested that catecholamines directly affect tumour cell behaviour and gene expression by growth-promoting effects and possible chemotactic activity of norepinephrine-producing organs to recruit tumour cells (adrenal gland and brain are the common sites of metastasis for several sites of malignancies). In addition, catecholamines have been shown to have anti-apoptotic effects on cancer cells and may render tumour cells resistant to chemotherapeutic drugs (Yang 2010). The variable effects of catecholamines can potentially be explained by the variable expression of nine adrenergic receptor isoforms and other factors, including catecholamine effects on cancer cells versus immune or endothelial cells (Wackerhage *et al.* 2022).

In the context of PPGL, severe catecholamine excess and its systemic effects may not only activate BAT, but also further exacerbate the negative impact of aBAT activity. The mechanistic pathways involving hypermetabolism, cancer cachexia, malnutrition and cardiovascular risks support the plausibility of aBAT being an independent determinant of survival. However, further research (both preclinical and clinical) based on prospective studies is required to delineate these pathways more clearly in the context of aBAT in patients with PPGL.

Conclusions

Based on complex association between catecholamine levels and activation of BAT in patients with PPGL, our study investigated the potential role of aBAT as a marker of catecholamine excess and potential subsequent clinical outcomes in these patients. While the presence of aBAT significantly correlated only with elevated plasma normetanephrine concentration, the observed trends towards reduced survival in aBAT-positive patients suggest a potential link between BAT activation and more aggressive disease state. Although small, our study and the used robust statistical approach enrich the limited pool of existing data, allowing for future secondary analyses and thereby adding significant value to the cumulative knowledge in this domain. Future research should focus on generating data from larger prospective cohort and clarifying the underlying mechanisms of BAT activation beyond sympathetic stimulation, exploring further metabolic and molecular

‘being’ factors in PPGL, and investigating the prognostic implications of BAT activity.

Declaration of interest

EO received an honorarium from Krka. GKD received research grants from NIHR, Novo Nordisk, UK Research Foundation and DDM, and payment or honoraria for lectures, presentations, speakers’ bureaus, manuscript writing or educational events from Novo Nordisk, Rhythm Pharmaceuticals, J&J/Ethicon and Medtronic. SCV received research grants, payment or honoraria for lectures, presentations or educational events from Novo Nordisk, Eli Lilly, Medtronic and Krka. GKD, EO and SCV report that there is no conflict of interest that could be perceived as prejudicing the impartiality of the work reported. Other authors did not report conflicts of interest.

Funding

GKD received NIHR Southeast London Clinical Research Network (CRN) ‘Greenshoots’ Investigator Award, which allowed protected time to complete this work. This work did not receive any specific grant from any funding agency in the public, commercial or not-for-profit sector.

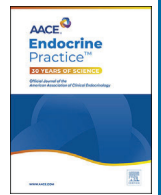
Acknowledgements

We would like to extend our gratitude to Aparajita Roy, Raissa Minhas, Jessica Kearney and Asma Omran for their contributions to the data collection process.

References

- Abdul Sater Z, Jha A, Hamimi A, *et al.* 2020 Pheochromocytoma and paraganglioma patients with poor survival often show brown adipose tissue activation. *J Clin Endocrinol Metab* **105** 1176–1185. (<https://doi.org/10.1210/clinem/dgz314>)
- Al-Harthy M, Al-Harthy S, Al-Otieschan A, *et al.* 2009 Comparison of pheochromocytomas and abdominal and pelvic paragangliomas with head and neck paragangliomas. *Endocr Pract* **15** 194–202. (<https://doi.org/10.4158/ep.15.3.194>)
- Bartness TJ, Vaughan CH & Song CK 2010 Sympathetic and sensory innervation of brown adipose tissue. *Int J Obes* **34** (Supplement 1) S36–S42. (<https://doi.org/10.1038/ijo.2010.182>)
- Beijer E, Schoenmakers J, Vijgen G, *et al.* 2012 A role of active brown adipose tissue in cancer cachexia? *Oncol Rev* **6** e11. (<https://doi.org/10.4081/oncol.2012.e11>)
- Blondin DP, Nielsen S, Kuipers EN, *et al.* 2020 Human brown adipocyte thermogenesis is driven by β 2-AR stimulation. *Cell Metab* **32** 287–300 e7. (<https://doi.org/10.1016/j.cmet.2020.07.005>)
- Brooks SL, Neville AM, Rothwell NJ, *et al.* 1981 Sympathetic activation of brown-adipose-tissue thermogenesis in cachexia. *Biosci Rep* **1** 509–517. (<https://doi.org/10.1007/bf01121584>)
- Cannon B & Nedergaard J 2004 Brown adipose tissue: function and physiological significance. *Physiol Rev* **84** 277–359. (<https://doi.org/10.1152/physrev.00015.2003>)
- Cero C, Lea HJ, Zhu KY, *et al.* 2021 β 3-Adrenergic receptors regulate human brown/beige adipocyte lipolysis and thermogenesis. *JCI Insight* **6** e139160. (<https://doi.org/10.1172/jci.insight.139160>)
- Dong K, Wei G, Sun H, *et al.* 2023 Metabolic crosstalk between thermogenic adipocyte and cancer cell: dysfunction and therapeutics. *Curr Opin Pharmacol* **68** 102322. (<https://doi.org/10.1016/j.coph.2022.102322>)

- Dwivedi AK, Mallawaarachchi I & Alvarado LA 2017 Analysis of small sample size studies using nonparametric bootstrap test with pooled resampling method. *Stat Med* **36** 2187–2205. (<https://doi.org/10.1002/sim.7263>)
- Eisenhauer EA, Therasse P, Bogaerts J, *et al.* 2009 New response evaluation criteria in solid tumours: revised RECIST guideline (version 1.1). *Eur J Cancer* **45** 228–247. (<https://doi.org/10.1016/j.ejca.2008.10.026>)
- Fassnacht M, Arlt W, Bancos I, *et al.* 2016 Management of adrenal incidentalomas: European society of endocrinology clinical practice guideline in collaboration with the European network for the study of adrenal tumors. *Eur J Endocrinol* **175** G1–G34. (<https://doi.org/10.1530/eje-16-0467>)
- Fenzl A & Kiefer FW 2014 Brown adipose tissue and thermogenesis. *Horm Mol Biol Clin Investig* **19** 25–37. (<https://doi.org/10.1515/hmbci-2014-0022>)
- Hadi M, Chen CC, Whatley M, *et al.* 2007 Brown fat imaging with (18)F-6-fluorodopamine PET/CT, (18)F-FDG PET/CT, and (123)I-MIBG SPECT: a study of patients being evaluated for pheochromocytoma. *J Nucl Med* **48** 1077–1083. (<https://doi.org/10.2967/jnumed.106.035915>)
- Iyer RB, Guo CC & Perrier N 2009 Adrenal pheochromocytoma with surrounding brown fat stimulation. *AJR Am J Roentgenol* **192** 300–301. (<https://doi.org/10.2214/ajr.08.1166>)
- Jalloul W, Moscalu M, Moscalu R, *et al.* 2023 Off the beaten path in oncology: active brown adipose tissue by virtue of molecular imaging. *Curr Issues Mol Biol* **45** 7891–7914. (<https://doi.org/10.3390/cimb45100499>)
- Jung SM, Sanchez-Gurmaches J & Guertin DA 2019 Brown adipose tissue development and metabolism. *Handb Exp Pharmacol* **251** 3–36. (https://doi.org/10.1007/164_2018_168)
- Kitamura K, Kangawa K, Kawamoto M, *et al.* 1993 Adrenomedullin: a novel hypotensive peptide isolated from human pheochromocytoma. *Biochem Biophys Res Commun* **192** 553–560. (<https://doi.org/10.1006/bbrc.1993.1451>)
- Kontogeorgos G, Scheithauer BW, Kovacs K, *et al.* 2002 Growth factors and cytokines in paragangliomas and pheochromocytomas, with special reference to sustentacular cells. *Endocr Pathol* **13** 197–206. (<https://doi.org/10.1385/ep:13:3:197>)
- Ma J, Huang M, Wang L, *et al.* 2015 Obesity and risk of thyroid cancer: evidence from a meta-analysis of 21 observational studies. *Med Sci Monit* **21** 283–291. (<https://doi.org/10.12659/msm.892035>)
- Marlatt KL & Ravussin E 2017 Brown adipose tissue: an update on recent findings. *Curr Obes Rep* **6** 389–396. (<https://doi.org/10.1007/s13679-017-0283-6>)
- Md Nor MN, Healy K, Feeney J, *et al.* 2024 Brown adipose tissue activation on ¹⁸F-FDG-PET/CT manifesting as cachexia in a patient with pheochromocytoma. *JCEM Case Rep* **2** luae082. (<https://doi.org/10.1210/jcemcr/luae082>)
- Nedergaard J, Bengtsson T & Cannon B 2007 Unexpected evidence for active brown adipose tissue in adult humans. *Am J Physiol Endocrinol Metab* **293** E444–E452. (<https://doi.org/10.1152/ajpendo.00691.2006>)
- Nishio M & Saeki K 2020 The remaining mysteries about brown adipose tissues. *Cells* **9** 2449. (<https://doi.org/10.3390/cells9112449>)
- Onyema MC, Ostarijas E, Zair Z, *et al.* 2024 The role of active brown adipose tissue in patients with pheochromocytoma or paraganglioma. *Endocr Pract* **31** 208–214. (<https://doi.org/10.1016/j.eprac.2024.11.003>)
- Paré M, Darini CY, Yao X, *et al.* 2020 Breast cancer mammospheres secrete adrenomedullin to induce lipolysis and browning of adjacent adipocytes. *BMC Cancer* **20** 784. (<https://doi.org/10.1186/s12885-020-07273-7>)
- Pfannenberger C, Werner MK, Ripkens S, *et al.* 2010 Impact of age on the relationships of brown adipose tissue with sex and adiposity in humans. *Diabetes* **59** 1789–1793. (<https://doi.org/10.2337/db10-0004>)
- Puar T, Van Berkel A, Gotthardt M, *et al.* 2016 Genotype-dependent brown adipose tissue activation in patients with pheochromocytoma and paraganglioma. *J Clin Endocrinol Metab* **101** 224–232. (<https://doi.org/10.1210/jc.2015-3205>)
- Sampath SC, Sampath SC, Bredella MA, *et al.* 2016 Imaging of brown adipose tissue: state of the art. *Radiology* **280** 4–19. (<https://doi.org/10.1148/radiol.2016150390>)
- Santhanam P, Solnes L, Hannukainen JC, *et al.* 2015 Adiposity-related cancer and functional imaging of brown adipose tissue. *Endocr Pract* **21** 1282–1290. (<https://doi.org/10.4158/ep15870.ra>)
- Shellock FG, Riedinger MS & Fishbein MC 1986 Brown adipose tissue in cancer patients: possible cause of cancer-induced cachexia. *J Cancer Res Clin Oncol* **111** 82–85. (<https://doi.org/10.1007/bf00402783>)
- Szatko A, Glinicki P & Gietka-Czernel M 2023 Pheochromocytoma/paraganglioma-associated cardiomyopathy. *Front Endocrinol* **14** 1204851. (<https://doi.org/10.3389/fendo.2023.1204851>)
- Terada E, Ashida K, Ohe K, *et al.* 2019 Brown adipose activation and reversible beige coloration in adipose tissue with multiple accumulations of 18F-fluorodeoxyglucose in sporadic paraganglioma: a case report. *Clin Case Rep* **7** 1399–1403. (<https://doi.org/10.1002/ccr3.2259>)
- Villarroya F & Vidal-Puig A 2013 Beyond the sympathetic tone: the new brown fat activators. *Cell Metab* **17** 638–643. (<https://doi.org/10.1016/j.cmet.2013.02.020>)
- Wackerhage H, Christensen JF, Ilmer M, *et al.* 2022 Cancer catecholamine conundrum. *Trends Cancer* **8** 110–122. (<https://doi.org/10.1016/j.trecan.2021.10.005>)
- Wang Q, Zhang M, Ning G, *et al.* 2011 Brown adipose tissue in humans is activated by elevated plasma catecholamines levels and is inversely related to central obesity. *PLoS One* **6** e21006. (<https://doi.org/10.1371/journal.pone.0021006>)
- Wilkenfeld C, Cohen M, Lansman SL, *et al.* 1992 Heart transplantation for end-stage cardiomyopathy caused by an occult pheochromocytoma. *J Heart Lung Transplant* **11** 363–366.
- Yang EV 2010 Role for catecholamines in tumor progression: possible use for beta-blockers in the treatment of cancer. *Cancer Biol Ther* **10** 30–32. (<https://doi.org/10.4161/cbt.10.1.12260>)
- Zhang R, Gupta D & Albert SG 2017 Pheochromocytoma as a reversible cause of cardiomyopathy: analysis and review of the literature. *Int J Cardiol* **249** 319–323. (<https://doi.org/10.1016/j.ijcard.2017.07.014>)



Review Article

The Role of Active Brown Adipose Tissue in Patients With Pheochromocytoma or Paraganglioma



Michael C. Onyema, MD ¹, Eduard Oštarijaš, MD ², Zoulikha Zair, MD ¹, Aparajita Roy, MD ¹, Raísa Minhas, MD ¹, Fannie Lajeunesse-Trempe, MD, MSc ^{1,3,4}, Jessica Kearney, MD ¹, Eftychia E. Drakou, MD, MSc ⁵, Ashley B. Grossman, MD, FMedSci ^{6,7,8}, Simon JB. Aylwin, MD, PhD ¹, Silvija Canecki-Varžić, MD, PhD ^{2,9}, Georgios K. Dimitriadis, MD, MSc, PhD ^{1,10,*}

¹ Department of Endocrinology ASO/EASO COM, King's College Hospital NHS Foundation Trust, London, United Kingdom

² Doctoral School of Clinical Medical Sciences, Medical School, University of Pecs, Pecs, Hungary

³ Department of Nutrition, Laval University, Quebec City, Canada

⁴ Faculty of Pharmacy, Laval University, Quebec City, Canada

⁵ Department of Clinical Oncology, Guy's Cancer Centre - Guy's and St Thomas' NHS Foundation Trust, London, UK

⁶ Green Templeton College, University of Oxford, Oxford, UK

⁷ Centre for Endocrinology, William Harvey Institute, Barts and the London School of Medicine, London, UK

⁸ Neuroendocrine Tumour Unit, Royal Free Hospital, London, UK

⁹ J. J. Strossmayer University of Osijek, Faculty of Medicine, Osijek, Croatia

¹⁰ Faculty of Life Sciences and Medicine, School of Cardiovascular and Metabolic Medicine and Sciences, Obesity, Type 2 Diabetes and Immunometabolism Research Group, King's College London, London, United Kingdom

ARTICLE INFO

Article history:

Received 6 September 2024

Received in revised form

24 October 2024

Accepted 12 November 2024

Available online 16 November 2024

Key words:

brown adipose tissue

BAT

pheochromocytoma

paraganglioma

positron emission tomography

computed tomography

systematic review

ABSTRACT

Objectives: Metabolically-active brown adipose tissue (aBAT) is a common finding on ¹⁸fluorodeoxyglucose positron emission tomography (FDG-PET) imaging in patients with pheochromocytoma or paraganglioma (PPGL). In addition to its clinical significance, we aimed to explore the prevalence of this finding on FDG-PET imaging in patients with PPGL.

Methods: We conducted a systematic review and meta-analysis of prospective and retrospective studies. Publications were identified through searches in MEDLINE/PubMed, Embase, and SCOPUS from inception until 2022-11-26, with an update check performed on 2024-05-02. Eligible studies included patients with PPGL who had completed FDG-PET imaging. Data on catecholamine levels stratified by the presence of aBAT were extracted and pooled using the random-effects model with the inverse variance method. For the quantitative synthesis, we used standardized mean differences and meta-analysis of proportions. A risk of bias assessment was performed using the Quality in Prognostic Studies tool.

Results: Our search yielded 6 studies suitable for inclusion. Pooled data showed a statistically significant positive difference in isolated demethylated catecholamine levels in aBAT positive groups compared to aBAT negative. No significant differences were found in multiple domains, including tumor size, tumor burden, germline mutations, or location. The proportion of patients with PPGL who present with aBAT stands at approximately 25%.

Conclusions: The demethylated metabolite levels could have potential use in predicting the presence of active brown adipose tissue in patients with PPGL. There is no convincing evidence of increased aBAT prevalence in patients with PPGL and germline mutations. There was, however,

Abbreviations: aBAT, active brown adipose tissue; BAT, brown adipose tissue; CAC, cancer-associated cachexia; F-DA, ¹⁸F-6-fluorodopamine; FDG-PET, ¹⁸fluorodeoxyglucose positron emission tomography; PPGL, pheochromocytoma or paraganglioma; SMD, standardized mean differences; SUV, standardized uptake value; WAT, white adipose tissue.

* Address correspondence to Dr Georgios K Dimitriadis, Department of Endocrinology ASO/EASO COM, King's College Hospital NHS Foundation Trust, Denmark Hill SE5 9RS, London, United Kingdom.

E-mail address: georgios.dimitriadis@kcl.ac.uk (G.K. Dimitriadis).

<https://doi.org/10.1016/j.eprac.2024.11.003>

1530-891X/© 2024 AAACE. Published by Elsevier Inc. This is an open access article under the CC BY license (<http://creativecommons.org/licenses/by/4.0/>).

evidence suggesting that the presence of aBAT may confer poorer outcomes and decreased life expectancy.

© 2024 AACE. Published by Elsevier Inc. This is an open access article under the CC BY license (<http://creativecommons.org/licenses/by/4.0/>).

Introduction

Adipose tissue is commonly identified in 2 distinct forms in humans and mammals – white adipose tissue (WAT) and brown adipose tissue (BAT). WAT functions primarily as an excess energy reservoir whilst remaining an active endocrine organ. On the other hand, it is widely known that BAT has an important role to play in thermoregulation with its much higher concentration of mitochondria and its notable abundance in newborn infants and hibernating animals.¹

With progress into adulthood, BAT mass significantly decreases. The remnants are typically located in the neck, mediastinum, axilla, retroperitoneum, and abdominal wall. Catecholamine stimulation of BAT leads to an increased number of brown fat cells, lipolysis, glucose transport and uncoupled protein-1 expression, resulting in heat generation.²

Human BAT is traditionally thought to primarily express β_3 -adrenoreceptors with increased norepinephrine stimulation compared to that of WAT,³ although in vitro studies have shown that thermogenesis may actually be driven by β_2 -adrenoreceptor stimulation.⁴

Due to increased ¹⁸F-fluorodeoxyglucose accumulation related to norepinephrine stimulation, activated brown adipose tissue (aBAT) is a frequent incidental finding on fluorodeoxyglucose positron emission tomography (FDG-PET) imaging in patients with pheochromocytomas or paragangliomas (PPGLs), which may result in false-positive reporting of tumor tissue.² The notion of FDG uptake in aBAT is supported by several studies performed in both rodents and humans, and case reports have demonstrated the resolution of this radiologic finding after PPGL resection.^{5,6}

Studies examining patients with PPGL have revealed an aBAT rate from 7.8% to 42.8% on FDG-PET imaging, correlating with elevated plasma catecholamine levels, but without any correlation with the specific germline mutations found.^{7–10} In one study, this radiologic finding was linked to significantly increased mortality.¹⁰ There is a lack of standardization in the realms of diagnostic cut-offs for standardized uptake values (SUVs) for aBAT on FDG-PET, but most commonly, this threshold lies between 1.0 and 2.0.¹¹ In previous studies of patients with PPGL, an SUV cut-off of > 1.5 has been used.^{8,10} However, little is known about the precise relationship of aBAT with PPGL and catecholamine levels. There is only one brief narrative review covering this area, according to our current knowledge: this included 3 original research studies, with a conclusion that on FDG-PET, the aBAT detection rate was 27.4% in a pooled cohort of 146 patients (compared to 6.1% in patients with no evidence of PPGL), but no formal meta-analysis was performed.¹²

The main aims of this study were to expand the existing knowledge regarding the incidence of aBAT in PPGL and the possible clinical implications of this finding. This included a better understanding of the possible correlation of aBAT with biochemistry, mutational status, tumor burden, survival/patient outcomes, and patient demographics. We have performed a thorough literature search of available evidence in the form of original research studies followed by a detailed statistical analysis of the results, with the intention of acquiring information to potentially provide valuable clinical insight, including prognostication.

Methods

The study design was set as a systematic review and meta-analysis of original research studies. A protocol was created using the PICO (population, intervention, control, outcomes) framework and registered in the International Prospective Register of Systematic Reviews under the number CRD42021276073 and was conducted based on the Preferred Reporting Items for Systematic Reviews and Meta-Analyses 2020, with the checklist available in the [Supplementary Materials](#) (number 1).

Study Eligibility

The review assessed only peer-reviewed publications in English. We used all of the following inclusion criteria:

- All prospective and retrospective studies examining aBAT in patients with PPGL (randomized controlled trials, observational, cohort, and other).
- Diagnosis of PPGL based on biochemistry, pathognomonic imaging, and/or histology.
- Patients to have completed FDG-PET imaging.

In line with the Cochrane Collaboration's recommendations,¹³ case reports and case series were excluded from the quantitative synthesis as these reports do not provide denominator data.

Search Strategy

The following search key was utilized, with Medical Subject Headings terms in mind: ((brown adipose) OR (brown fat) OR BAT) AND (paragangliom* OR phaeo* OR pheo* OR pheochromocytoma OR paraganglioma) AND (fdg OR pet OR (pet ct) OR positron OR (positron emission tomography computed tomography))

We searched for publications in the following databases: MEDLINE/PubMed, Embase, and SCOPUS. The time frame was set as all studies published from inception until 26 November 2022, with an update check performed on 2 July 2024 in MEDLINE/PubMed, Embase, and SCOPUS. No language filter or any other filters were selected.

Data Collection

Afterward, we imported the abstracts extracted from the search into Covidence (Veritas Health Innovation; <http://www.covidence.org>), a systematic review management tool. Two reviewers then independently performed parallel reviews of all selected abstracts for relevance according to our protocol requirements. From these relevant abstracts, full-text reviews were subsequently performed to select the final appropriate eligible studies for inclusion in the systematic review. Any conflicts between reviewers regarding the inclusion or exclusion of any particular study would be decided from the ultimate decision of an assigned third reviewer.

If an article was unavailable, an email was sent to the study authors to request the full text. Additionally, preliminary results from our group's own cohort study from a single-center experience are included in the statistical analysis. The results, however, will be

presented both with and without it, with the subset available in [Supplementary Materials](#) (number 2).

Risk of Bias Assessment

A qualitative assessment using the Quality in Prognostic Studies tool was performed on all selected studies by 2 reviewers for the potential risk of bias and to help understand the validity of the presented findings. The following 6 domains were assessed and tabulated for each study: study participation, study attrition, prognostic factor measurement, outcome measurement, study confounding, and statistical analysis and reporting. Each domain was discussed and mutually agreed between reviewers as either low, moderate, or high risk of bias, or N/A if “not applicable.” Any disputes were ultimately decided by an assigned third reviewer. The summary of per-study risk of bias assessment is available in the [Supplementary Materials](#) (number 3).

Statistical Analysis

The collected continuous data were initially retrieved into a predefined spreadsheet and subsequently pooled into combined groups of metabolites, ie normetanephrine with metanephrine, and norepinephrine with epinephrine, using the equations for combining groups described in the Cochrane handbook.¹³ We used the random-effects model with the inverse variance method and restricted maximum-likelihood tau-estimation to pool such quantitative data, and to calculate the summary results based on effect sizes. Subsequently, the results were expressed using forest plots as standardized mean differences (SMD) with respective 95%–CIs. Afterwards, a cumulative meta-analysis, using the chronological criterion, was also performed in order to assess the evolution and trends in the data over time, with results plotted on a cumulative forest plot.

Studies were also analyzed using a meta-analysis of proportions with respective 95%–CIs, both as standard and cumulative meta-analytical methods, after each of which a forest plot was generated.

We assessed the statistical heterogeneity using the I^2 statistic for its quantification and the chi-square for the presence of heterogeneity. The heterogeneity quantification statistic was interpreted as low (< 30%), moderate (30% to 50%), substantial (50% to 90%), or considerable (75% to 100%), according to the Cochrane guidelines. Publication bias was to be assessed using Egger’s test of intercept and by visual inspection of funnel plots should the number of selected studies per plot exceed $k = 10$.

All analyses were performed using R statistical software (version 4.4.0, The R Foundation)¹⁴ and *meta* package (version 7.0.0).¹⁵

Results

Search and Selection

Our database search yielded a total of 145 records, 6 of which we deemed eligible for inclusion in our review. A flow-chart of the process is outlined in [Fig. 1](#).

Risk of Bias

At the risk of bias assessment, we found all studies to be eligible for inclusion in this systematic review. An overview by Quality in Prognostic Studies domains is shown in [Fig. 2](#). Detailed results of the analysis can be found in the [Supplementary Material](#).

Highlights

- Concentration of demethylated metabolites (normetanephrine and norepinephrine, vs non-“nor” forms) was significantly higher in patients with active brown adipose tissue (aBAT), indicating their potential as predictive markers in patients with paraganglioma (PPGL)
- The addition of our study to the existing ones in meta-analytical synthesis reduced overall heterogeneity, supporting consistency of results across studies
- Elevated catecholamine concentrations in patients with PPGL were linked to the presence of aBAT on imaging and inversely related to weight/body mass index
- No significant differences in tumor characteristics or life expectancy were noted among patients with PPGL, with or without aBAT
- Although increased mortality was observed in patients with PPGL and aBAT, broader implications for cancer outcomes remain unconfirmed and necessitate further research

Clinical Relevance

This systematic review identifies potential markers for detecting active brown adipose tissue (aBAT) in patients with pheochromocytoma or paraganglioma (PPGL). With meta-analysis increasing the level of evidence in this field, this review could help in refining prognosis and guiding further research into its implications for patient outcomes.

Quantitative Synthesis

The meta-analysis of pooled data showed a statistically significant positive difference in isolated normetanephrine/norepinephrine (SMD = 0.70; CI 0.37, 1.03) catecholamine levels between the aBAT positive ($N = 69$) and negative ($N = 210$) groups, with a low level of heterogeneity ($I^2 = 20\%$, $P = .29$). Isolated metanephrine/epinephrine levels indicated a negative, albeit statistically insignificant, mean difference between the groups (SMD -0.15 ; CI $-0.47, 0.16$). When combined, however, normetanephrine/norepinephrine and metanephrine/epinephrine levels also showed statistically a significant positive difference between the aBAT positive ($N = 67$) and negative ($N = 188$) groups (SMD 0.51; CI 0.18, 0.85) with low, statistically insignificant heterogeneity ($I^2 = 24\%$, $P = .26$) ([Fig. 3](#)).

After performing a cumulative meta-analysis on the combined groups of metabolites in chronological order, the SMD showed variation over time, with initially substantial heterogeneity ($I^2 = 57\%$) reducing over time to low ($I^2 = 24\%$), as well as the confidence interval of the results, indicating a decrease in P -value despite only one study in isolation showing statistical significance ([Figs. 3 and 4](#)).

The proportion of pheochromocytoma patients who also had aBAT was 26% (CI 20%, 32%), with moderate, albeit statistically insignificant, heterogeneity ($I^2 = 32\%$, $P = .18$) ([Fig. 5](#)).¹⁶

Qualitative Synthesis

The studies included were primarily conducted on a retrospective basis, with a PPGL diagnosis being made multi-modally. Cohort samples analyzed ranged from 28 to 205 patients. The included studies revealed a clear correlation between the elevation of catecholamine tracers and the predisposition to increased

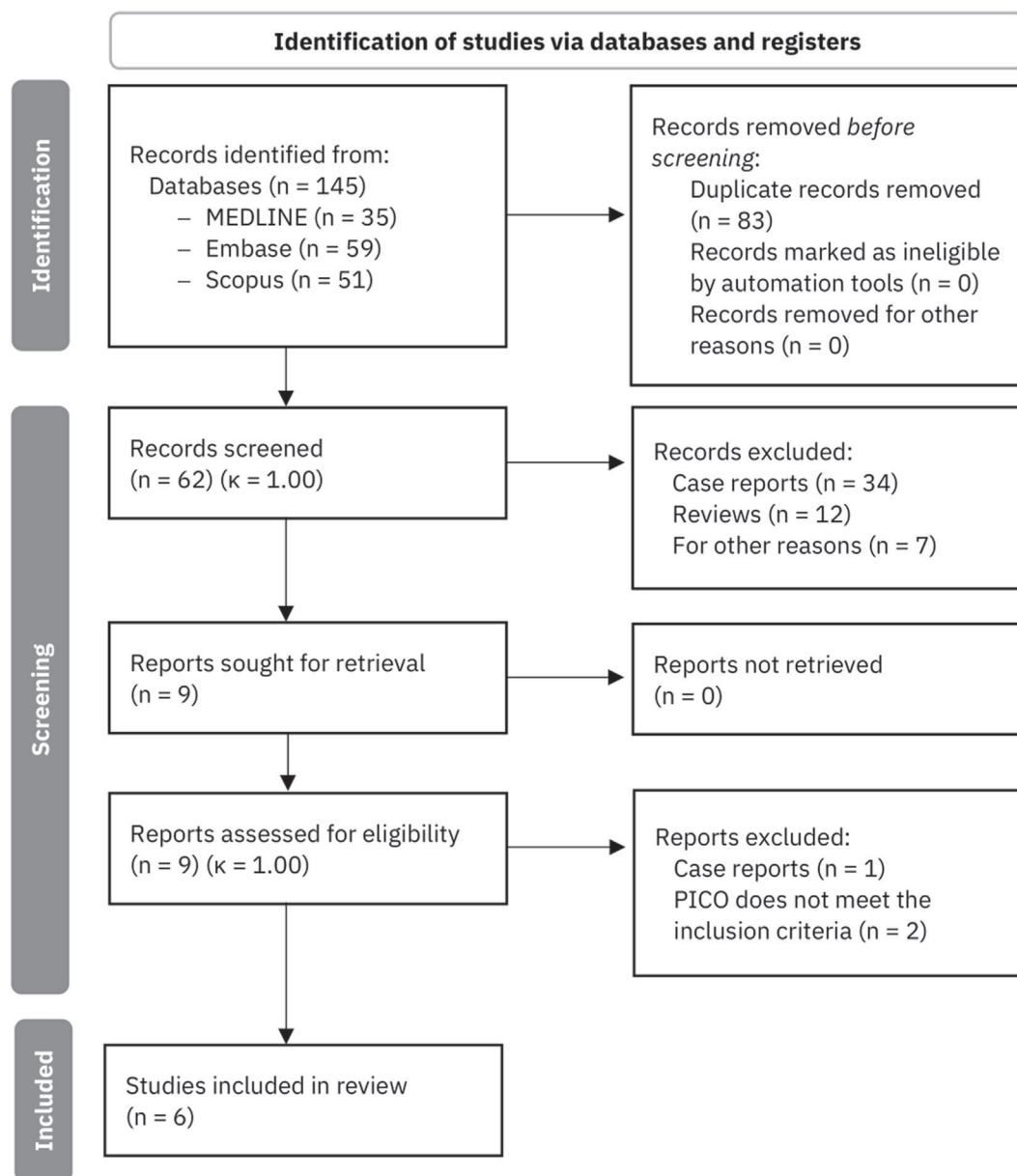


Fig. 1. Study selection flowchart.

BAT activity. For 12 out of 12 patients with non-secreting PPGLs (normal catecholamine assessment) across 2 studies, BAT activation was absent.^{6,7}

In the study by Puar et al⁸, aBAT on FDG-PET was identified by an SUV_{max} value > 1.5. Three studies analyzed SUV_{max} values in their PPGL cohorts displaying aBAT with mean values of 6.76, 4.0 and

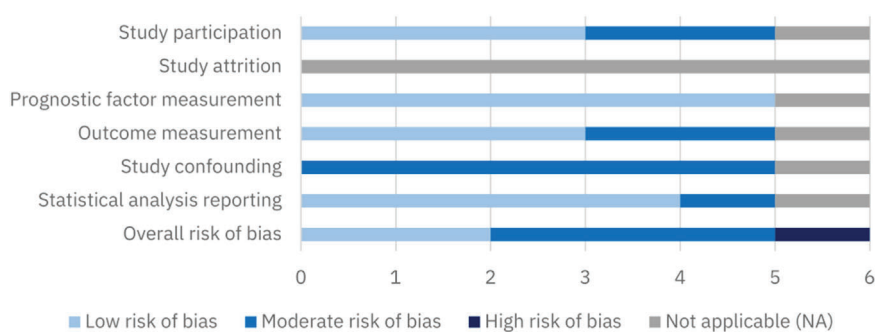


Fig. 2. Risk of bias assessment overview.

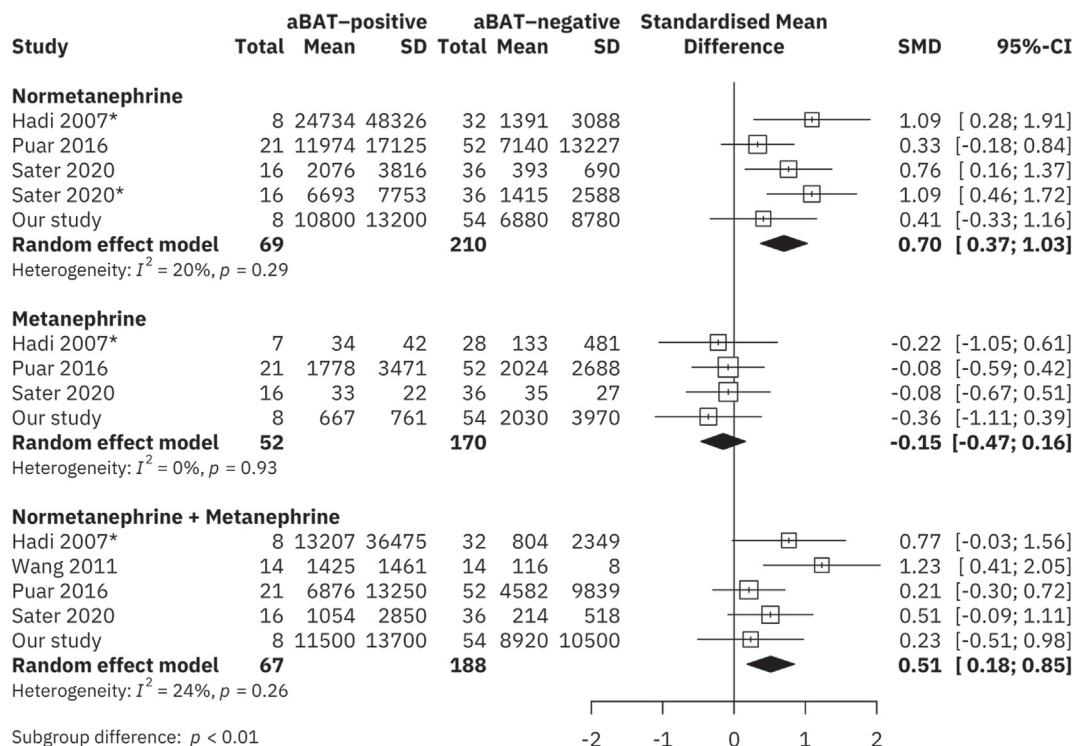


Fig. 3. Forest plot showing mean differences in levels of different catecholamines. * asterisk indicates (nor)epinephrine instead of (nor) metanephrine. aBAT = active brown adipose tissue.

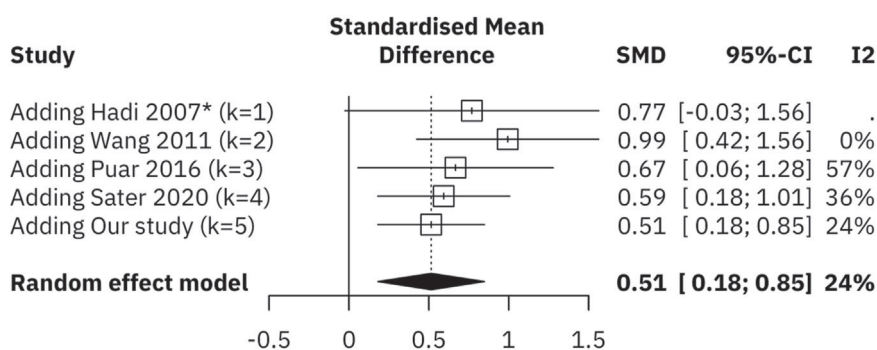


Fig. 4. Forest plot of cumulative meta-analysis of catecholamine level means. SMD = standard mean differences.

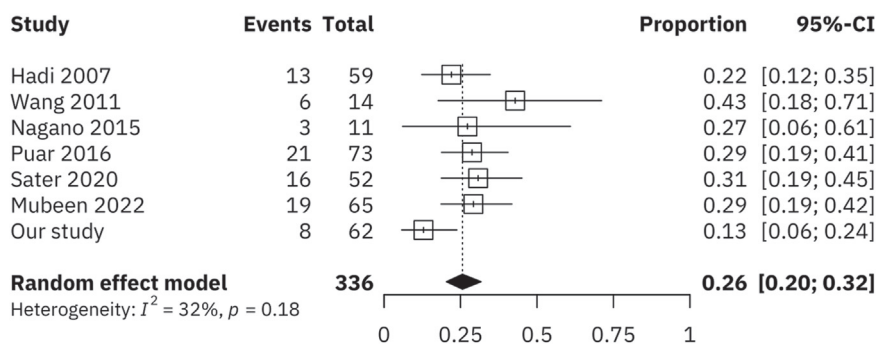


Fig. 5. Forest plot showing proportions of patients with PPGL presenting with aBAT.

4.91, respectively.^{6–8} In the study by Puar et al, a subgroup analysis showed that the highest mean SUV_{max} values belonged to those with cluster 1 germline mutations (von hippel lindau, succinate dehydrogenase) compared to cluster 2 (rearranged during transfection, neurofibromatosis type 1, MYC-associated factor X) and sporadic tumors. Nevertheless, this study demonstrated no statistically significant association between germline mutations and the prevalence of BAT activation.

In the study by Sater et al,¹⁰ 16 patients were identified with PPGL and concurrent aBAT. Approximately 70% of patients from this cohort were found to have combined cluster 1 or cluster 2 mutations. Kaplan–Meier survival analysis revealed that presence of activated BAT was linked to decreased overall survival when compared to the control group not expressing aBAT (HR 5.80, 95% CI, 1.05–32.05; $P = .02$) with an associated 5.8-fold increased chance of death attributed to tumor progression. Of note, all deaths (4/4) in the aBAT group from this study were in those with succinate dehydrogenase mutations. Death in the aBAT group was noted to occur at a younger age with markedly higher norepinephrine levels (22.10 ± 8.00 vs $0.48 \pm 0.27 \times ULN$). No other study which was included performed an analysis of mortality in aBAT cohorts.

The studies included in our quantitative synthesis revealed a trend toward a lower age at diagnosis in aBAT cohorts, as well as an observed inverse relationship between aBAT presence and waist circumference/body mass index. In comparisons of patients with PPGL and aBAT vs patients with PPGL without aBAT, no significant differences were found in multiple domains, including tumor size, tumor burden, or tumor location. There were also no significant differences found in systolic and diastolic blood pressure, lipid profiles, thyroid function, fasting blood glucose, or gender.

In the study by Hadi et al,⁹ alternative imaging for activated BAT was reviewed, the only study to do so. They concluded that of 83 patients with PPGL imaged with ¹⁸F-DG-PET, 19.2% had aBAT. With those imaged with ¹⁸F-6-fluorodopamine (F-DA) PET (67 patients with PPGL), 17.9% had aBAT: F-DA PET images BAT through localization of sympathetic innervations in these areas in a similar manner to ¹²³I-meta-iodobenzylguanidine.

Discussion

Pooling comparable data proved challenging because not all studies will have measured the same parameters for catecholamine assessment, depending on assay availability in their laboratory. Furthermore, some studies combined the measured variables while others did not. For all these reasons, we had to assess the retrieved information by combining all the values prior to their analysis and standardizing the data.

Concentrations of demethylated metabolites, prefixed with nor- (ie, normetanephrine and norepinephrine), showed statistically significant higher mean values in aBAT positive groups compared to the aBAT negative, suggesting its potential use in predicting the presence of active brown adipose tissue in patients with PPGLs. During the analysis of the cumulative meta-analytical results, it was noticed that the pattern of increased catecholamine levels was consistent over studies, concomitant with a decrease in heterogeneity, resulting in the shortening of confidence intervals and increased statistical significance. Adding the results from our study, although statistically insignificant in isolation, reduced the total pooled heterogeneity by 12%, as well as the confidence interval and P -value, thereby demonstrating its importance in contributing to the overall results and predicting equivalent results in further studies.

Furthermore, it was noticed that the inclusion of our study's proportions of patients with PPGL and aBAT tends to be on the low side compared to other studies, increasing the heterogeneity of the results. However, the cumulative result is changed by only 3% after

its inclusion, indicating that the proportion of patients with PPGL who present with aBAT is stable at around one quarter. While we were also unable to obtain the full text of the study performed by Mubeen et al, we have nevertheless included their result because it showed accordance with other reviewed papers.

Strengths and Limitations

This systematic review with a meta-analysis adds further confirmation to the close association of elevated catecholamines and the predisposition to aBAT on functional imaging in patients with PPGL. From the studies included, an inverse relationship between aBAT and weight/BMI was noted. This is already an established area of interest as it is acknowledged that BAT in humans may have a pivotal role in weight regulation and thus may form the basis of a therapeutic target in obesity.¹⁷ It is postulated that BAT activation and expansion in various forms of cancer may be a notable contributor to cancer-associated cachexia (CAC) associated with the cancer hypermetabolic state and mediated through increased energy expenditure via UCP-1 activity.¹⁸ However, recent large retrospective case control studies have failed to demonstrate significant links between aBAT and CAC or increased mortality.^{19,20} Animal models suggest a greater association between aBAT and CAC than comparable results in human studies.²¹ Whilst data presented in this quantitative synthesis indicated increased all-cause mortality in patients with PPGLs and aBAT, there is insufficient evidence of such an association in patients with other cancer types from retrospective clinical studies. Subsequently, the hypothesis that aBAT confers poorer outcomes in cancer patients cannot be generalized but requires further investigation in prospective clinical studies.

Multiple domains of patient characteristics were assessed in cohorts with PPGL with no statistically significant differences noted in aBAT patients, including tumor size, burden, and location. Notably, aBAT has been shown to be visualized on other imaging modalities, including F-DA PET, due to the likely localization of sympathetic innervations. However, this meta-analysis is based on 6 eligible studies and, given the variability in study designs, sample sizes, and measurement parameters, the conclusions thus may not be fully generalizable. Further analysis of aBAT in patients with PPGL with imaging methods alternative to FDG-PET may add more valuable information to a growing knowledge base.

Conclusions

Life expectancy and germline mutation associations were not extensively reviewed in the included studies. From the data available, there is no convincing evidence of increased aBAT prevalence in patients with PPGL and germline mutations. There was, however, evidence of increased all-cause mortality in those patients with PPGL and aBAT compared to patient controls with PPGL without aBAT. These are both areas of important interest that would benefit from continued and more extensive future research, as would the potential association of aBAT in patients with cancer cachexia. At this stage, it could be postulated that the presence of aBAT may confer poorer outcomes or life expectancy in patients with PPGLs.

Disclosure

G.K.D. has in the past received research grants from the NIHR, Novo Nordisk UK Research Foundation, and DDM, as well as payment or honoraria for lectures, presentations, speakers' bureaus, manuscript writing, or educational events from Novo Nordisk, Rhythm Pharmaceuticals, J&J/Ethicon, and Medtronic. E.O. has received an honorarium for a lecture by Krka. S.C.V. has received research grants, payment or honoraria for lectures, presentations,

or educational events from Novo Nordisk, Eli Lilly, Medtronic, and Krka.

References

1. Richard AJ, White U, Elks CM, et al. Adipose tissue: physiology to metabolic dysfunction. In: *Endotext*. South Dartmouth (MA): MDText.com, Inc; 2000.
2. Iyer RB, Guo CC, Perrier N. Adrenal pheochromocytoma with surrounding brown fat stimulation. *AJR Am J Roentgenol*. 2009;192:300–301. <https://doi.org/10.2214/AJR.08.1166>
3. Cero C, Lea HJ, Zhu KY, Shamsi F, Tseng YH, Cypess AM. beta3-Adrenergic receptors regulate human brown/beige adipocyte lipolysis and thermogenesis. *JCI Insight*. 2021;6. <https://doi.org/10.1172/jci.insight.139160>
4. Blondin DP, Nielsen S, Kuipers EN, et al. Human Brown adipocyte thermogenesis is driven by beta2-AR stimulation. *Cell Metab*. 2020;32:287–300.e287. <https://doi.org/10.1016/j.cmet.2020.07.005>
5. Nedergaard J, Bengtsson T, Cannon B. Unexpected evidence for active brown adipose tissue in adult humans. *Am J Physiol Endocrinol Metab*. 2007;293:E444–E452. <https://doi.org/10.1152/ajpendo.00691.2006>
6. Terada E, Ashida K, Ohe K, Sakamoto S, Hasuzawa N, Nomura M. Brown adipose activation and reversible beige coloration in adipose tissue with multiple accumulations of 18F-fluorodeoxyglucose in sporadic paraganglioma: a case report. *Clin Case Rep*. 2019;7:1399–1403. <https://doi.org/10.1002/ccr3.2259>
7. Wang Q, Zhang M, Ning G, et al. Brown adipose tissue in humans is activated by elevated plasma catecholamines levels and is inversely related to central obesity. *PLoS One*. 2011;6:e21006. <https://doi.org/10.1371/journal.pone.0021006>
8. Puar T, van Berkel A, Gotthardt M, et al. Genotype-dependent brown adipose tissue activation in patients with pheochromocytoma and paraganglioma. *J Clin Endocrinol Metab*. 2016;101:224–232. <https://doi.org/10.1210/jc.2015-3205>
9. Hadi M, Chen CC, Whatley M, Pacak K, Carrasquillo JA. Brown fat imaging with (18)F-6-fluorodopamine PET/CT, (18)F-FDG PET/CT, and (123)I-MIBG SPECT: a study of patients being evaluated for pheochromocytoma. *J Nucl Med*. 2007;48:1077–1083. <https://doi.org/10.2967/jnumed.106.035915>
10. Abdul Sater Z, Jha A, Hamimi A, et al. Pheochromocytoma and paraganglioma patients with poor survival often show brown adipose tissue activation. *J Clin Endocrinol Metab*. 2020;105:1176–1185. <https://doi.org/10.1210/clinem/dgz314>
11. Sampath SC, Sampath SC, Bredella MA, Cypess AM, Torriani M. Imaging of brown adipose tissue: state of the art. *Radiology*. 2016;280:4–19. <https://doi.org/10.1148/radiol.2016150390>
12. Santhanam P, Treglia G, Ahima RS. Detection of brown adipose tissue by (18) F-FDG PET/CT in pheochromocytoma/paraganglioma: a systematic review. *J Clin Hypertens*. 2018;20:615. <https://doi.org/10.1111/jch.13228>
13. Higgins JPT, Thomas J, Chandler J, Cumpston M, Li T, Page MJ, Welch VA, eds. *Cochrane Handbook for Systematic Reviews of Interventions*. 2nd ed. John Wiley & Sons; 2019.
14. *R: A language and Environment for Statistical Computing*. Vienna, Austria: ScienceOpen, Inc; 2024.
15. Balduzzi S, Rücker G, Schwarzer G. How to perform a meta-analysis with R: A practical tutorial. *Evid Based Ment Health*. 2019;22:153–160.
16. USCAP 2022 Abstracts: Endocrine Pathology (356–371). *Mod Pathol*. 2022;35(Suppl 2):476–492. <https://doi.org/10.1038/s41379-022-01035-5>
17. Santhanam P, Solnes L, Hannukainen JC, Taïeb D. Adiposity-related cancer and functional imaging of brown adipose tissue. *Endocr Pract*. 2015;21:1282–1290. <https://doi.org/10.4158/EP15870.RA>
18. Vaitkus JA, Celi FS. The role of adipose tissue in cancer-associated cachexia. *Exp Biol Med*. 2017;242:473–481. <https://doi.org/10.1177/1535370216683282>
19. Becker AS, Zellweger C, Bacanovic S, et al. Brown fat does not cause cachexia in cancer patients: a large retrospective longitudinal FDG-PET/CT cohort study. *PLoS One*. 2020;15:e0239990. <https://doi.org/10.1371/journal.pone.0239990>
20. Eljalby M, Huang X, Becher T, et al. Brown adipose tissue is not associated with cachexia or increased mortality in a retrospective study of patients with cancer. *Am J Physiol Endocrinol Metab*. 2023;324:E144–E153. <https://doi.org/10.1152/ajpendo.00187.2022>
21. Beijer E, Schoenmakers J, Vijgen G, et al. A role of active brown adipose tissue in cancer cachexia? *Onco Rev*. 2012;6:e11. <https://doi.org/10.4081/oncol.2012.e11>